

UNCLASSIFIED

AD 270 454

*Reproduced
by the*

**ARMED SERVICES TECHNICAL INFORMATION AGENCY
ARLINGTON HALL STATION
ARLINGTON 12, VIRGINIA**



UNCLASSIFIED

NOTICE: When government or other drawings, specifications or other data are used for any purpose other than in connection with a definitely related government procurement operation, the U. S. Government thereby incurs no responsibility, nor any obligation whatsoever; and the fact that the Government may have formulated, furnished, or in any way supplied the said drawings, specifications, or other data is not to be regarded by implication or otherwise as in any manner licensing the holder or any other person or corporation, or conveying any rights or permission to manufacture, use or sell any patented invention that may in any way be related thereto.

CATALOGED BY
AS AD INC.
270 454

THERMAL RADIATION PROPERTIES OF MATERIALS

270 454

R. A. SEBAN
R. E. ROLLING

UNIVERSITY OF CALIFORNIA

JUNE 1961

ASTIA
JUN 27 1962

XEROX
-2-7-

AERONAUTICAL SYSTEMS DIVISION

NOTICES

When Government drawings, specifications, or other data are used for any purpose other than in connection with a definitely related Government procurement operation, the United States Government thereby incurs no responsibility nor any obligation whatsoever; and the fact that the Government may have formulated, furnished, or in any way supplied the said drawings, specifications, or other data, is not to be regarded by implication or otherwise as in any manner licensing the holder or any other person or corporation, or conveying any rights or permission to manufacture, use, or sell any patented invention that may in any way be related thereto.

Qualified requesters may obtain copies of this report from the Armed Services Technical Information Agency, (ASTIA), Arlington Hall Station, Arlington 12, Virginia.

This report has been released to the Office of Technical Services, U. S. Department of Commerce, Washington 25, D. C., for sale to the general public.

Copies of ASD Technical Reports and Technical Notes should not be returned to the Aeronautical Systems Division unless return is required by security considerations, contractual obligations, or notice on a specific document.

THERMAL RADIATION PROPERTIES OF MATERIALS

*R. A. SEBAN
R. E. ROLLING*

UNIVERSITY OF CALIFORNIA

JUNE 1961

**DIRECTORATE OF MATERIALS & PROCESSES
CONTRACT No. AF 33(616)-6630
PROJECT No. 7360**

**AERONAUTICAL SYSTEMS DIVISION
AIR FORCE SYSTEMS COMMAND
UNITED STATES AIR FORCE
WRIGHT-PATTERSON AIR FORCE BASE, OHIO**

FOREWORD

This report was prepared by the Institute of Engineering Research, University of California, Berkeley, California, under USAF Contract No. 4F 33(616)-6630. The contract was initiated under Project 7360, "Materials Analysis and Evaluation Techniques", Task No. 73603, "Thermodynamics and Heat Transfer". It was administered under the direction of the Materials Central, Directorate of Advanced Systems Technology, Wright Air Development Division, with Mr. Robert A. Winn acting as project engineer.

The report covers work conducted from July 1959 through September 1960. The project was under the direction of R. A. Seban, Professor of Mechanical Engineering, principal investigator, and R. E. Colling, research engineer.

Grateful acknowledgement for their various contributions is due to: R. Eberhart, research assistant; D. Russell, C. Woodson, and E. Anderson, engineering aids; and to Professor H. A. Johnson for frequent consultation on various problems.

ABSTRACT

Methods are described for the measurement of total normal emittance, in air, for temperatures up to 2500°F; for normal spectral reflectance, in air, at low temperature; for wavelengths from 0.30 to 25 microns and in air, at 1000°F, from 1 to 25 microns. Results of this type are given for twenty samples of different materials and the measured total emittances are generally within 5% of values predicted from reflectance measurements.

Reflectances were also measured as a function of angle for wavelengths of the order of 1 micron, to give absorptances as a function of angle of incidence that are useful in the appraisal of solar irradiation.

A spectral emittance unit is described and the preliminary results from it for samples at 1400°F show general agreement with the measured values of spectral reflectance.

PUBLICATION REVIEW

This report has been reviewed and is approved.

FOR THE COMMANDER:



Jules I. Wittebort
Chief, Thermophysics Branch
Physics Laboratory
Materials Central

TABLE OF CONTENTS

	Page
1.0 Introduction	1
2.0 Definitions and Analyses	2
2.1 Reflection	2
2.2 Absorption and Emission	4
3.0 Spectral Reflectance Determinations	6
3.1 The Heated Cavity System	6
3.2 Beckman Spectroreflectometer	13
3.3 Integrating Sphere for Variable Incidence	18
4.0 Total Normal Emittance	22
4.1 Electrically Heated Unit	23
4.2 Gas Heated Unit	23
4.3 Radiometer	25
4.4 Thermocouple Installation	26
5.0 Spectral Emittance	29
6.0 Roughness	34
7.0 Characteristics of Selected Materials	36
7.1 Nature of the Results	36
8.0 Total Emittance and Spectral Reflectance Results	43
9.0 Comparison With Other Results	47
10.0 Angular Dependence of the Absorptance	51
11.0 Plastic Samples	57
11.1 Total Emittance	57
11.2 Spectral Reflectance	57
11.3 Translucent Plastic	58
11.4 Reflectance of Plastic Samples at Short Wavelengths	60
12.0 Summary and Conclusions	66
13.0 Results for the Various Samples	69
13.1 Chromate on Stainless Steel	71
13.2 Chromate Coatings on Various Materials	73
13.3 Chromate on 302 Stainless Steel	75
13.4 Chromate on 420 Stainless Steel	77
13.5 Chromate on Inconel	79
13.6 M 252 (S.S. 4781)	81
13.7 HS 25 (S.S. 8178)	83
13.8 Rene 41 (S.S. 8080)	85
13.9 Niobium Dipped in Al-Si	87

TABLE OF CONTENTS (CONTINUED)

	Page
13.10 Niobium Dipped in Al-Cr-Si	89
13.11 PRF-5	91
13.12 PFR-4	92
13.13 Stainless Steel 286	93
13.14 Inconel	95
13.15 Boron Carbide Coating	97
13.16 Alclad Solar Absorber	99
13.17 Astrolite	101
13.18 Fl20	103
13.19 CTL 37-9	105
13.20 WWRONE-2	107
14.0 Nomenclature	109
15.0 References	110

LIST OF FIGURES

FIGURE		PAGE
1.	Angular relations for reflectance	2
2.	Tilting cavity system	6
3.	Functions used in computing reflectance results	8
4.	Air cooled sample holder	10
5.	Effect of error in sample temperature	11
6.	Effect of error in reference temperature . .	12
7.	Comparison of measured r_{ϕ} and r_u	14
8.	Spectral reflectance of MgO	15
9.	Beckman DK-2 sphere	16
10.	Reflectance determined by different systems . .	19
11.	Variable angle integrating sphere	20
12.	Arrangement used in emittance measurements . .	22
13.	Gas fired emittance stand	24
14.	Thermocouple attachment	26
15.	Spectral emittance stand	30
16.	Spectral emittance results	32
17.	Typical roughness indications	35
18.	Wavelength subdivisions for total emittance . .	40
19.	Wavelength subdivisions for solar reflectance .	41
20.	Effect of sample temperature on reflectance . .	45
21.	Comparison of results for Inconel	48
22.	Comparison of total emittance values	49
23.	Angular reflectance of polished samples	52

LIST OF FIGURES (CONTINUED)

FIGURE		PAGE
24.	Angular reflectance of roughened samples. . . .	53
25.	Angular reflectance of various materials. . . .	55
26.	Spectral reflectance of various materials . . .	61
27.	Spectral reflectance of various materials . . .	62
28.	Spectral reflectance of various materials . . .	63
29.	Spectral reflectance of various materials . . .	64
30.	Spectral reflectance of various materials . . .	65
31.	Spectral reflectance of various materials . . .	66

1.0 INTRODUCTION

To extend the amount of available information on the thermal radiation properties of materials used in space applications, such properties have been determined for a number of selected materials. These have been determined in air, at atmospheric pressure, at room and at elevated temperatures, but they are applicable in other environments provided there is no essential change in the surface from that which was tested.

The primary results are total normal emittances at surface temperatures from 500°F to 2500°F and spectral reflectances of cold samples for wavelengths from 0.30 to 25 microns, and with sample temperatures up to 1100°F for wavelengths from 1 to 25 microns. The spectral results permit a calculation of total normal emittances, and comparison with the measured total normal emittances indicates that this property should be predictable within 5% in the temperature range from 500 to 3000°F from the spectral reflectance values.

Additional results are presented for the dependence of the reflectance on the angle of incidence, at wavelengths of the order of 1 micron, a characteristic that is particularly important in respect to the absorption of solar radiation. Some spectral emittance results are also presented in the wavelength range from 1 to 15 microns, but the scope of these results is limited because satisfactory operation of the device for these determinations was substantially delayed. The results that are presented support the measured values of the spectral reflectance.

Because of the variety of definitions that are involved with respect to the reflectance and emittance, these are first presented; the section on definitions is followed by others devoted to the description of the systems used for the realization of the results. A table in Section 7 defines the kind of results that were obtained for each of the samples and this table indicates the location, in Section 13, of the detailed results for each. Sections 8 to 12 are commentaries on various features of the results; Section 11 refers specifically to the plastic samples, for which only limited results were obtained. These materials are of high thermal resistance, making the precise determination of surface temperature impossible in those instances of measurement when a high heat flux existed through the sample. This proved to be a major impediment in determining satisfactory results for plastics.

Manuscript released for publication 3 October 1960 as a WADD Technical Report.

2.0 DEFINITIONS AND ANALYSES

Despite the relative standardization of the definitions of reflectance and emittance, enough ambiguity remains to make it convenient to restate these definitions. They are given in as general a way as possible, beginning with the reflectance in a prescribed direction for irradiation at a specified angle of incidence, though this reflectance was not measured in the experimental work described in the report. All relations here and in the remainder of the report are for monochromatic radiation unless they are specifically qualified as being for total radiation.

2.1 Reflectance

We consider the irradiation of a material of area A_1 by a black surface of area A , which is normal to the length r connecting the areas, and which length is at an angle ϕ with respect to the normal to area A_1 . For A and A_1 both small, the irradiation is

$$\frac{E}{\pi} \cos \frac{\Delta A_1}{r^2}$$

and per unit area of A_1 and per unit solid angle $\Delta A/r^2$ it is $\frac{E}{\pi} \cos \phi$.

This irradiation is in part reflected, and in general the reflection is distributed in an arbitrary way over the entire hemisphere above the surface. In the direction μ, ψ [the azimuthal angle ψ is measured from the plane of the incident radiation], the intensity of the reflection is $R_{\mu, \psi; \phi}$, and a reflection coefficient can be defined as

$$r_{\mu, \psi; \phi} = \frac{R_{\mu, \psi; \phi}}{\frac{E}{\pi} \cos \phi} \quad 2.1.1$$

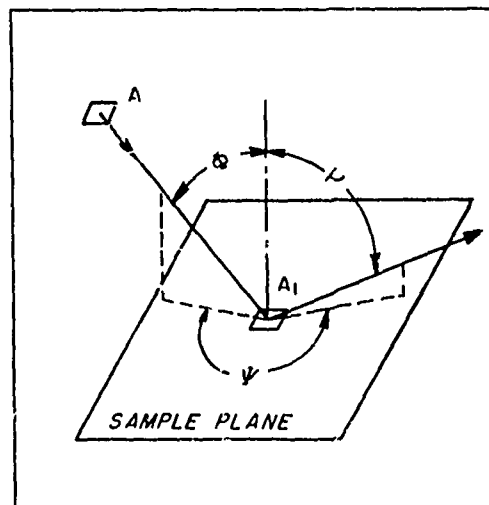


Figure 1.

This is similar to the coefficient defined by Münch,⁽¹⁾ who, however, multiplied by 2π the right side of Equation 2.1.1.

The total reflected radiation is obtained by integrating the intensity of the reflection over the 2π steradians of solid angle over surface A_1 .

$$R_\phi = \int_0^{2\pi} R_{\mu, \psi; \phi} d\Omega \quad 2.1.2$$

This is the reflection that is measured by an integrating sphere when the sample is irradiated in a prescribed direction, ϕ and it is convenient to define a reflection coefficient as:

$$r_\phi = \frac{R_\phi}{\frac{E}{\pi} \cos \phi} \quad 2.1.3$$

This is the limit to which the definitions may be carried without some specification of the nature of the reflection. In this sense it is important to consider it in terms of two common definitions, of specular and diffuse reflection. In specular reflection the intensity $R_{\mu, \psi; \phi}$ is zero everywhere except at $\mu = \phi, \psi = \pi$, so that R_ϕ is the same as $R_{\phi, \pi; \phi}$; there is then no distinction between r_ϕ and $r_{\mu, \psi; \phi}$. According to electromagnetic theory all smooth surfaces are specular reflectors.

Diffuse reflection, also specified as reflection from a "matt surface", postulates that the intensity of the reflection follows Lambert's Law, $R_{\mu, \psi; \phi} = \frac{R_\phi}{\pi} \cos \mu$, so that Equation 2.1.1 becomes

$$r_{\mu, \psi; \phi} = \frac{r_\phi \cos \mu}{\pi} \quad 2.1.4$$

The results of Eckert(2) and of Münch(1) indicate that this is a poor approximation to most surfaces of engineering interest.

Because there are a number of technical applications, particularly in reflectance measurements, in which the sample is irradiated diffusely and the reflection measured only in the direction μ, ψ , the equations are presented for this special case. The reflected intensity that is observed is

$$R_{\mu, \psi} = \int_0^{2\pi} r_{\mu, \psi; \phi} \frac{E}{\pi} \cos \phi d\Omega \quad 2.1.5$$

But because of the uniformity of the irradiation with respect to azimuthal angle ψ the intensity $R_{\mu, \psi}$ is the same for all azimuthal

angles, as is evident by expansion of Equation 2.1.5 to the form

$$R_{\mu\psi} = \frac{E}{\pi} \int_0^{\pi/2} \int_0^{2\pi} r_{\mu,\psi;\phi} \cos \phi \sin \phi d\psi d\phi$$

A more compact form is possible by defining a reflectance

$$r_{\mu\phi} = \int_0^{2\pi} r_{\mu,\psi;\phi} d\psi$$

A reflectance is often defined for this kind of measurement as the ratio of the intensity R_{μ} to that of the irradiation in the same direction

$$r_{\mu} = \frac{R_{\mu}}{\frac{E}{\pi} \cos \mu} = \frac{1}{\cos \mu} \int_0^{\pi/2} r_{\mu\phi} \cos \phi \sin \phi d\phi \quad 2.1.6$$

For a specular reflector, of course, $r_{\mu} = r_{\mu,\psi;\phi}$, and for a diffuse reflector $r_{\mu,\phi} = \frac{2\pi r_{\phi} \cos \mu}{\pi}$. The latter case produces no essential simplification of Equation 2.1.6 unless r_{ϕ} happens to be constant, in which case integration is possible, to yield $r_{\mu\phi} = r_{\phi}$, also a constant.

2.2 Absorption and Emission

For an opaque material, the radiation that is not reflected is absorbed, so that $(1-r_{\phi})$ is the fraction of the irradiation incident at angle ϕ that is absorbed. When the irradiation is received from a diffuse black body the hemispherical absorptivity is

$$\alpha = \frac{1}{\pi} \int_0^{2\pi} (1-r_{\phi}) \cos \phi d\Omega \quad 2.2.1$$

When the sample is at the temperature of the source of the irradiation then total absorbed energy must be emitted as ϵE_T . A statement of Kirchhoff's Law for the total radiation is

$$\alpha_T = \epsilon_T \quad 2.2.2$$

And on a monochromatic basis this is

$$\int \alpha E d\lambda = \int \epsilon E d\lambda$$

Since α and ϵ depend on λ , and E depends on λ and T , the applicability of Kirchhoff's Law requires that $\alpha = \epsilon$.

As in the case of the reflectance, an emittance can be defined as the ratio of the intensity of the emission to that of a black body at the same temperature in the same direction

$$\epsilon_{\mu} = \frac{I}{\frac{E}{\pi} \cos \mu}, \quad \epsilon = \frac{1}{\pi} \int_0^{2\pi} \epsilon_{\mu} \cos \mu d\Omega \quad 2.2.3$$

where symmetry about the normal has been assumed.

In terms of this definition, and the reflectance r_{μ} for diffuse irradiation, the intensity of the radiosity of the surface at any point can be stated as

$$\epsilon_{\mu} \frac{E}{\pi} \cos \mu + r_{\mu} \frac{E}{\pi} \cos \mu$$

Then, if the radiosity is always to be equal to that of a black body, we must have

$$\epsilon_{\mu} + r_{\mu} = 1 \quad 2.2.4$$

The reflectance r_{μ} is the one that can be measured with diffuse irradiation, as it is defined by Equation 2.1.6. The other reflectances defined in Section 2.1, however, can be related to r_{μ} and hence to ϵ_{μ} only within the restriction of additional assumptions. With specular reflectors, $r_{\mu, \phi; \phi} = r_{\phi} = r_{\mu}$ so that the emittance ϵ_{μ} is determined by r_{ϕ} with angle ϕ equal to angle μ . If the surface is a diffuse reflector, and if r_{ϕ} is independent of angle, then $r_{\mu} = r_{\phi}$, constant and then ϵ_{μ} is also constant. Lambert's Law is thus obtained for the angular distribution of emission.

3.0 SPECTRAL REFLECTANCE DETERMINATIONS

Spectral reflectances are of value for the deduction of the absorptance and of the emittance, and the usefulness of a particular technique hinges largely upon the degree to which the reflectance measurements that are obtained can be used to deduce these desired values. In the present work two methods were used, a heated cavity system providing hemispherical irradiation which was approximately diffuse, and integrating spheres in which was measured the total reflection from an incident beam of monochromatic energy. In one of these spheres there was provision for variation of the angle of incidence. As indicated in the definitions of the previous section, it is from the heated cavity system that an emittance may be most directly deduced, but the heating requirements are such that the minimum useful wavelength for that system is of the order of 1 micron, so that the sphere, with a more uncertain indication, is needed to extend the range to shorter wavelengths. Since the cavity system was used from 1 to 25 microns, and reflectances were measured with a sphere in the range from 0.3 to 2.7 microns, there is a substantial overlap in the two kinds of results that should assist in their discrimination. But these two kinds of reflectance are random enough in the various samples so that there is produced no experimental appraisal of their similarity or difference.

3.1 The Heated Cavity System

This system has as its essential element a heated cavity which is nearly isothermal. The method which permits the determination of reflectivity in the region 1.0 to 25 microns, was developed by Gier and Dunkle and has been described by Gier⁽³⁾. Thermal energy from the cavity walls irradiates a 7/8" disk held in a water or air cooled sample holder at the inner surface of the cavity. The external optics are so arranged that a 3/8" diameter center section of the sample is viewed at 7° to its normal. This energy is chopped and focused on the inlet slits of the Perkin-Elmer Model 83 monochromator, detected therein with a vacuum thermocouple, with the thermocouple output amplified by a Perkin-Elmer Model 107 amplifier and displayed on a Brown potentiometer indicator. By physically tilting the cavity the image of a similar area in the reference region can be placed on the monochromator inlet slits.

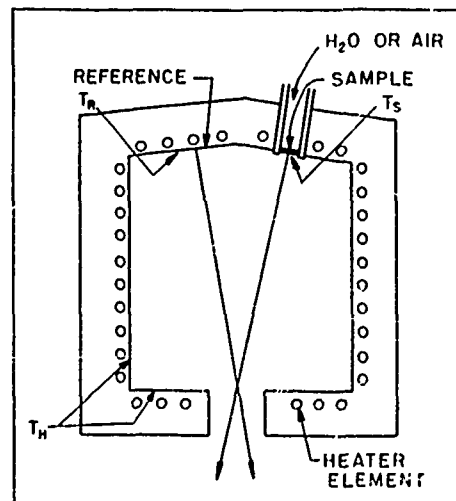


Figure 2.-Tilting Cavity System

When the sight is on the sample, the intensity observed is, per unit area of sample

$$r_{\mu} G_H + \epsilon_{\mu} E_s$$

Here G_H is the presumed diffuse irradiation of the sample, which is realized except for non-uniformity of the radiosity of the cavity walls and the area of the observation port at the bottom of the cavity. The maximum observed temperature difference in the cavity, occurring during the use of the water cooled sample holder, was 15°F between the relatively uniform temperature of the sides and bottom of the cavity, hereafter assumed to be uniform at T_H , and the lower temperature T_R , of the reference area. The area of the cavity opening produced an angle factor of 0.02 at the sample, resulting in a slightly high estimated value for G_H . This error does not exist for a purely specular sample since all of the viewed energy for this case originates from a small area at the bottom of the cavity.

When the sight is on the reference the intensity observed is $G_H r_{\mu} = \epsilon_{\mu} E_R$. This area is heavily oxidized nickel, giving a high value for ϵ_{μ} , thus the results are ultimately appraised as though $\epsilon_{\mu}=1$ $r_{\mu}=0$, though actually when $T_H > T_R$ the radiosity of this surface is a little higher than the estimate that is used.

The detector output is a linear function of the observed intensity, and the system constants, including amplifier gain, path attenuation, etc., are combined into a constant K . The detector output when viewing the reference is then:

$$S_R = K (G_R E_R + r_R G_H - E_c) \quad 3.1.1$$

(Here the subscript μ , indicating the nature of ϵ and r is deleted and the distinguishing subscripts on G , r , etc. refer to the reference, cavity, and sample. Subscript c refers to the chopper blade which is viewed by the monochromator when it obscures the cavity during the chopping process.) When viewing the sample the output is

$$S_s = K [r_s G_H + (1-r_s) E_s - E_c] \quad 3.1.2$$

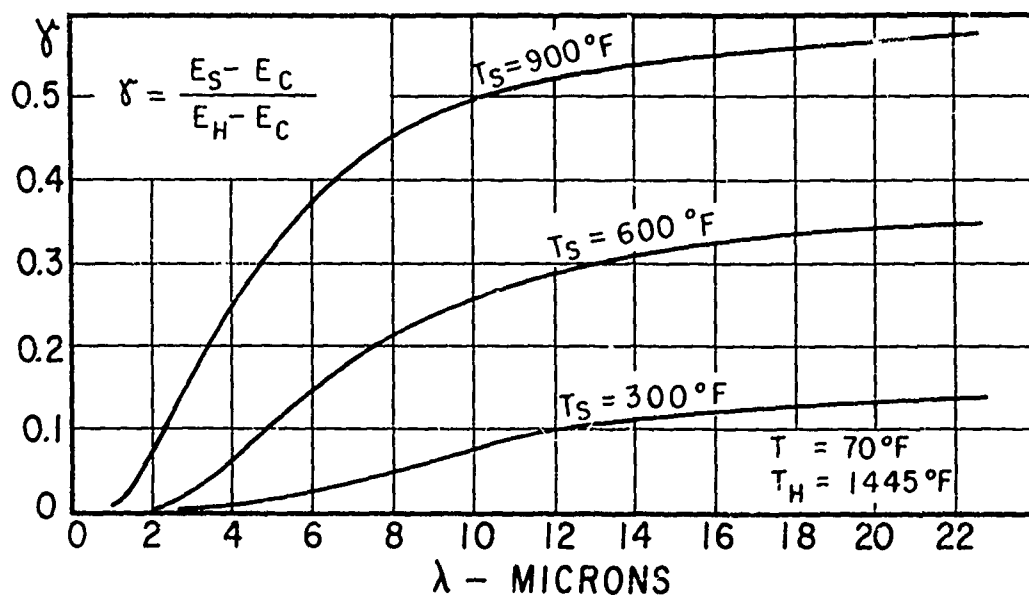
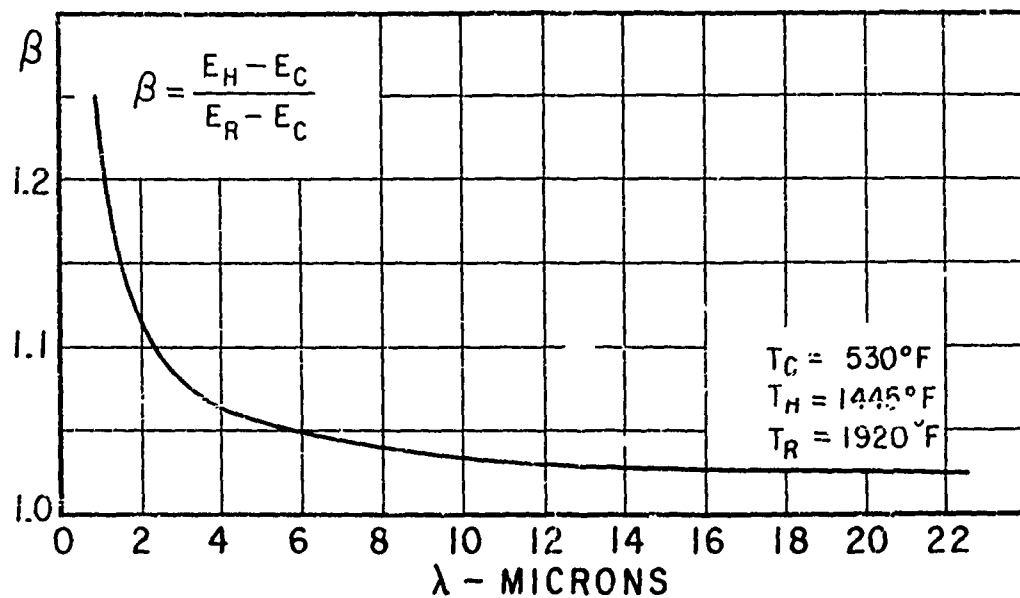


Figure 3. - Wavelength dependence of functions used in computing reflectance results.

where $1-r_s = \epsilon_s$ has been taken in accordance with Equations 2.2.4 and 2.1.6. Combination of Equations 3.1.1 and 3.1.2 eliminates the constant K of the response of the over-all system and the resulting ratio S_s/S_R is considered in terms of further assumptions necessary to the evaluation of the reflectance. These involve the assumption that the emittance of the reference area is unity, so that its radiosity is E_R , and that the emittance of the rest of the cavity is also unity, making its radiosity, and consequently the irradiation of the sample, equal to E_H . With these assumptions the response ratio becomes:

$$\frac{S_s}{S_R} = \frac{r_s E_H + (1-r_s) E_s - E_c}{E_R - E_c} \quad 3.1.3$$

With the water cooled sample holder, the emission from the sample is much less than its irradiation from the cavity, $E_s \ll E_H$. Though the sample temperature is not measured in cold runs, it is easily shown to be of the order of that of the surroundings, so that $E_s \approx E_c$. Then Equation 3.1.3 becomes:

$$\frac{S_s}{S_R} = r_s \frac{E_H - E_c}{E_R - E_c} = r_s \beta \quad 3.1.4$$

Actually the reflectance r_s is evaluated as S_s/S_R , which assumes $E_H = E_R$, and then the contribution of the factor $(E_H - E_c)/(E_R - E_c)$ is considered in an error analysis. Figure 3 indicates the magnitude of the ratio $(E_H - E_c)/(E_R - E_c)$ for conditions more severe than typical, with the cavity at 1450°F and the reference area at 1420°F. The error is seen to be significant at short wavelengths. When it exceeded 2% the results were evaluated according to Equation 3.1.4.

To obtain results at elevated sample temperatures the water cooled sample holder was replaced by the air cooled sample holder, the essential aspects of which are shown in Figure 4. By restriction of the air supply, high sample temperatures could be obtained; the determination of the sample temperature became necessary for evaluation of the experimental results.

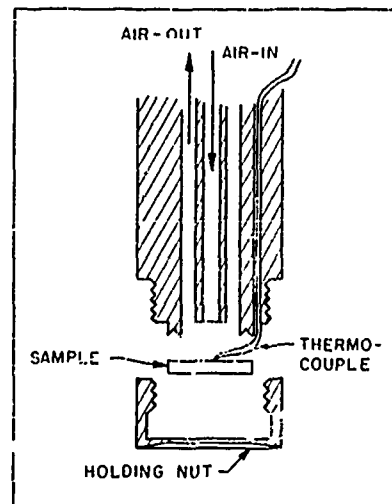
These temperatures were obtained by means of a thermocouple which was welded to the back of the sample disk, with the wires removed from the holder through tube fittings provided for them. The sample emittance was evaluated from the observed temperature T_s with Equation 3.1.3 then giving the reflectance of the sample as

$$r_s = \frac{S_s}{S_R} \left[\frac{E_R - E_c}{E_H - E_s} \right] + \left[\frac{E_c - E_s}{E_H - E_s} \right]$$

or with $\beta = \frac{E_H - E_C}{E_R - E_C}$

and $\gamma' = \frac{E_S - E_C}{E_H - E_C}$

we have
$$r_s = \frac{\left[\frac{S_S}{S_R} \frac{1}{\beta} - \gamma' \right]}{[1 - \gamma']}$$



The calculation of the quantities β and γ' is aided by a tabulation of $E/\sigma T^5$ as a function of λT , where tables may be compiled in the form of a function

Figure 4.-Air Cooled Sample Holder

$$C(\lambda T) = \frac{E}{\sigma T^5}$$

Using Planck's equation required values, then

$$E = \frac{C_1}{\lambda^5 (e^{C_2/\lambda T} - 1)}$$

for tabulation of the

$$\gamma' = \frac{C_S \left(\frac{T_S}{T_C} \right)^5 - C_C}{C_H \left(\frac{T_H}{T_C} \right)^5 - C_C}$$

Less apparent than the labor of calculating the results but more important for their appraisal is the loss of sensitivity of the detector to the reflected energy as the sample temperature becomes high. The major part of the detector output is then due to emission from the sample. Therefore errors in the measurement of the sample temperature and of the difference between T_S and T_C become of greater significance as the temperature of the sample increases. Figure 5 presents the error Δr for typical operating conditions, with a sample temperature of 1000°F, and shows the effect of a 20°F error in the sample temperature.

For the same conditions, Figure 6 presents the effect of differences between T_R and T_H , with a 100°F difference being the basis of

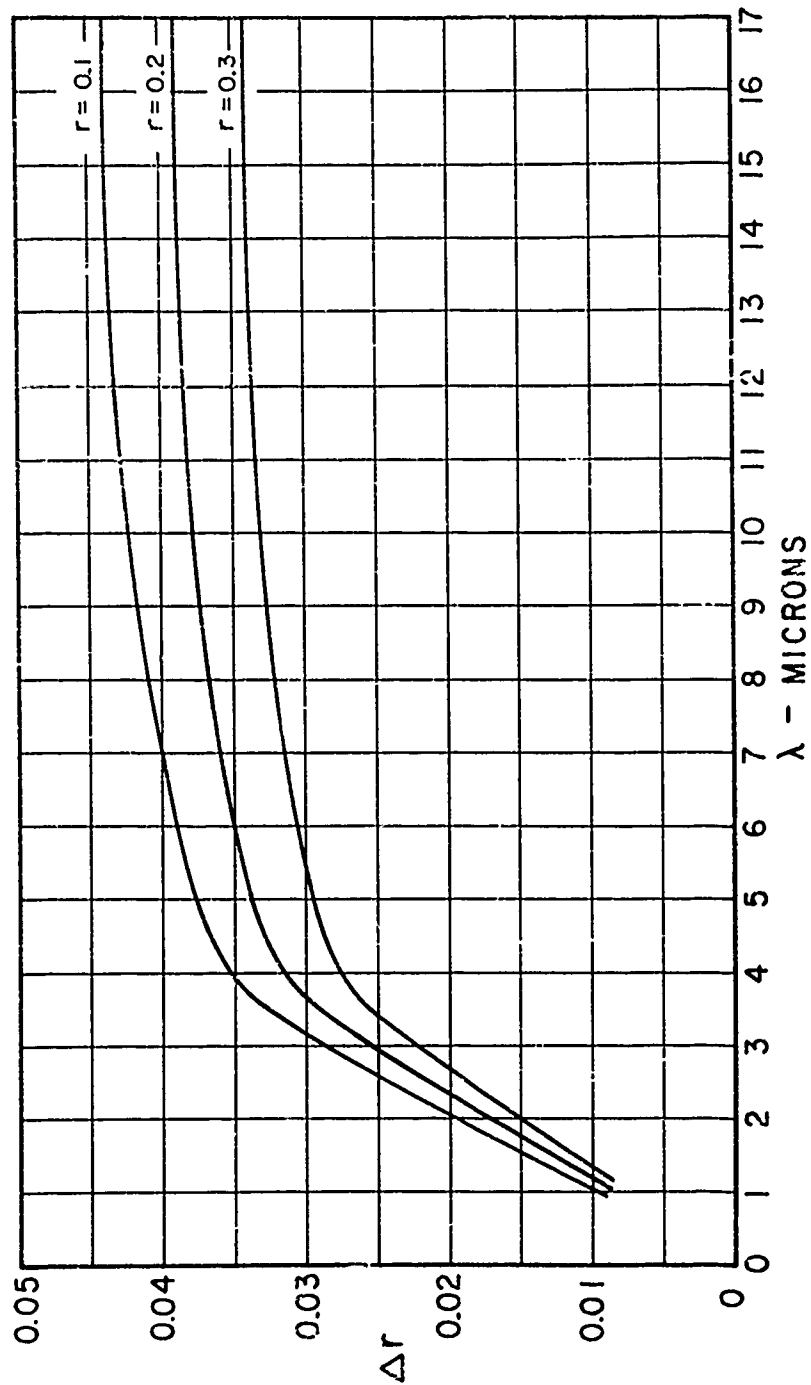


Figure 5. - Possible variation in r due to measurement error of 20°F in T_S . Conditions: $T_S = 1000^\circ\text{F}$; $T_i = 1400^\circ\text{F}$; $T_C = 700^\circ\text{F}$.

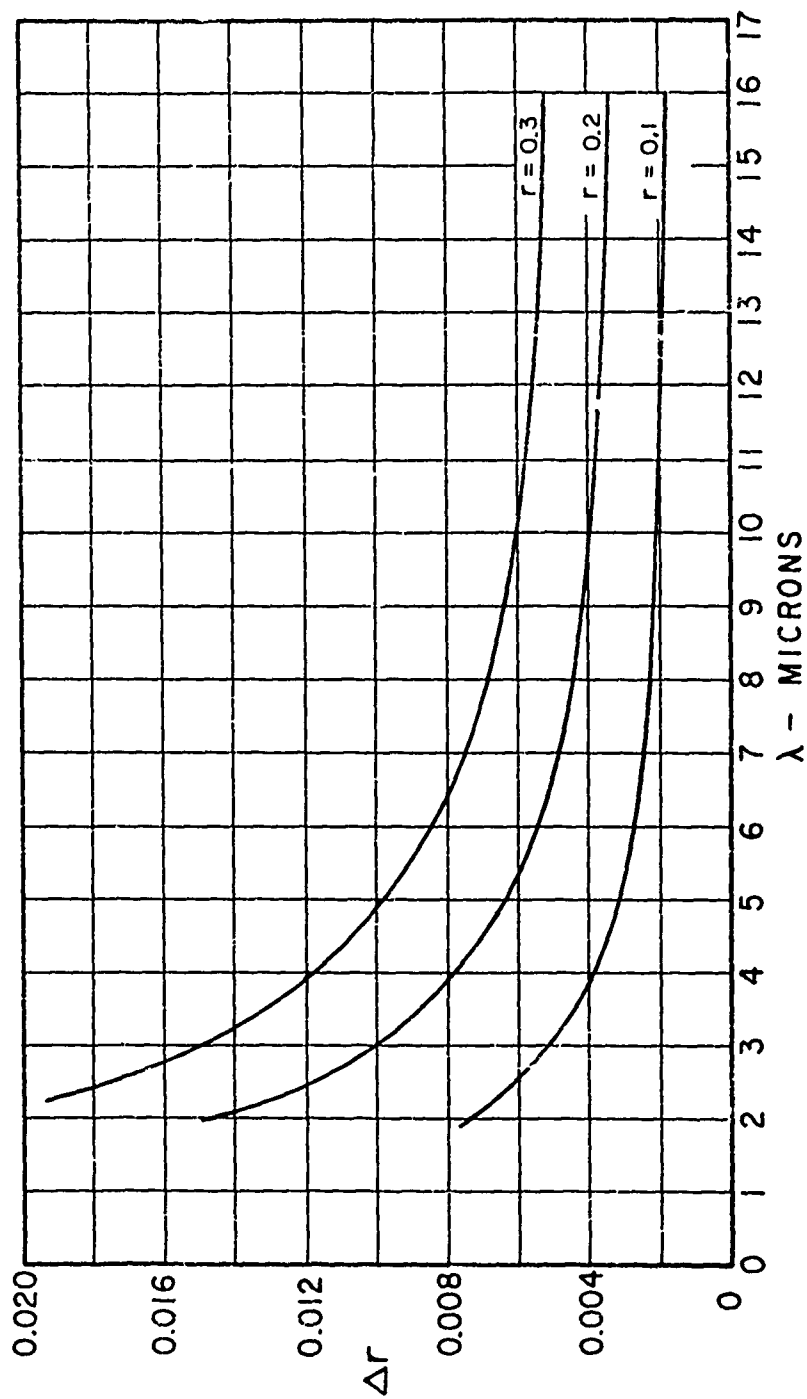


Figure 6. - Possible variation in r due to measurement error of 20°F in T_R . Conditions: $T_H = 1400^\circ\text{F}$; $T_R = 1400^\circ\text{F}$; $T_C = 70^\circ\text{F}$.

the presentation. This indicates the error due to the assumption of $\beta = 1$ in the calculations, though actually the temperature difference was usually less than 10°F and the reduced error can be obtained proportionately from Figure 6. In any case the calculation of the reflectance from Equation 3.1.4 is used only where Figures 5 and 6 indicate that a specific error computation is necessary to obtain satisfactory results.

3.2 Beckman Spectroreflectometer

For short wavelengths, from 0.3 to 2.7 microns, reflectance data were obtained from a standard Beckman DK2 spectrometer with a spectroreflectance attachment. This is a comparison type integrating sphere device in which, in normal observation, the sample and reference are irradiated with a beam of monochromatic energy at an angle of 4° to the normal. The instrument is ratio-recording so that the output record is the ratio of the reflectance of the sample to that of a smoked magnesium oxide reference surface, the measured reflectance being r_s as defined by Equation 2.1.3. Reversed operation is possible, with total irradiation from a luminous source being directed into the sphere at the normal detector location and the detector located in the normal lamp position. The irradiation is then approximately diffuse, but this is rendered uncertain by the high energy requirements in this mode of operation. In practice, a photoflood lamp was used at the detector port, and at least that region had a radiosity in excess of the remainder of the sphere. With this operation the reflectance that is measured approximates r_μ , Equation 2.1.6, with the instrument actually indicating the ratio of the standard and sample reflectances. The detection is monochromatic, as the reflected energy passes through the spectrometer toward the detector.

Figure 7 shows two reflectance ratios for a sample judged to be reasonably diffuse, for both modes of operation. There is little difference, and such behavior was typical for most samples. This is surprising since in theory r_ϕ and r_μ , $\phi = \mu = 4^\circ$ would be equal only if the reflection were specular or if it were diffuse with a reflectance r_ϕ independent of angle of incidence.

Reflectance ratios were translated to reflectances by adopting a standard for the reflectance of the MgO reference, which was smoked to a thickness of 1/8 inch. Figure 8 shows some of the available data for the reflectance of MgO, with an indication of the reflectance adopted for the interpretation of the results in this report.

Because the response of the sphere is sensitive to the geometrical nature of the reflection [i.e., to $r_{\mu, \phi, \epsilon}$], additional partial corrections are necessary when the geometrical distribution of this reflectance differs in the reference and in the sample. Neglecting the holes in the sphere and the absorption by the detector, the response of the detector to irradiation by flux W of the presumably diffuse reference is

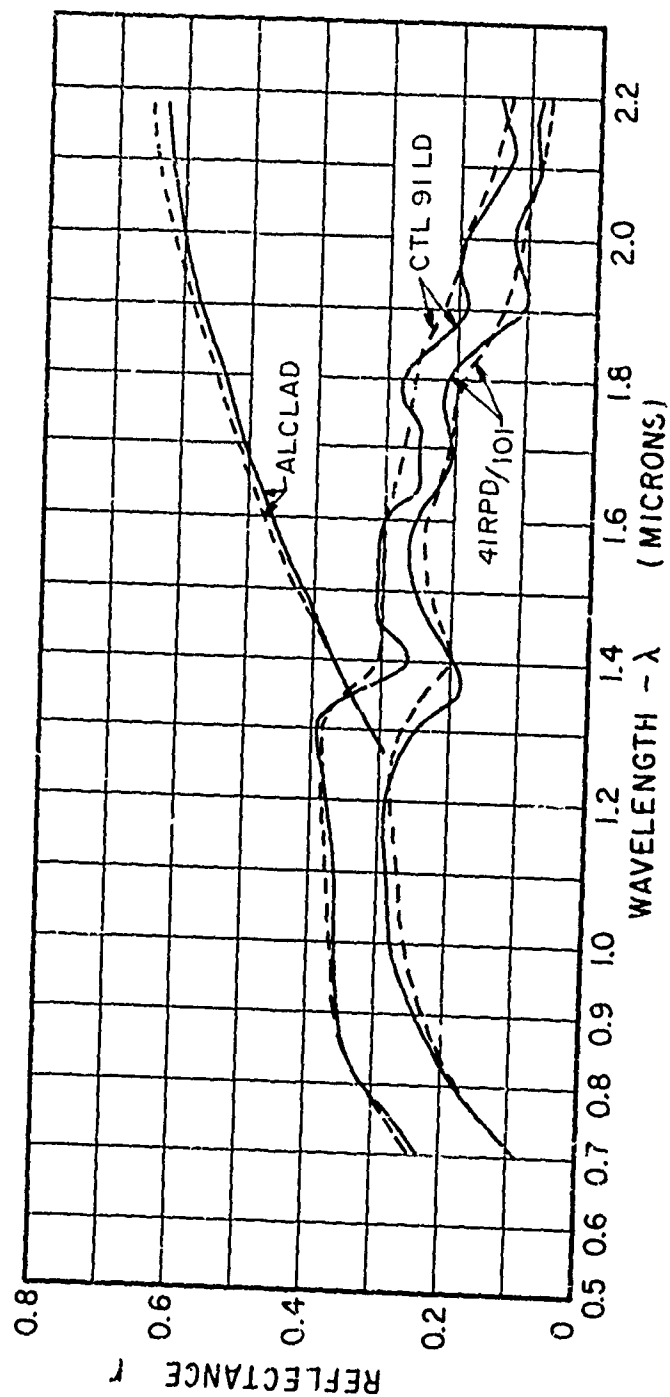


Figure 7. - Comparison of data taken in Beckman DK2 with normal and reversed operation. Dashed lines, reverse operation giving r' ; solid lines normal, r .

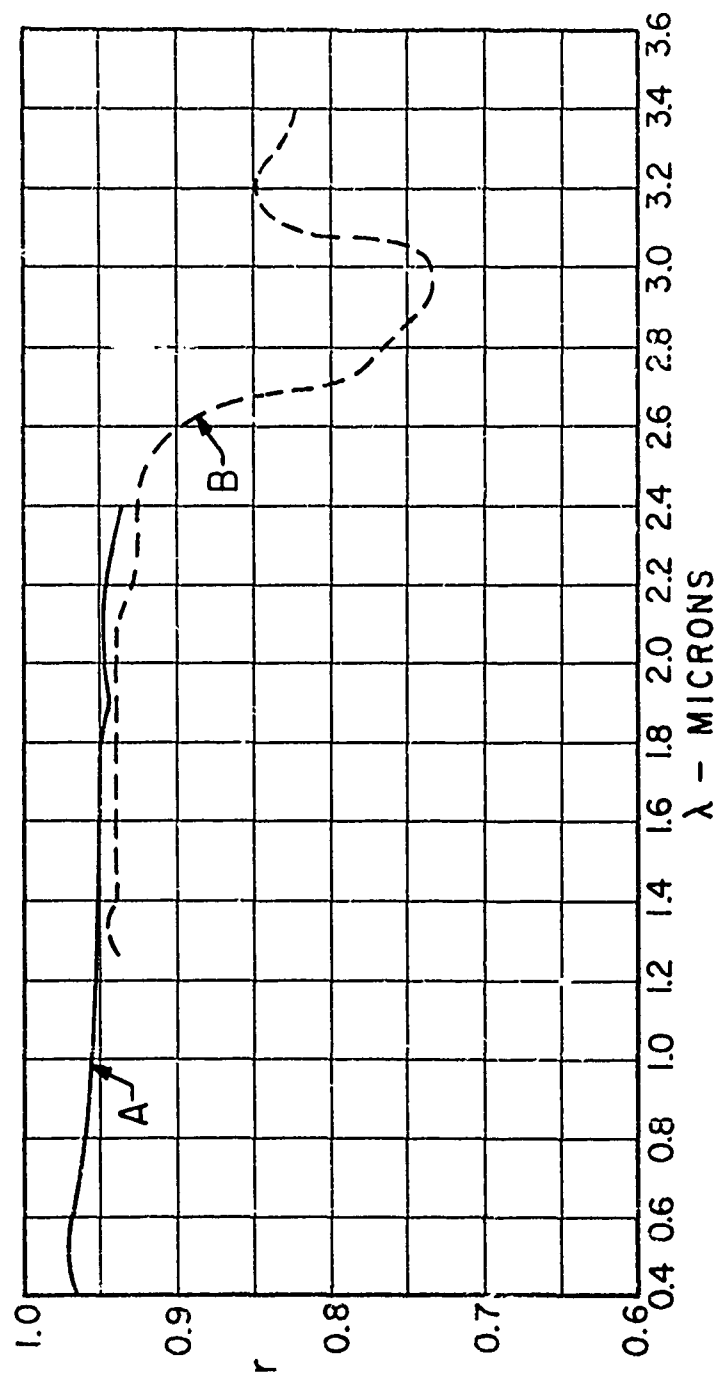


Figure 8. - Normal spectral reflectance of MgO. Curve A, National Bureau of Standards; Curve B, heated cavity reflectometer.

$$W r_s \left[\frac{1}{1-r_s} \right]$$

3.2.1

where r_s is the reflectance of the reference and r_0 is the reflectance of the presumably diffuse MgO on the sphere wall. This was approximately 1/16 inch thick, deposited electrostatically by the method of Waldron and Tellex⁽⁴⁾. Here the factor $\left[\frac{1}{1-r_s} \right]$ will be altered if the openings in the sphere are accounted for [see Jacquez⁽⁵⁾] and the equivalent factor can be evaluated on the assumption of diffuse reflection in all reflections. When so determined, this factor is often called the sphere efficacy. For a diffuse sample, the irradiation of the detector, appraised as above, will be proportional to

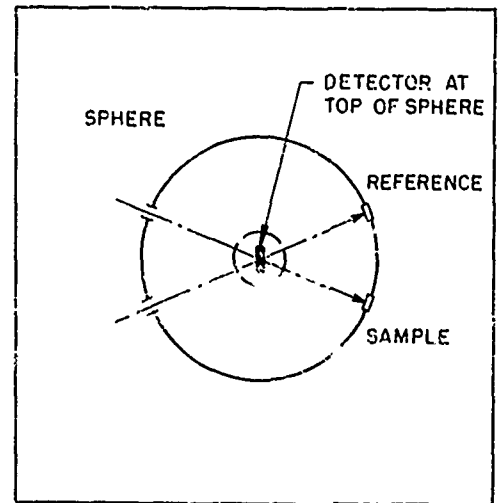


Figure 9.-Beckman DK2 Sphere

$$W r_s \left[\frac{1}{1-r_s} \right]$$

3.2.2

and then the ratio of the detector readings will be r_s/r_0 .

If, however, the sample is not a diffuse reflector, the response is altered in a way that is in part clarified by the limiting case of a specular reflector. Then none of the first reflection falls on the detector but all is incident on the sphere wall (actually in the region between the two inlet ports). There it is diffusely reflected and from there on the action of the sphere is as though this energy had been diffusely reflected originally. In this case the detector irradiation is proportional to

$$W r_s r_0 \left[\frac{1}{1-r_s} \right]$$

3.2.3

and the recorded ratio is r_s/r_0 . This is not exactly true because the energy loss through the apertures occurs on the first and later reflections from the reference, but only on the second wall reflection of the energy initially reflected from the sample. The difference is small however, and the sphere efficacy has been assumed to be the same in both cases.

Shields coated with MgO were used at the detector location in an attempt to eliminate the first reflection from the reference and thus, while reducing the over-all sphere efficacy, to produce a proportional response for both the sample and reference. While the use of these shields tended to increase the measured reflectance of highly specular samples the results were still less than known values.

Suppose now that the sample is neither specular nor diffuse but that the reflected energy is wholly in the region 0 to 30°. Then none of the first reflection impinges on the detector and the response would tend to be like that for a specular sample, except that the inlet ports occupy 4% of the sphere area within the 0 to 30° limit. Thus a substantial fraction of the reflection will be lost entirely and what remains will produce a detector response like that indicated for a specular sample. Unfortunately, not enough is known about the nature of the reflectance $\rho_{\mu, \psi, \phi}$ to permit an appraisal of this possible effect. It is clear, however, that with a truly diffuse reflector used as a reference, (and the MgO is presumably diffuse, though there is remarkably little evidence available for this) the response ratio will always be less than the reflectance of the sample.

Other sources of error are also possible in the operation of the sphere when a sample has a surface which is grooved in a given direction. It is possible to orient such a sample with respect to the detector such that a strong or weak first reflection strikes the detector. This effect was particularly noted when plastic laminated samples were run, since the fibers in these samples tended to have a preferred specular direction.

Another source of error arises in the operating technique used with the DK2 spectrometer. In setting a zero energy level by use of a shutter on the sample beam, care must be used to be sure that the shutter completely blocks the incident beam. Stops were used by the manufacturer to provide a fixed position of the shutter when zeroing, however, the stops were slightly out of position allowing approximately 3% of the energy to enter the sphere. This can result in the use of an erroneous scale expansion for the following run, and operating procedures were initiated to avoid this source of error.

The proper ratio amplification of the detector output depends considerably upon the correct phasing of mechanical breaker points which limit the duration of the signal received from the reference and sample excitation of the detector at the amplifier. The breaker points in question are subject to vibration and wear, and as a result their phasing must be subjected to frequent verification.

There must be additional effects that contribute to the uncertainty of the reflectance indicated by the Beckman system, and Figure 10 demonstrates the combination of such effects and similar ones that may exist in the sphere described in Section 3.3. Reflectance values on typical materials are presented as obtained from the Beckman unit

and from the sphere described in Section 3.3, both of which measured r_ϕ , with ϕ close to zero, and from the heated cavity, which measured r_ν , with ν close to zero.

The polished copper is a specular reflector, and the results obtained from the variable angle sphere, that is described in Section 3.3, are in good agreement with values found by Betz⁽⁶⁾, though this agreement is not shown on the Figure. The values obtained from the Beckman unit have been adjusted for the reflectance of the sphere wall. The wall reflectance was determined from an aluminum disk which was coated with magnesium oxide to about the same thickness as the Beckman sphere wall. These reflectances, deduced in this way from the indication of the Beckman reflectometer, are lower than those found from the variable angle sphere. The results from the cavity exceed slightly those from the sphere.

Lower reflectances are again indicated for the Beckman unit for the stainless steel, for which the Beckman results were also treated as though the sample were specular. Closer correspondence is obtained for the plastic Fl20, but with the boron carbide, treated as diffuse, the results for the Beckman unit are again below those of the sphere. With this poor and relatively diffuse reflector, there is no clue to the large ratio of the reflectances indicated from the two units.

The conclusion that may be drawn from the presentation of Figure 10 is one of an uncertainty in the measured reflectance which is of the order of 0.05 in the reflectance, with the DK2 results tending to be lower than the others. This must be borne in mind in considering the results where the DK2 values are given, that device being used because of its speed in accommodating the large number of samples involved.

3.3 Integrating Sphere for Variable Incidence

Reflectances r_ϕ , at variable angle of incidence ϕ , were obtained from a separate sphere which received spectral energy from the Perkin Elmer monochromator. Detection was by lead sulfide and photomultiplier detectors, and the detector output was sensed by the Perkin Elmer 107 amplifier, as used in the heated cavity system. Variable incidence was achieved by mounting the sample and the reference on a rotatable holder at the center of the sphere as indicated in Figure 11, so that various angles of incidence could be obtained. When either sample or reference was exposed, the other was contained within a housing, so that the sphere operated as a substitution sphere. The presence of the sample holder complicates the algebraic appraisal of the sphere operation, but since the holder was coated with AgO a qualitative consideration indicates that the sphere efficacy should not be much different than it would be for the same sphere without the holder.

In this sphere, with energy rate W of the sample or of the reference, with the geometric nature of the reflection from each being the same, the irradiation of the detector is proportional to

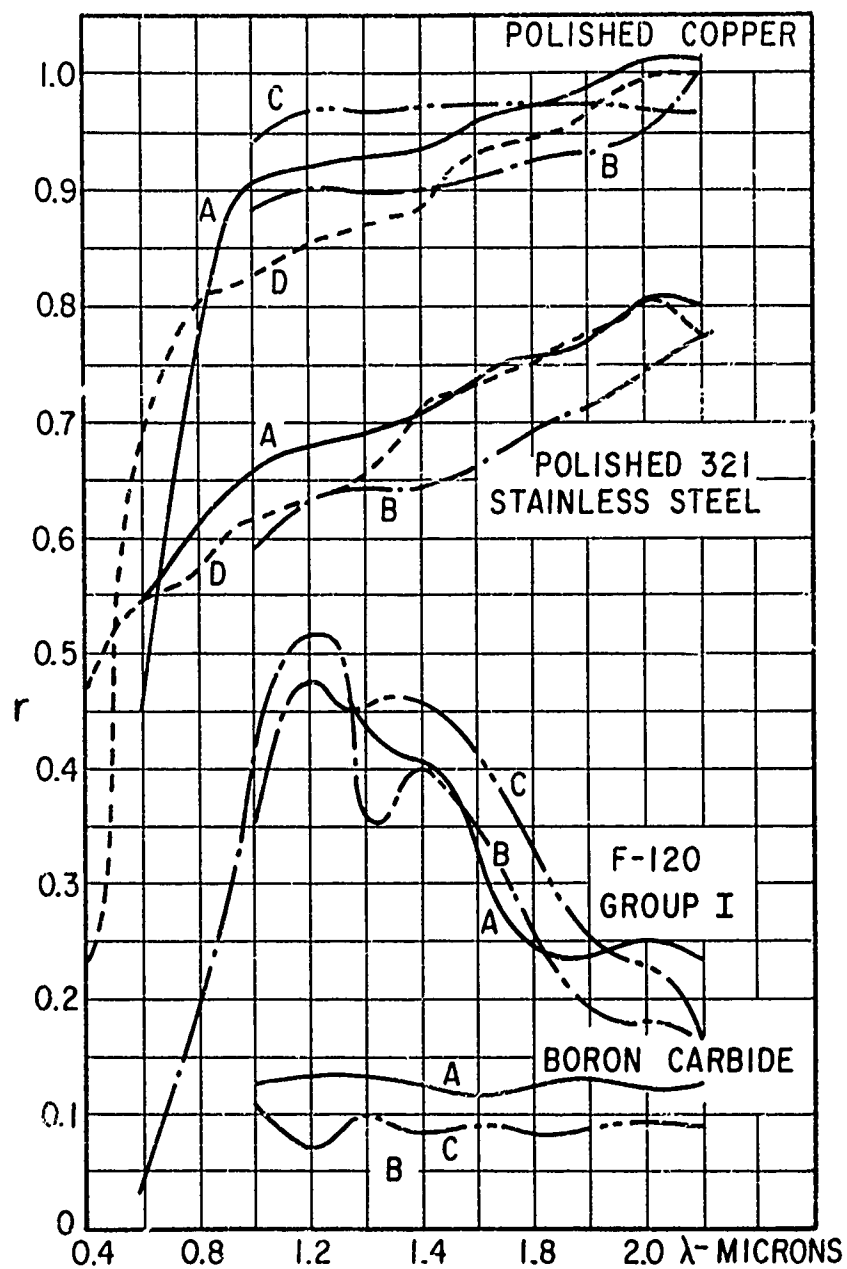


Figure 10. - Reflectance determined by different systems. Curve A, integrating sphere; Curve B, Beckman DK2; Curve C, tilting cavity; Curve D, reference No. 5.

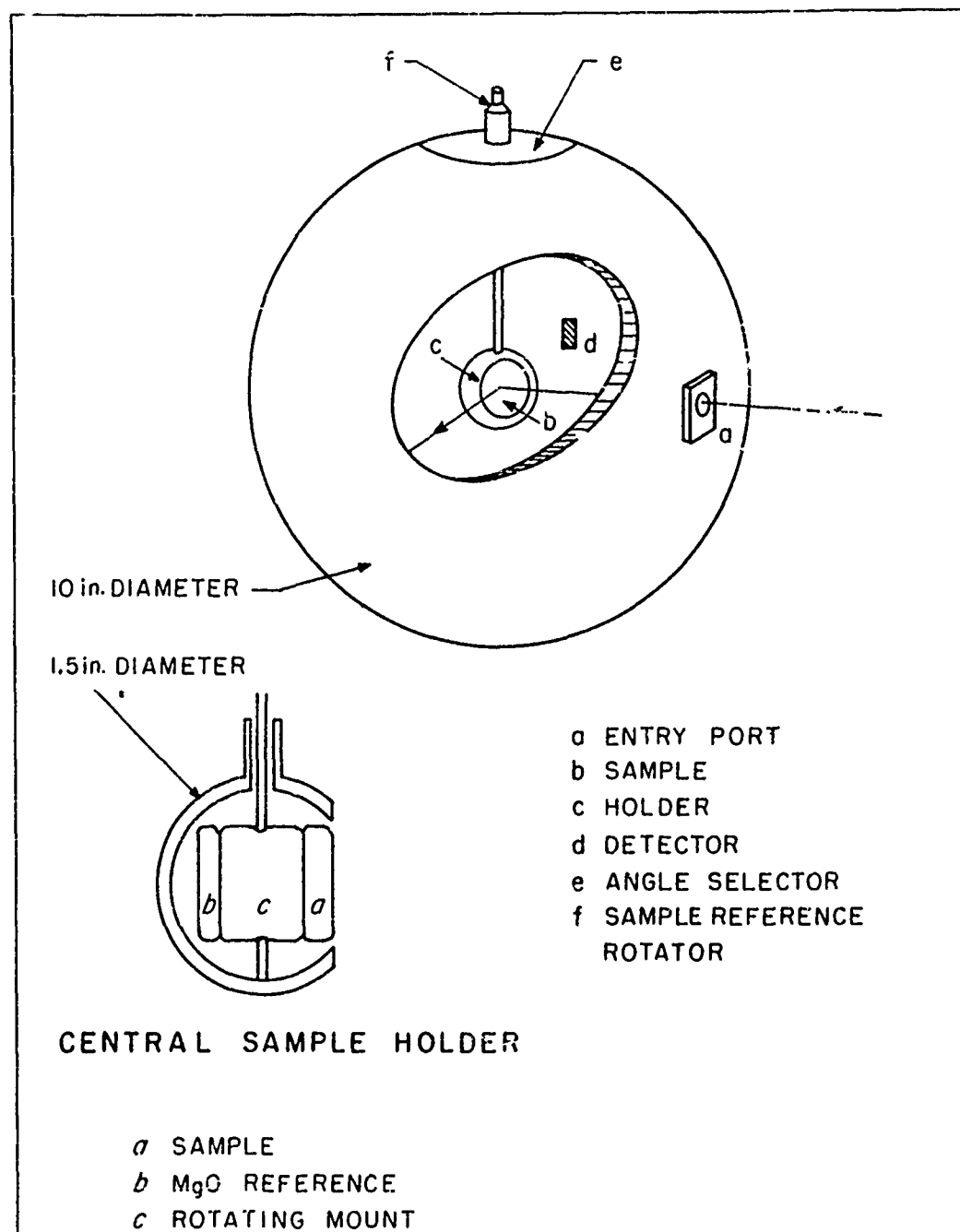


Figure 11. - Variable Angle integrating sphere.

$$W r_s r_s \left[\frac{1}{1-r_s} \right]$$

3.3.1

where r_s is the reflectance of the presumably diffuse sphere wall and r_s the reflectance of the sample. The ratio of the detector output for sample and reference is consequently the ratio of the reflectances, except for a small change in sphere efficacy when the sample and reference are interchanged, a change considered to be negligible in the interpretation of the results.

When the geometrical nature of the reflectance is not the same for the sample and for the reference then there arise difficulties best illustrated by the consideration of a specular sample. When the angle of incidence is of the order of 45° the sample holder eclipses from the detector the first reflection $W r_s r_s$, though the major part of this reflection is incident on the sphere walls and the intercepted part is reflected again to them. Thus, when the shadowing occurs the detector irradiation is

$$W r_s^2 r_s \left[\frac{1}{1-r_s} \right]$$

3.3.2

and the ratio of the response in this condition to that for the MgO reference is $r_s r_s / r_s$, where r_s is the reflectance of the sphere walls. This lower value occurs with specular samples for angles of incidence from 41 to 54° . It could be eliminated by movement of the detector to a position immediately below the sample holder, but this modification will not completely ameliorate the difficulty associated with specular reflectors. The wall coating is apparently not a sufficiently diffuse reflector to eliminate an effect due to the position of the bright spot on the sphere caused by the first reflection. As spot location changes, the irradiation of the detector from the first reflection on the sphere wall apparently changes, introducing slight additional errors which depend on the angle of incidence.

With the unit as described, reflectances r_s were obtained for $50^\circ < \phi < 80^\circ$, the latter limit imposed by the situation in which the incident energy fully covered the sample.

4.0 TOTAL NORMAL EMITTANCE

The determination of the total normal emittance was made with samples in air, heated from the back, with sample temperatures measured with thermocouples. The radiation was detected with a calibrated radiometer, the view of which was limited by shields to a small angle factor at normal incidence. The response of the thermopile detector then gave the part of the radiation of the detector that was due to the observed sample area as

$$G_T = K(V_1 - V_2)$$

Here K is the instrument constant as determined by calibration, V_1 the voltage output of the thermopile when observing the sample, V_2 the thermopile output when observing a black shield at the temperature of the shields and surroundings.

The irradiation of the receiver strip by the sample is

$$F_{ds} \epsilon_T \sigma T_s^4$$

where F_{ds} is the shape factor of the sample area with respect to the radiometer strip. The emittance ϵ_T is consequently determined as

$$\epsilon_T = \frac{K(V_1 - V_2)}{F_{ds} \sigma T_s^4}$$

4.0.1

The need for a precise determination of the surface temperature establishes classes of materials for which the emittance can be determined with reasonable confidence. Good results are obtainable with metals, which are good conductors and to which thermocouple wires can be attached by welding without radical alteration of the surface. With coated metals the situation is less satisfactory, due both to difficulty in affixing the thermocouple wires and to possible thermal resistance in the coating itself.

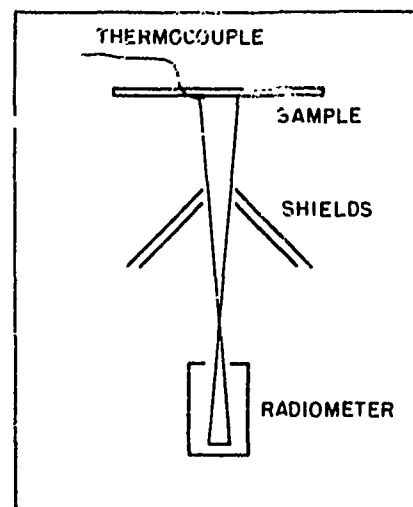


Figure 12

Finally, the technique of heating the sample from the back causes almost insurmountable difficulties with plastics, with which the temperature variation through the sample becomes enormous, in consequence of which sufficiently precise determination of the surface temperature is almost impossible. For this reason, the results for all the plastics are treated separately in Section 11.

Two back heated units were used in the present program. An electric furnace heating unit provided sample temperatures up to 1750°F and a gas heated unit provided for temperatures up to 2500°F. Both produced heating at the top of the sample, with the test surface facing downward.

4.1 Electrically Heated Unit

The electrically heated unit consists of a small electric furnace, 6" x 6" x 14" interior dimensions, mounted with the furnace door removed and open side downward. A hinged sample holding door holds 6" x 6" samples against the furnace opening. The 30" height between the furnace bottom and the floor is screened but not sealed to prevent drafts. A swinging door on one side enables the introduction of the radiometer and shield assembly on tracks provided for it. Radiometer reference readings are taken outside the enclosure and the radiometer is placed under the furnace only for the brief reading period.

The radiometer shields are made of aluminum sheets painted black on the inside. They are conical in shape with cone opening angle of 45° and an opening provided at the top of the cone to produce the desired shape factor. For the electric stand two sets of cones were used to provide shape factors which would limit the total energy to a desired maximum value over the full range of temperatures. For operation from 300° to 1200°F the shape factor used was 0.00776 and for 1200°F to 1700°F the shape factor was 0.00308. In low and high temperature operation, the area sighted was 2-7/8" and 2" respectively, with the top of the conical shields 2-5/8" from the sample with the shields of large angle factor and 3-5/8" from the sample with the shields giving a low factor.

The maximum sample temperature is limited by the emissivity of the sample and the maximum allowable furnace temperature, the latter being of the order of 2000°F.

4.2 Gas Heated Unit

A gas heated unit, actually intended initially as a prototype for a refined unit which ultimately was not built, was used for sample heating with hot gas from an oxyacetylene flame produced by a multiport burner. The burner used was a Victor 12ML heating torch head. Convection heating of this type enables the attainment of somewhat higher temperatures, but involves difficulties in the spatial variation of the heat transfer coefficient, very high gas temperatures near the sample, and hot gas disposal. Because of the latter and the crude form of the

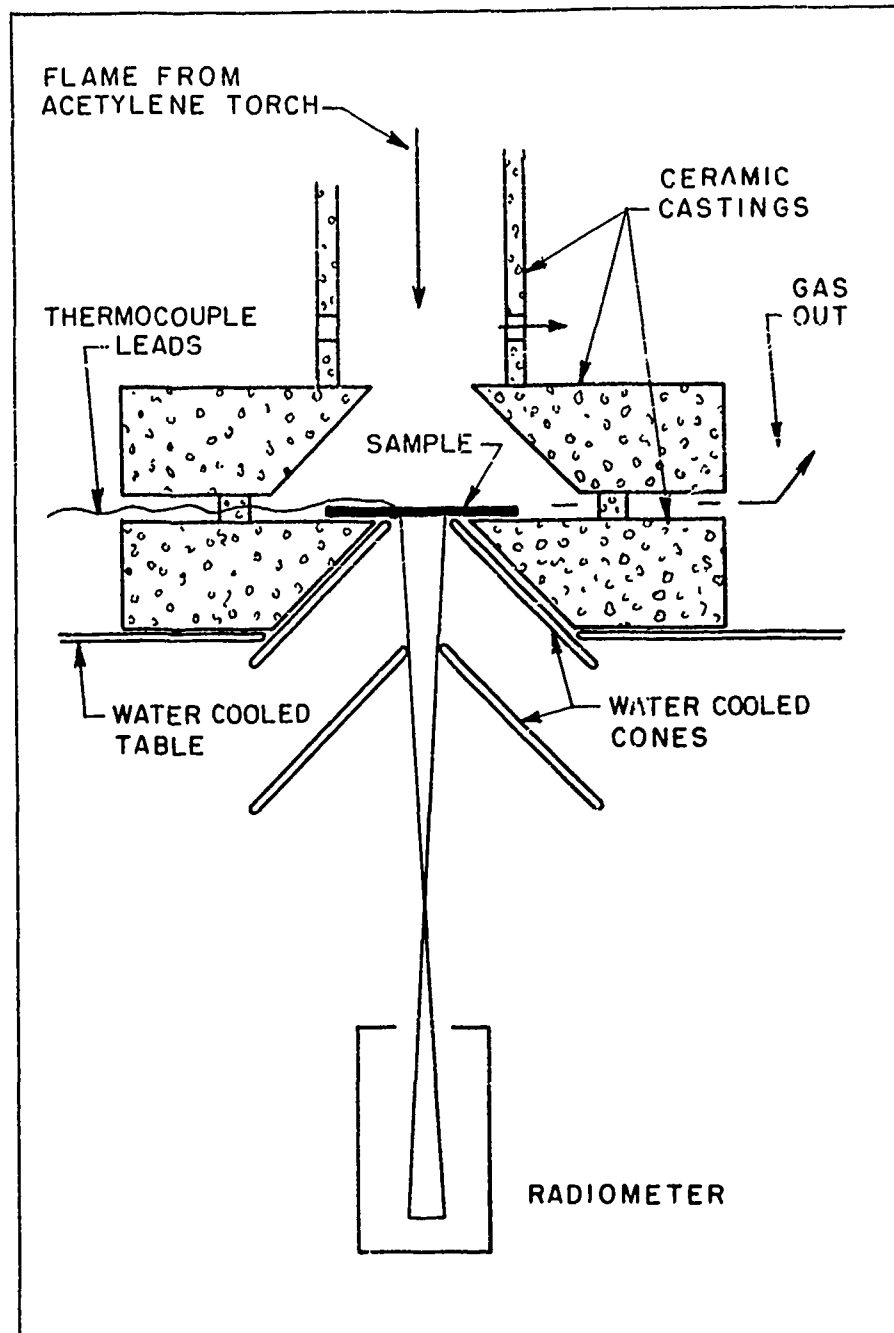


Figure 13. - Gas fired emittance stand.

apparatus, operation was in an outdoor location.

Figure 13 shows schematically the nature of the unit. The sample lays upon a formed cylinder of castable ceramic, (Norton Alundum 33I), which in turn is supported by a water cooled table. The hot gas from the torch is confined by surrounding ceramic sections and exhausts around the edge of the cylinder just above the location of the sample. Thus the hot gas circulation is exclusively produced by the aspirating affect of the burner itself; in general this was insufficient to avoid the effect of wind pressure in changing slightly the direction and magnitude of the total gas flow rate. Despite the use of shields around the unit, small but significant changes of sample temperature occurred in the presence of slight gusts of wind.

Exceptionally uniform distributions of sample temperature were realized at temperatures below 2500°F. Observation of the sample face with an optical pyrometer indicated uniformity to within 5°F, even with metallic samples as thin as 0.013 inches, in which substantial equalization of temperatures by conduction effects would not be expected.

Shields were placed below the sample to eliminate spurious radiation and reflection from the supporting ceramic, and to define the shape factor for the radiometer. These were usually placed so that the shape factor was 0.000609 and the sample area viewed by the radiometer was a circle 1-3/4" in diameter. An alignment bar registering on the two shields was used to locate the radiometer. The bottom shield defined the shape factor, and the primary function of the top shield was the elimination of any direct radiation to the inside of the bottom shield and from the sides of the ceramic holder to the sample itself. The effectiveness of this latter protection depended on the closeness of the top shield to the sample; this was subject to variation from the design specification by deformation of the sample during heating. The gap from the top shield to the sample was of the order 1/8 to 1/4 inches, producing a shape factor from sample to gap of 0.06, with a consequent maximum error of $F(1-\epsilon_r)/\epsilon_r$ in the observed emittance. Since the emittance of the materials was large, this error was not of great consequence.

The shields are water cooled, with inlet near the top ring and outlet below. Some details are apparent in Figure 13.

4.3 Radiometer

Measurements were made with total directional radiometers of the Gier-Dunkle type, described by Gier⁽⁷⁾, calibrated against cavities at temperatures of about 1200°F and 700°F, and with a check on a standard sample at 300°F. The standard sample used was a surface grooved brass plate, painted on the viewed surface with a diffuse black paint resulting in a plate emittance of 0.97 at 300°F. These determinations, made at various angle factors, were reduced to a radiometer constant

$K = W_T / \Delta V$, which was generally consistent to 1.5%. These

radiometers, while affording direct impingement of the radiation on the receiver strip, suffer from an inherently large shape factor to the surroundings of 0.0352, which is necessary because of the length of the receiver strip itself. Thus, in operation, the receiver strip sees much area external to the radiometer itself, and careful shielding is required. However, the possibility of stray irradiation is still large, and for high temperature applications a focussing instrument is in many ways an advantage. The forte of the type of instrument used is in its high response in the low temperature range.

4.4 Thermocouple Installation

The crucial element in emittance measurement is the determination of the surface temperature, and here a major problem is the relation of the detector indication to the average temperature of the area viewed by the radiometer. With metallic samples, thermocouples were welded to the surface, each wire separately. For temperatures below 2000°F, 30 gage chromel-alumel couples were used, with duplex asbestos and glass insulation. Details of the thermocouple attachment are shown in Figure 14. The part of the viewed area actually covered by wire was less than 0.2% of the total viewed by the radiometer in the electrically heated stand.

At the higher temperatures associated with operation in the gas fired unit, 30 gage platinum-platinum-10% rhodium thermocouples were used. These were welded to metallic samples and were held near the viewed surface. With this technique approximately 0.3% of the viewed area was occupied by wire or cement. Reference junctions were located away from the heated area, with chromel-alumel couples used to establish the reference junction temperatures.

An alternative scheme involved bringing the bare wires from the viewed surface through a hole in the sample plate, 1/4 inch from the point of their attachment, then along the back of the sample, protecting them there with Norton 1139 alundum cement and using the cement around the hole in an attempt to prevent thermocouple shorting. The effectiveness of the latter procedure was not conclusive and the entire arrangement was short lived,

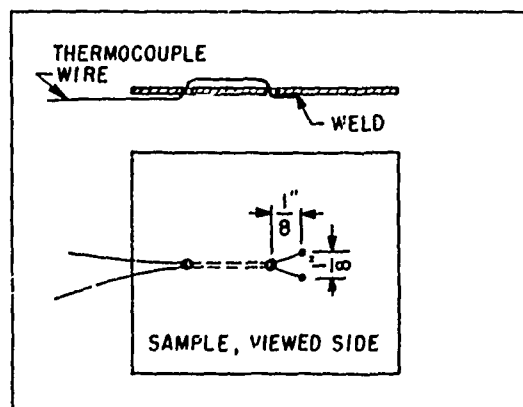


Figure 14.

for the cement, projecting into the hot gas stream, was soon ablated by it. When the thermocouple wire was exposed it immediately melted. One test, made with a dual installation of couples, with leads passing out the front and the back, indicated a 10 to 25°F excess temperature for the couple passing out the back of the sample. If this difference is appraised as solely due to the nature of the thermocouple installation, assuming no shorts in the leads passing through the plate and out the back, it indicates a $\pm 5\%$ uncertainty in the measured emittance.

Temperatures were obtained from the thermocouple response by means of the standard Leeds and Northrup calibration tables so that inaccuracy in the calibration is absorbed as an error into the emittance determination. Aging of the wires, involving a change in calibration with time of use is a factor in this regard, and the table presents some typical results where the standard is a platinum-platinum-10% rhodium thermocouple having a Bureau of Standards calibration.

Calibration Errors in Typical Thermocouple
Installations after 4 Hours at 1900°F

<u>Thermocouple</u>	<u>Indication is low by °F</u>
Chromel-Alumel	
welded junction	13
welded to tab of Inconel	4
Platinum-Platinum-10% Rhodium	
welded junction	7
welded to tab of Inconel	5

The thermocouple response decreases with age so that the apparent temperature is below the true value. Differences of the type shown in the table would lead to errors of 2-1/2% in the emittance at 2000°F.

Thermocouples could not be attached securely to the plastic samples and the technique employed for them is indicated in Section 11.1. Certain of the metallic samples (coated Molybdenum) did not permit attachment of the thermocouples by welding. Welds, if made, would deteriorate; separation of the wires ultimately occurred because of poor weldability or because of oxidation of the base metal. As an alternate, pressure type thermocouples were applied, being made of 20 gage chromel-alumel wires sharpened to conical tips having a cone opening angle of 17° with a tip .007" in diameter. Analytical estimates indicate that the temperature of the contact area should be near that of

the surface provided that there is negligible thermal resistance at that interface. But electrical continuity is achievable while a substantial thermal contact resistance may remain. Thus, the temperature indicated will increase as the force on the thermocouple prongs is increased, which reduces the thermal resistance. When the technique was used with an Inconel sample at 1500°F, the prong thermocouple indicated a temperature 40°F less than did the welded couple. With Cb coated with Al-Cr-Si at 1000°F, the difference was 230°F, due apparently to the different coating that existed on the surface of the material. The prong thermocouple as applied in this instance was not viewed with confidence, and total emittance results are not quoted for the Cb coated with Al-Cr-Si, Cb coated with Al-Si, and the PFR5 samples, except partially where the welded thermocouple appeared to give reasonable results.

5.0 SPECTRAL EMITTANCE

Measurements of normal spectral emittance were made with a system composed of a heated cavity, a small electric furnace for heating the sample, and the optics necessary to focus energy from the sample and from the cavity onto the inlet slits of the monochromator. This device was put into operation late in the program and the results obtained from it are limited. Thus, they are regarded as preliminary and are given in this section to demonstrate their nature rather than being included in Section 13 with the other final results.

Figure 15 illustrates schematically the nature of the device, by which energy alternately from the cavity and from the sample could enter the monochromator system through the diaphragm and the chopper. The general operation of this unit is similar to the tilting cavity of the reflectance system except that the tilting mirror supplants the movement of the cavity and sample that would be needed to place them alternately in the line of sight. This relative simplification of the mechanical elements of the system is at the expense of great sensitivity to the alignment of the tilting mirror. The tilting mirror must effect coincidence of the positions of the two images on the monochromator inlet slits, such that the optical paths within the monochromator are identical. At the present time it is not completely clear that the mechanical advantage of the tilting mirror system over one involving mechanical exchange of cavity and sample position is a sufficient one when it is compared to the disadvantage of the difficulty of optical alignment. This alignment is made more difficult because the off axis spherical mirror produces focal lines at the diaphragm location to make imaging difficult. After the beam leaves the chopper it is focused on the inlet slits of the monochromator by a set of mirrors which improve the situation and give a definite focus at the inlet slits.

In operation, with energy arising at the cavity ultimately reaching the thermocouple detector, the amplified and rectified detector output is:

$$S_R = K [E_R - E_c]$$

where E_R is the monochromatic emissive power of the cavity, E_c that due to the temperature of the chopper, and the constant K depends on path absorption, slit width, optical gain of the system and electrical gain of the amplifier. When the sight is on the sample, with the same mechanical and electrical settings on the monochromator, the response is:

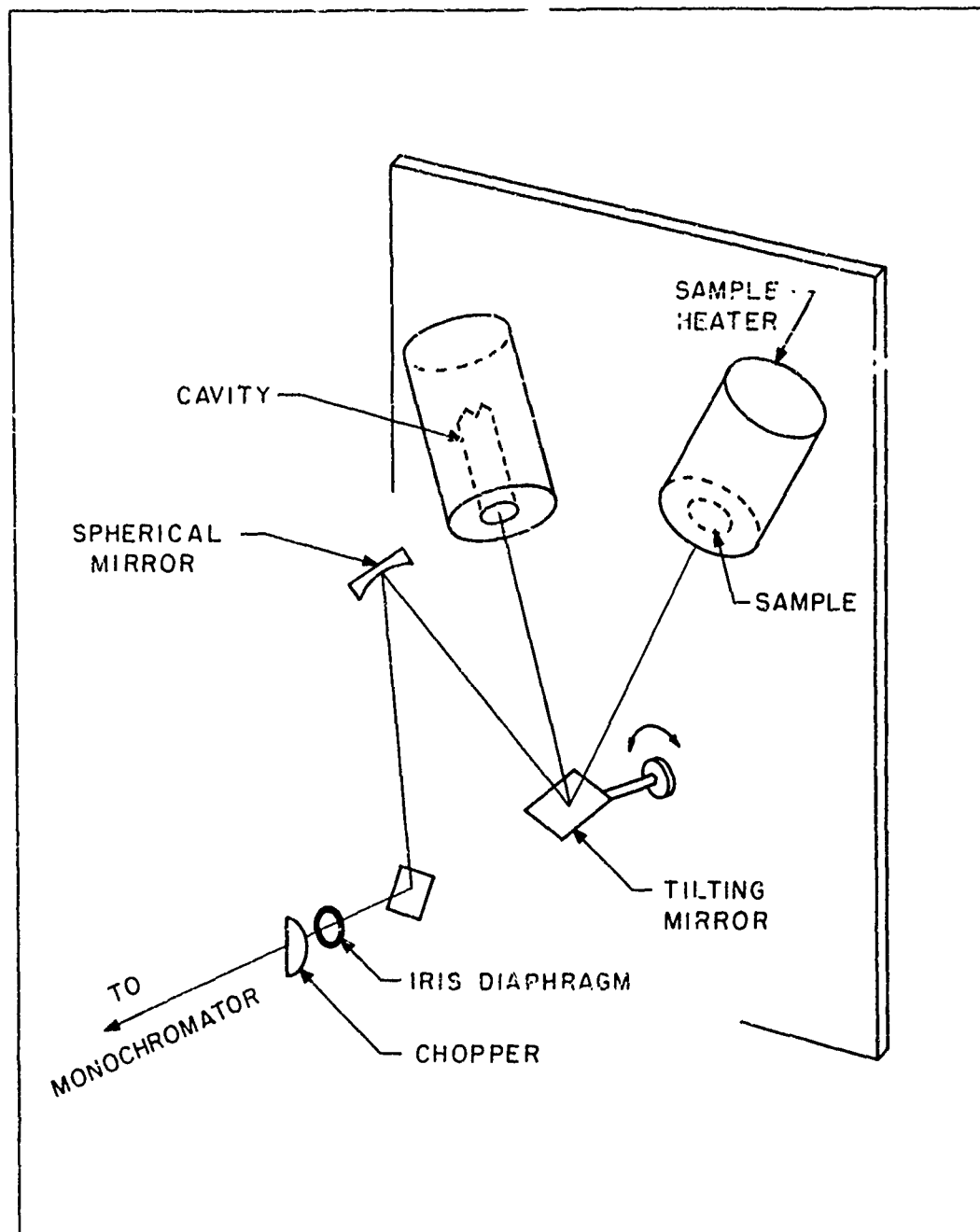


Figure 15. - Spectral emittance stand

$$S_s = K[\epsilon E_s + r_s G_\infty - E_c]$$

5.0.2

Now the irradiation, G_∞ , of the sample from the surroundings is substantially from regions at temperature T_∞ , so that with small error, G_∞ can be set equal to E_c , to give for the ratio of the response magnitudes:

$$S_s / S_R = \epsilon \frac{E_s - E_c}{E_R - E_c} \quad 5.0.3$$

In operation, the temperatures of the cavity, T_R , and of the sample, T_s , are set close together but they must still be known with good accuracy. This latter requirement is easily visualized by considering a situation in which there actually exists an error ΔT in the sample temperature. We obtain from Equation 5.0.3

$$\frac{\Delta \epsilon}{\epsilon} = \frac{-\Delta E_s}{E_s - E_c}$$

and for short wavelengths this gives approximately:

$$\frac{\Delta \epsilon}{\epsilon} \approx - \frac{C_2}{\lambda} \frac{\Delta T_s}{T_s^2}$$

This error is large at short wavelengths and it diminishes as the wavelength increases. Typically, at 1340°F, an error of 20°F in the sample temperature produces an error, $\Delta \epsilon / \epsilon$ of 16% at 1 micron, 5% at 3 microns, and 1.6% at 10 microns. When the spectral emittance values are integrated to obtain the total emittance an error of 4.5% will exist in the result due to the varying error with wavelength. In a total emittance measurement made at the same temperature as is used for the spectral, and with the same temperature measurement error, the error in the result would also be 4.5%.

It is the error in the measurement of surface temperature, which cannot be appraised easily, that introduces the major error into the spectral emittance results.

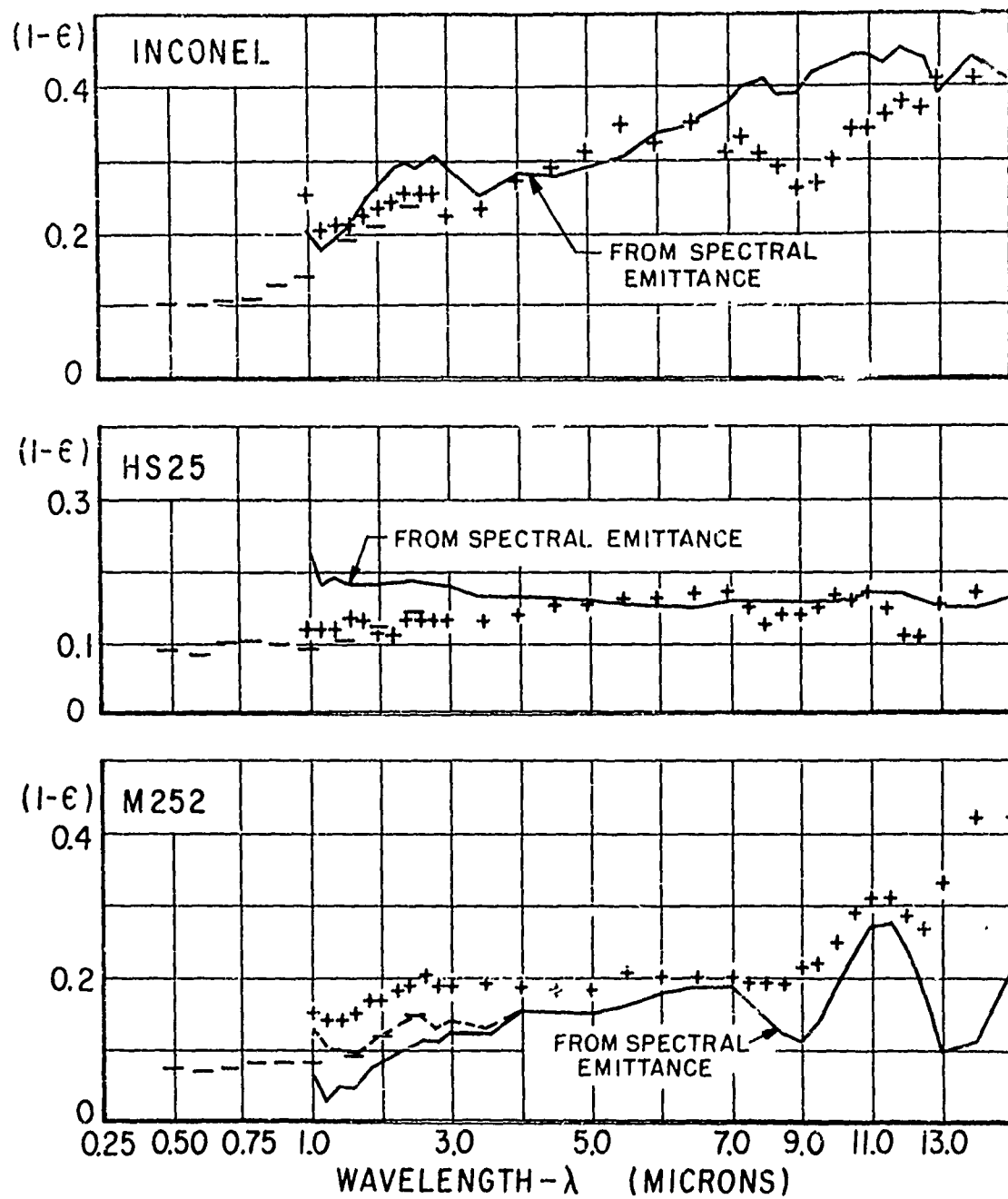


Figure 16. - Spectral emittance results.

Figure 16 shows some of the initial values obtained in the range 1 to 15 microns. The measured emittances are shown as $(1-\epsilon)$, so that they can be compared directly with the results for the spectral reflectance. Since the emittances were obtained with sample temperatures of the order of 1400°F, they ought to be compared to reflectances measured at similar temperatures. Figure 16 shows, however, reflectances measured with a cold sample, as representative of values of greatest assurance, with the realization that the reflectances at higher temperatures are indeed slightly different.

The emittances for Inconel correspond well with the reflectances in the range $1 < \lambda < 7$, although there are some differences in detail. From $7 < \lambda < 15$, however, the emittance values fail to reflect the minimum which occurs in the reflectance curve, so that on the reflectance scale the values differ by 50%. This may in part be due to a difference in samples, though the emittance sample, while different, had about the same thermal history as did the sample from which the reflectance was determined.

The results for HS25 show good correspondence but the agreement is tempered by the effect of difficulties in temperature measurement on this sample. Thermocouples attached to the front and the back indicated temperatures differing by 50°F, and the average of these temperatures was used as the basis of emittance evaluation. This serious difference was apparently due to poor welds and the consequent thermal resistance at the contact joint. Because of the doubt concerning the actual temperature, the differences between the results for reflectance and emittance in the region $\lambda < 5$ may be due to a small error in the temperature estimate.

For M252 there is again fair agreement between the measured emittances and the reflectance results, except at the extremes of the range of wavelengths. At low wavelengths this is doubtless due to error in the temperature measurement, and an "adjusted" curve shows the result of postulating a sample temperature 12°F higher than the measured value. This is a dramatic illustration of the sensitivity of the results at low wavelengths to errors in the temperature. But the possible 12°F deviation is really unsupportable in the case of this particular set of results, for which the indication of the thermocouples at the front and at the back of the sample differed by less than 2°F.

6.0 ROUGHNESS

In the expectation that the roughness of the surface might have an important influence on its reflectance, the roughness of the surface of most of the samples was determined by means of a Talysurf Model 3 Surface Measuring Instrument. This is a stylus device with an effective tip dimension of 2.5 microns, which by the manufacturer's specification should portray crests spaced 5 microns and more apart. Obviously, the true depth might not be reproduced due to the limited entry of the stylus, the complete dimensions of which are unknown. The response of the stylus is portrayed on a linear chart, with a horizontal reproduction of 254 microns per inch of chart and a variable vertical reproduction from 0.5 to 25 microns per inch of chart. For the samples examined, this latter ratio was commonly either 5 or 12.5. This large ratio of vertical to horizontal produces a record that exaggerates the roughness effect; this is shown in Figure 17 by a typical chart and its interpretation in which equal measures of horizontal and vertical distances are used. This transforms the irregular appearance of the record obtained from the instrument chart to an undulating curve.

No satisfactory specification has been found for the nature of the roughness. What has been done in most of the results is to specify the height of the fine structure and to indicate also the height of the greater variations in profile which occur with a much lower frequency, characterizing the latter by the linear distance between the large variations. Another specification that may be of significance is the total line length in the true coordinates, as this would indicate selectively the increase in surface area produced by the roughness. This involves a tedious calculation from the Talysurf record and was not done extensively. For the boron carbide coating, the increase of line length was only 2%, a result obvious from observation of the true profile in Figure 17. This implies, at least, that the surface area is not greatly magnified by the roughness and that any variation in the reflectance which might depend on the roughness effect would not do so through an increase in surface area alone.

Any survey of the effect of roughness on the radiation properties as they are presented in Section 13 for the various samples is limited by the uniqueness of the roughness for each sample and the lack of reflectance values for varying roughness for any particular sample. Moreover, most of the samples possessed a low reflectance due primarily to the dielectric properties of the coatings and less to the particular nature of the surfaces. Only with polished metals was there evident a pronounced effect, and within the time available for experimental work, this was observed only in the range from 0.7 to 2.7 microns. These results are not presented specifically, although they appear in part in Section 10, where the results for copper show a 10% reduction in reflectance due to a considerable increase in roughness. For bakelite, on the other hand, an increase of roughness produced no significant change from the already low reflectance of the polished material.

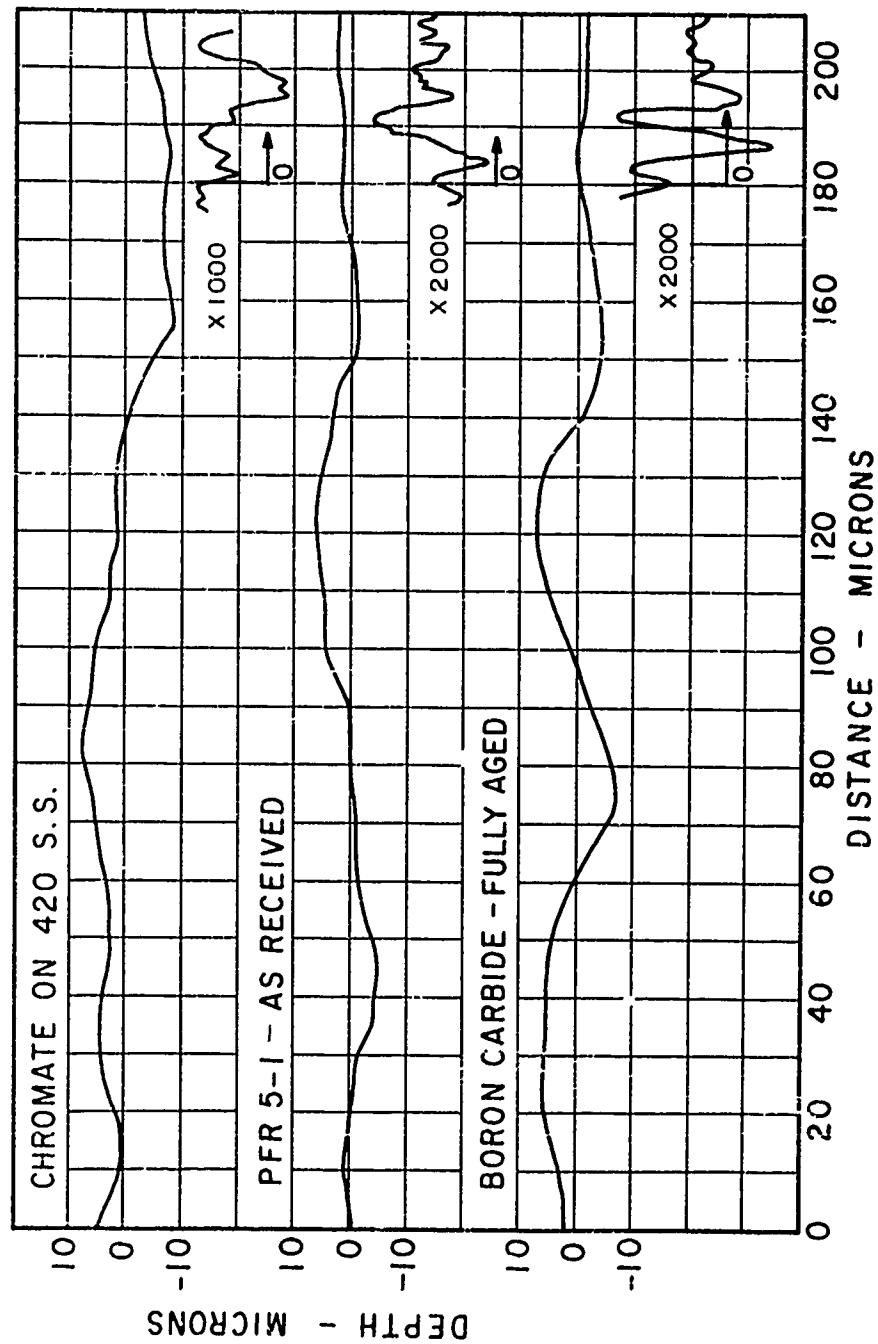


Figure 17. - Typical roughness characteristics of test materials. Inserts indicate record as presented by profilometer.

7.0 CHARACTERISTICS OF SELECTED MATERIALS

A primary objective of the research was the determination of the thermal radiation properties of a number of materials, the majority of which were furnished by WADD. Spectral and total radiation properties are involved, and it is important that these be compared, for there are uncertainties in each of the individual measurements which, through comparison, can be better appraised and which in aggregate can lead to a preferred evaluation of the properties of individual materials. Table I lists the materials, indicates the character of the results obtained for each, and specifies the location of the detailed results for each sample, as these are located in Section 13.

7.1 Nature of the Results

The results for each of the samples are given in a standard form; this section contains the list of the items used in that form with comments pertinent to each.

1. Material - Specification or WADD Number
2. Initial Treatment - Done after receipt of sample. Prior treatment, if specified, given in "Material" item.
3. Roughness - Talysurf indication (Section 6.0) expressed as the height of the fine structure together with a height and spacing for the longer irregularities.
4. Spectral Reflectance - These reflectances are those obtained from the heated cavity, being r_μ , Equation 2.1.6 with $\mu = 7^\circ$, for cold operation according to Equation 3.1.4 and for hot operation according to Equation 3.1.5, for the range 1 to 25 microns. In the range 0.3 to 2.5 microns the reflectance is r_ϕ , Equation 2.1.3, $\phi = 4^\circ$, as obtained from the Beckman DK2 reflectometer, with cold sample. These are distinguished by the separate line designations — r_μ , cold; — — — — r_μ , hot; r_ϕ , DK2.

The reflectances are presented graphically on an arbitrary abscissa scale which tends to give proportional weights to the reflectances when they are used for emittance calculation at high and low temperatures. Part of the data is repeated on a larger scale for 0 to 2.5 microns to aid in calculations of solar absorptance.

5. Total Normal Emittance
Measured - These are total normal emittances ϵ_T , obtained from the electrically heated stand, Section 4.1, and the gas heated stand, Section 4.2, calculated from Equation 4.0.1. The results are shown as points on a

TABLE 1 Range and Location of Results

Material	Total Emissance		Spectral Reflectance				Spectral Emissance	Results on page	Roughness
	1500 of	2000 of	DK2 .3-2.5 μ	Low T. Cavity 14-25 μ	Sphere .74-2.5 μ	Hot Cavity 14-25 μ			
<u>METALS *</u>									
1. Chromate on Mild St.	0.80	0.88	x	x		x		71	x
2. Chromate on 302 SS	0.75	0.79	x	x		x		75	x
3. Chromate on 420 SS	0.75	0.79	x	x	x	x		77	x
4. Chromate on Inconel	0.85	0.85	x	x		x		79	x
5. M252 (SS 4781)	0.78	0.80	x	x		x	x	81	x
6. HS25 (SS8178)	0.85	0.86	x	x	x	x	x	83	x
7. René 41 (SS 8080)	0.95	0.82	x	x		x		85	x
8. Nb/AlSi (Slurry dip)	0.81	0.82	x	x				87	x
9. Nb/AlCrSi (Slurry dip)	0.85	0.86	x	x				89	x
10. PFR 5-1	0.84	0.84	x	x				91	x
11. PFR 4								92	
12. CSA	0.92	0.45						93	
13. Inconel			x	x	x	x	x	95	
14. Iron Carbide	0.90	0.91	x	x	x	x		97	x
15. Alclad Solar Absorber	0.101	0.131	x ₁	x ₁	x ₁	x		99	x

MATERIAL	TOTAL ² EMITTANCE		SPECTRAL REFLECTANCE				SPECTRAL EMITTANCE	Results on page	Rough- ness
	1500 OF	2000 OF	DK2 .3 -2.5	Low T Cavity 1 -25	Sphere .7 -2.5	Hot Cavity 1 -25			
<u>PLASTICS**</u>									
16. Astrolite			x	x				101	
17. F-12C			x	x	x			103	
18. CTL 37-9X			x	x	x			105	
19. WWCNE-2 (Translucent)			x	x				107	

* NOTE: "Fully aged" data shown in Total Emittance and Spectral Reflectance columns, except where only "As Received" data was taken

1 "As Received" data - no cold Fully Aged data available.

2 "Total Emittance" values are (1 - integrated spectral reflectance values) from "Fully Aged" cold runs.

** NOTE: Only spectral reflectances of the following samples were obtained in the DK2 over the range 0.3 -2.5 . The reflectances are given on pages 61 to 66.

BV-1708S
BV-17085-W
DC-2104
DC-2104W
Epon 828
Epon 828W

Selection 5003W
Vibrin 135
Vibrin 135W
CTL 91-LD
Selection 5003

41-RSD/101
400-RPD-DG2106
HT-500
YN-25
Teflon

curve of emittance as a function of temperature. The designations are: \triangleright , rising temperature; \triangleleft , decreasing temperature; both from the electrically heated unit and \odot , gas heating.

Predicted - Normal total emittances, ϵ_T , have been predicted from the measured spectral reflectances, r_ν , from the heated cavity results for $1 < \lambda < 25$ and r_ϕ from the Beckman results for $\lambda < 1$ micron. As indicated in Section 2.2, the use of r_ν in this sense is correct while the use of r_ϕ presumes that $r_\nu = r_\phi$. More important is the implication contained in Section 3.3 that the Beckman results may give reflectances that are a little too low, but in the total emittance calculations those values are used only for $\lambda < 1$ and there is little energy in this region for $T < 3000^\circ\text{F}$. Finally, for poor reflectors, the error in the emittance, $(1-r)$, is not very great. Spectral reflectances chosen in this way were then integrated to obtain the total emittance:

$$\epsilon = \frac{1}{\sigma T^4} \int_0^\infty (1-r) E d\lambda \approx 1 - \frac{1}{\sigma T^4} \sum_{\Delta\lambda_i} \bar{r} \int_{\lambda_i}^{\lambda_i + \Delta\lambda_i} E d\lambda$$

Scales such as shown on Figure 18 were then constructed for twenty equal increments of $[\frac{1}{\sigma T^4}] \int_{\lambda_i}^{\lambda_i + \Delta\lambda_i} E d\lambda$. The average reflectance \bar{r} is an average with respect to energy, but in using an overlay such as shown on Figure 18 in connection with the plot of spectral reflectance results, averages were actually taken with respect to wavelength. Most of the subdivisions are small and the variation of reflectance in them is small, so the error is negligible. There is an error in the increment at highest wavelength, but since this encompasses at most only a twentieth of the total energy, the error is fractional here also.

The total reflectance $[\frac{1}{\sigma T^4}] \sum_{\lambda_i} \bar{r} \int_{\lambda_i}^{\lambda_i + \Delta\lambda_i} E d\lambda$ is obviously then the average of the twenty averages, $\bar{\bar{r}}$, selected for the wavelength increments of Figure 18. Emittances so obtained are shown graphically on the Figure which contains the measured values of total emittance, for both the "cold" reflectance and the reflectance measured at elevated temperature.

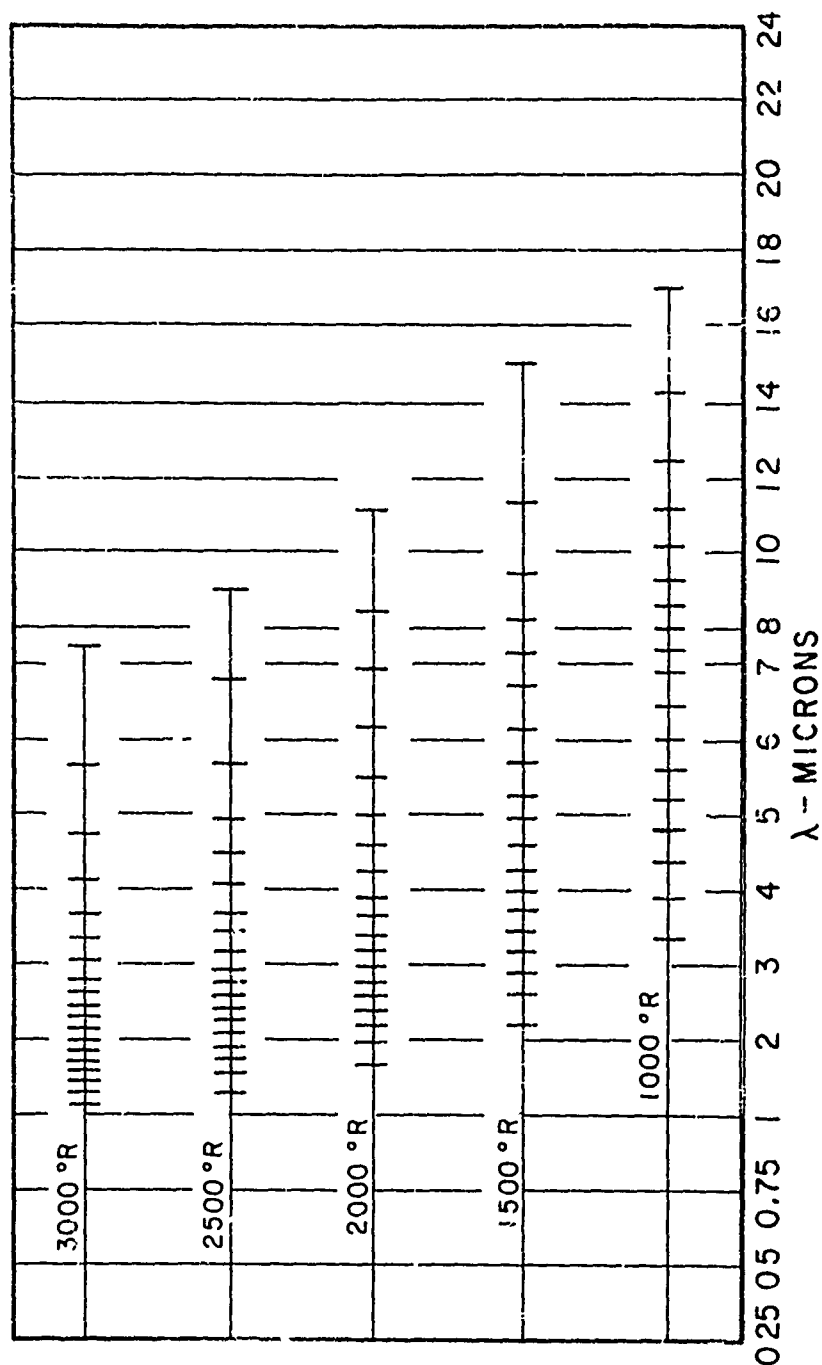


Figure 18. - Equal energy increments used in integrations for total emittances. 5% of total energy extends beyond each end limit of bands shown.

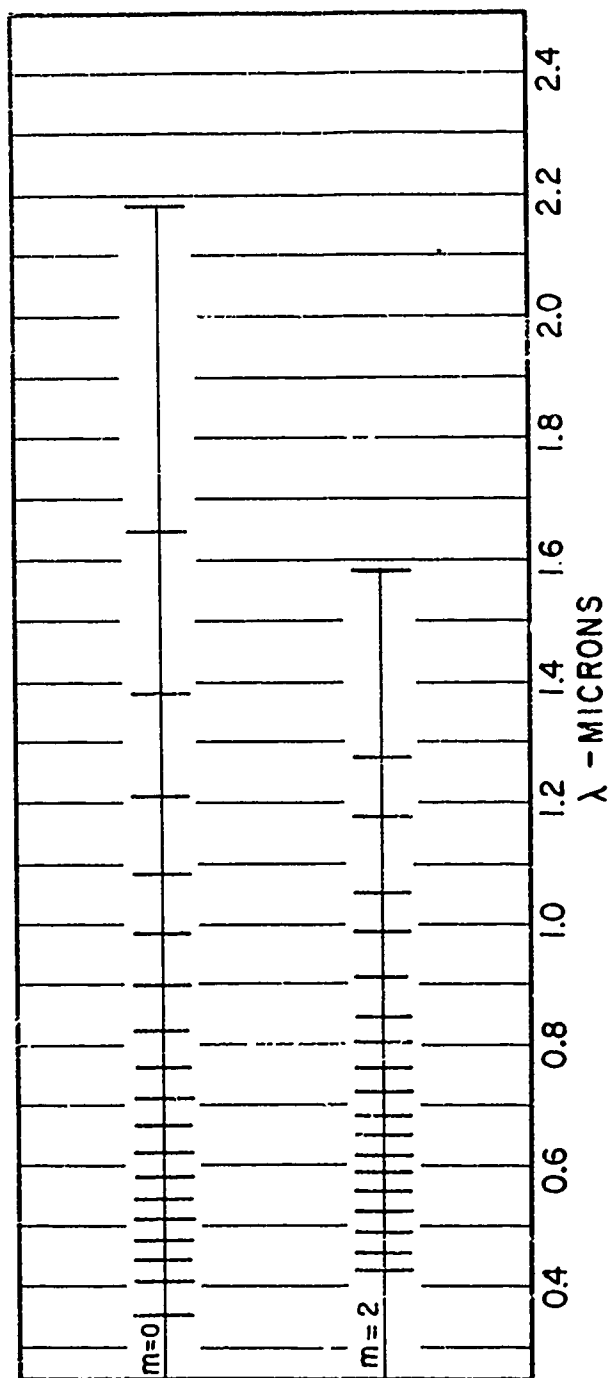


Figure 19. - Equal increments of solar energy used in integrations for solar reflectances. 5% of total energy extends beyond each end of increments shown. M^{u0} , outside earth's atmosphere; M^{-2} , sea level.

6. Solar Absorptances - For certain samples the solar absorptance has been calculated from the spectral reflectance data and the solar irradiation for zero air mass (outside the atmosphere) as given by Johnson⁽⁸⁾. The method of calculation is the same as that specified for the total emittance values and Figure 19 shows also the wavelength subdivisions used for the calculation of the absorptances. Figure 19 also contains the wavelength subdivisions for twenty equal energy increments for solar irradiation at sea level (air mass 2) as presented by Johnson.
7. Spectral Emittance - The spectral emittance system became operative so late in the program that the results so far obtained must be regarded as preliminary. For this reason, only a few results for spectral emittance are contained in Section 5, where the system is briefly described and the technique of its use is indicated.

8.0 TOTAL EMITTANCE AND THE SPECTRAL REFLECTANCE RESULTS

A primary use of the spectral reflectance results is in the prediction of the total emittance though they are obviously also essential in other applications such as the evaluation of radiant energy interchange between non-grey surfaces. It has been indicated in Section 7.1 that the reflectances measured in the cavity system should lead directly to values of the total normal emittance and that those from the integrating sphere systems should without much error be usable for such a calculation, provided that their influence is minimized by making that prediction for temperature levels less than 3000°F. Such predictions of the emittance have been made for all of the samples for which spectral reflectance results were obtained. In the present context this evaluation is of the greatest interest for those samples for which results were also obtained for the total normal emittance, since the comparison of measured and predicted values then demonstrates the degree to which the expected correspondence is obtained.

In general, the measured values of the total normal emittance exceed the predicted values. This is shown in detail in the presentation of results for each sample, and is summarized in Table 2, in which the experimental values are estimated from the trend of the results if an experimental value was not obtained for the particular temperature shown in the table. The predictions shown there are made from reflectance data obtained with a cold sample.

Table 2

<u>Material</u>	<u>Temperature °F</u>	<u>Measured</u>	<u>Predicted</u>
Rene 41	800	.79	.78
	1500	.845	.82
Boron Carbide	800	.93	.89
	1500	.96	.91
PRF5	800	.90	.84
	1500	.91	.84
Cb dipped in Al-Si	800	.83	.80
	1500	.85	.82
Inconel	800	.69	.68
	1500	.75	.73
M 252	800	.78	.77
	1500	.83	.80

The evidence shows the measured value to generally exceed the predicted one; the difference can be attributed to errors of measurement and to the possibility that the spectral reflectance at elevated temperatures differs from that which was measured at low temperatures. This latter effect does exist for metals, but its nature for non-conductors remains ambiguous and the reflectances measured at high temperature, with the air cooled sample holder, do not give definitive evidence in this regard. Those results, for a temperature of the order of 1000°F, are shown in the results section. They usually indicate a reflectance greater than that obtained with a cold sample. Emittances calculated from these reflectances would then be below the prediction of the Table to increase the disparity with the experimental results. This difference varies with the particular sample, and some of the difference between the "cold" and "hot" spectral reflectances may indeed be due to errors associated with the determination of the surface temperature, as indicated in Section 3.1. These are such as to always make the apparent reflectance greater than the true value, with a consequent prediction of lower emittance from the "hot" reflectance data. While this rationalizes the difference, no such adjustment will make the spectral reflectance results for the hot sample coincide with those of the cold sample. This is illustrated for two samples in Figure 20, which shows the "hot" and "cold" reflectance data for René 41, together with the "hot" results that would be obtained for a surface temperature 20°F in excess of that measured at the back of the sample. A similar presentation is made for the boron carbide, the temperature change in the results for the hot sample being 40°F. These increases in the temperature of the sample, above what was measured, were chosen rather arbitrarily, to bring the values of the reflectance obtained with the hot sample into closer coincidence with those reflectances obtained with the cold sample. For the boron carbide coating at least, there is reality in this appraisal. Considering the thickness of the coating, together with an arbitrarily assumed thermal conductivity of 1 Btu/hr.ft.°F, there is expected a temperature drop of 18°F through the cavity, under the operating conditions in which the hot reflectance results were obtained.

As indicated by Figure 20, the effect of temperature changes is primarily in the long wavelengths and the results at short wavelengths are almost unaltered. Thus, there remains a definite indication of some change in the reflectance as the surface temperature is increased, of such nature as to increase slightly the difference between the measured and predicted values of the emittance.

In considering the differences that exist between the predicted and the measured values of the emittance it is important to recognize that they differ only on the order of 5%, and that this difference is increased only slightly if the "hot" values of the reflectance are used in the calculations. This represents rather good agreement, especially in consideration of the possible errors that exist in the results for the total emittance and which tend to produce high values in that measurement.

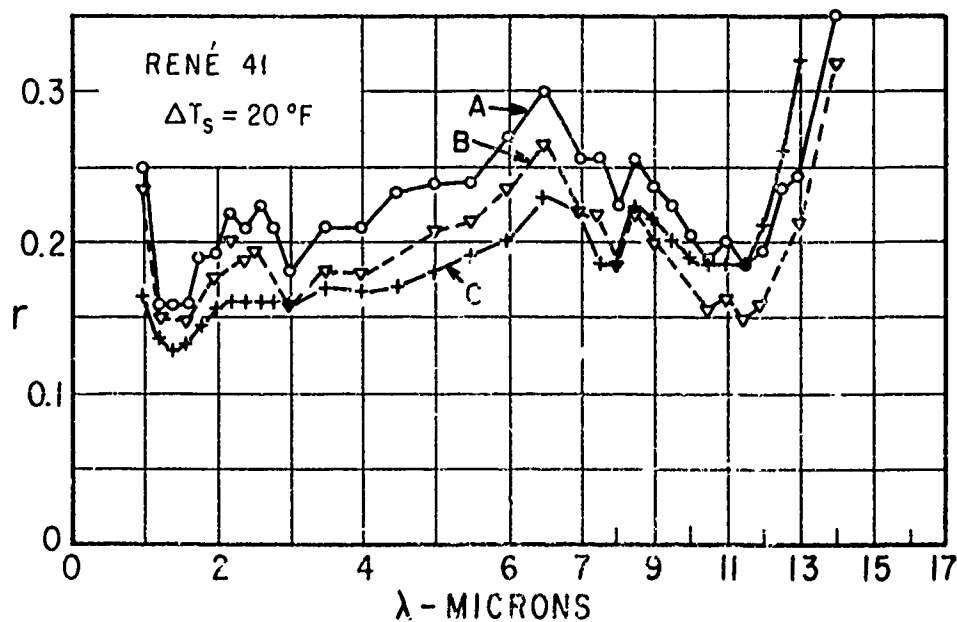
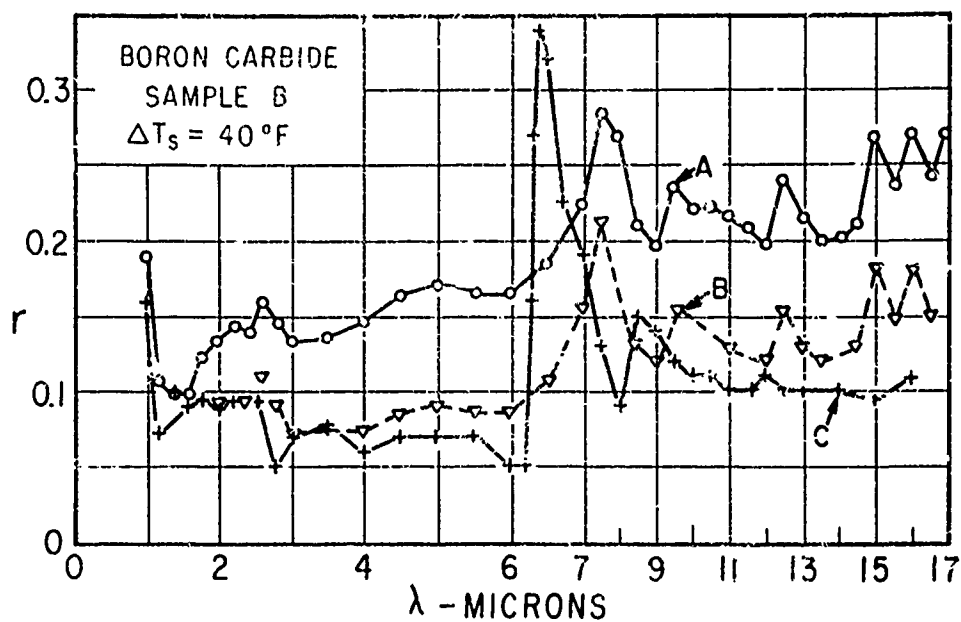


Figure 20. - Hot and cold reflectance data for two samples. Curve A, hot sample; Curve B, same as A assuming error of ΔT_s in sample temperature; Curve C, cold sample data.

The specification of the total normal emittance either from measurement or by calculation from the normal spectral reflectances leaves yet to be attained the value of the total hemispherical emittance, a value that must be found either by measurement or through knowledge of the geometrical distribution of the radiation. Direct measurements were not made in this program, they involve systems of the calorimetric type in which the total radiation leaving the sample surface in all directions is measured. Hence the total hemispherical emittance may be obtained from the present results only on the assumption that the ratio of the hemispherical to the normal emittance is practically unity. Eckert⁽²⁾ indicates this to be a fair approximation, except for specular surfaces of low emittance. Also, monochromatic results for the absorptance, given in Section 10, support such an assumption.

9.0 COMPARISON WITH OTHER RESULTS

It is significant to compare the results of this report with those of others, for similar materials, that have been obtained with differing experimental arrangements. One possible result of such a comparison is an evaluation of the effects of uncertainties in measurement and method of calculation. Comparisons, unfortunately, are themselves not absolute, for there is ample evidence of change in the surfaces of materials which experience different environmental histories and the consequent change of their radiation properties. In addition, for the materials reported on herein there exists only a meager amount of alternate data. It is significant, however, that in these cases there is a fair measure of correspondence between the results presented here and those available from other measurements.

Spectral emittance results have been presented by Harrison et.al.⁽⁹⁾ for oxidized Inconel; they reveal an insensitivity to sample temperature for $\lambda > 8$ and a pronounced temperature effect for $\lambda < 7$. Figure 21 shows these emittance results represented as reflectances, and contains also the present results for the "cold" reflectance as they are given on page 94. Fair correspondence is revealed in the region from 1 to 7 microns between the low temperature (945°F) emittance data and the reflectance data. For $\lambda > 5$, however, the NBS data is consistently lower than the measured reflectances, and the difference becomes large at $\lambda > 7$ microns. There is a suspicion that this may indicate a heavier oxide coating on the NBS specimen, but nothing definite can be said in this regard.

Total emittance values are also presented for Inconel on Figure 21, which is like that of page 95 except that additional comparative results are included. Two of these are predicted values from earlier measurements made on different samples in the heated cavity system, as reported by Etemad⁽¹⁰⁾. These show magnitude agreement with the present total emittance values because lower spectral reflectances were indicated for these samples. Values predicted from the NBS emittance data are also indicated and these differ markedly from the other predictions by their altered dependence on temperature.

Total emittance results are given by Clayton and Evans⁽¹¹⁾ for René 41, HS25, and M252 and these are compared in Figure 22 to the present results for these materials. There is a correspondence in magnitude in the results, particularly for the René 41 and for the HS25.

By taking a mean line through the results indicated by Clayton, these results exceed the present results found for the René 41 by 12% at 500°F, and are practically identical at 1700°F where, in fact, the present results show a scatter of over 5%. Only a single point is available for the HS25, at 1600°F, and this is identical to the present results at that temperature.

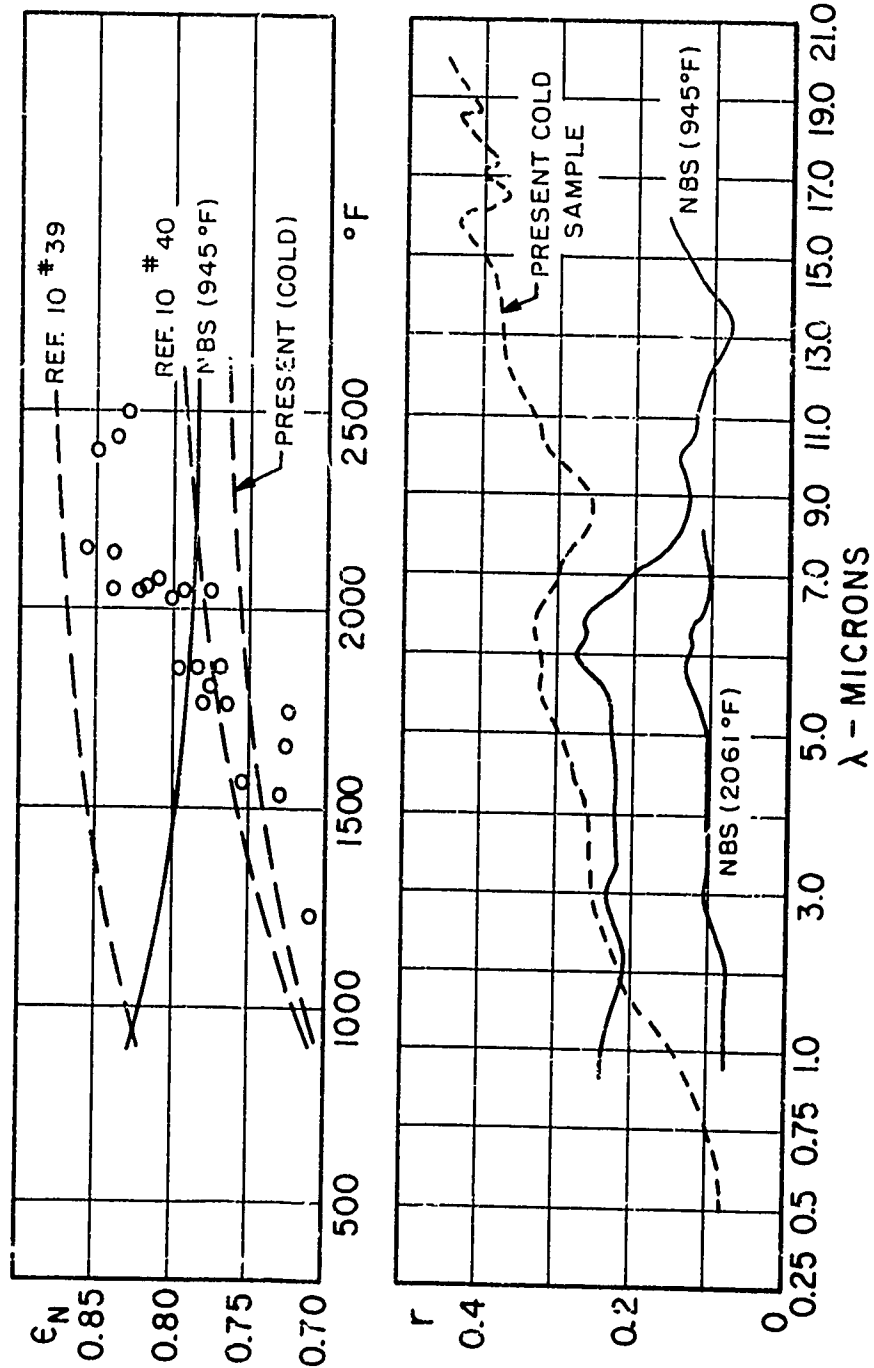


Figure 21. - Comparison of results for Inconel. Top curves show total emittance values, the circles being present measurements and prediction from the present reflectance results (page 95). The lower curve compares the present reflectance values with the NBS results.

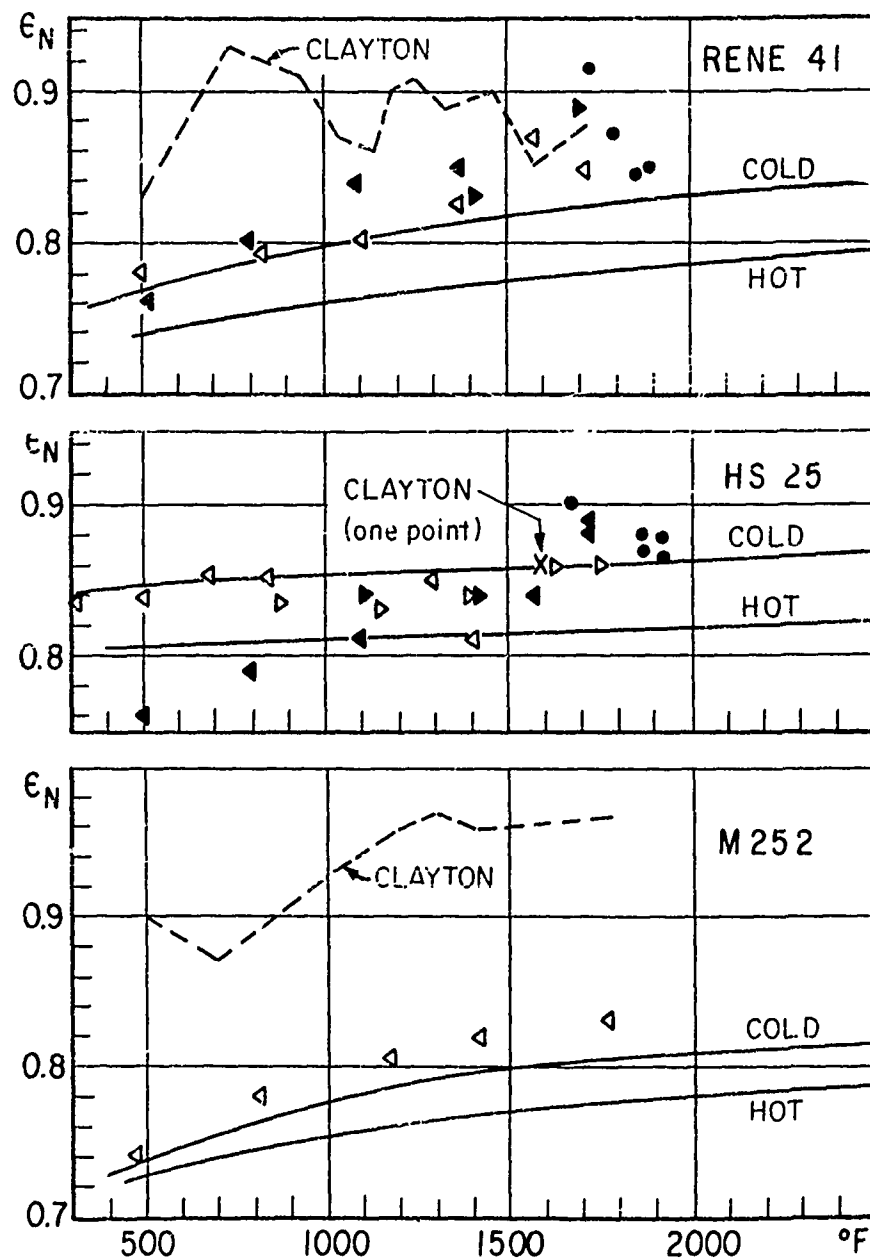


Figure 22. - Comparison of total emittance. Points are present results, solid curves integrated values from spectral reflectances. Dashed curve from Reference 11. Solid points from second sample of same material.

The greatest deviation exists in the results for M252, although there is evidence that the sample tested by Clayton was oxidized to a greater degree. The present emittances are 18% lower and confidence in their magnitude is inspired by their position, close to the prediction made from the reflectance results.

In appraising the results obtained by Clayton, it is important to note that these were obtained in reference to the emittance of a boron carbide coating, for which the emittance was assumed to be 0.98. The present results for boron carbide coatings, contained on page 97 are of interest in this connection. These reveal that while the emittance is actually of the magnitude used by Clayton, it may well be slightly less and it does indicate some variability with temperature. On this score, the results inferred with boron carbide as a reference may well be high, and this effect would be greater at the lower temperatures.

10.0 ANGULAR DEPENDENCE OF THE ABSORPTANCE

Measurements with the integrating sphere described in Section 3.3 produced values of the reflectance, r_ϕ , for varying angles, ϕ , of incident radiation. These are more useful when converted to angular absorptance $\alpha_\phi = 1 - r_\phi$; absorptance as a function of angle of incidence becomes important when point radiation sources are involved, as exemplified by the solar irradiation of a satellite or space vehicle. The angle of incidence between the sun's rays and normal to the satellite surface has a strong influence on the amount of energy it reflects and absorbs.

It is important to note again that angular absorptance is related to angular emittance only for a completely specular surface. For such a surface it would be possible, given r_ϕ , to determine the angular emittance. This relation will not hold for surfaces with both specular and diffuse reflecting characteristics; the sphere does not directly indicate the specularity of the surface.

Figure 23 presents results at 1.2 microns for polished samples which were specular, or approximately so. In the range 41° to 54° , as mentioned on Section 3.3, the sphere produced results which were multiplied by some fraction of the wall reflectance. When the first reflection was completely shielded from the detector by the sample holder, at 45° incidence, the multiplication was by the wall reflectance itself. This reflectance was determined from a sample coated with a similar thickness of MgO and the results at 45° in Figure 23 were corrected for this effect, to orient a broken line indicative of appropriate values in the region of uncertainty. Other curves show the prediction from electromagnetic theory for pure copper and for a dielectric of index of refraction equal to 2.0. The experimental curve for copper agrees with theory in magnitude, but contains variations in detail; there are secondary effects believed to be associated with the movement of the specular first reflection around the sphere wall. These gave rise to increasing reflectance from 0 to 20 degrees, and a decrease beyond 60 degree incidence. The results for smooth bakelite show the 45° dip, but all other effects are masked by the low reflectance of this material. Good correspondence is indicated with respect to the prediction for a dielectric from electromagnetic theory.

Figure 24 presents results for roughened specular reflectors. The copper sample was roughened by a grid of grooves of 45° opening angle, 0.005 inches (127 microns) deep; the surface created is an array of pyramids. The 24ST aluminum and bakelite samples were roughened with sandpaper, the scratches all running parallel. The average spacing and depth of the coarse grooves is given, as is the peak to peak depth of the fine structure, as measured with the Talysurf Profilometer; all readings follow in microns:

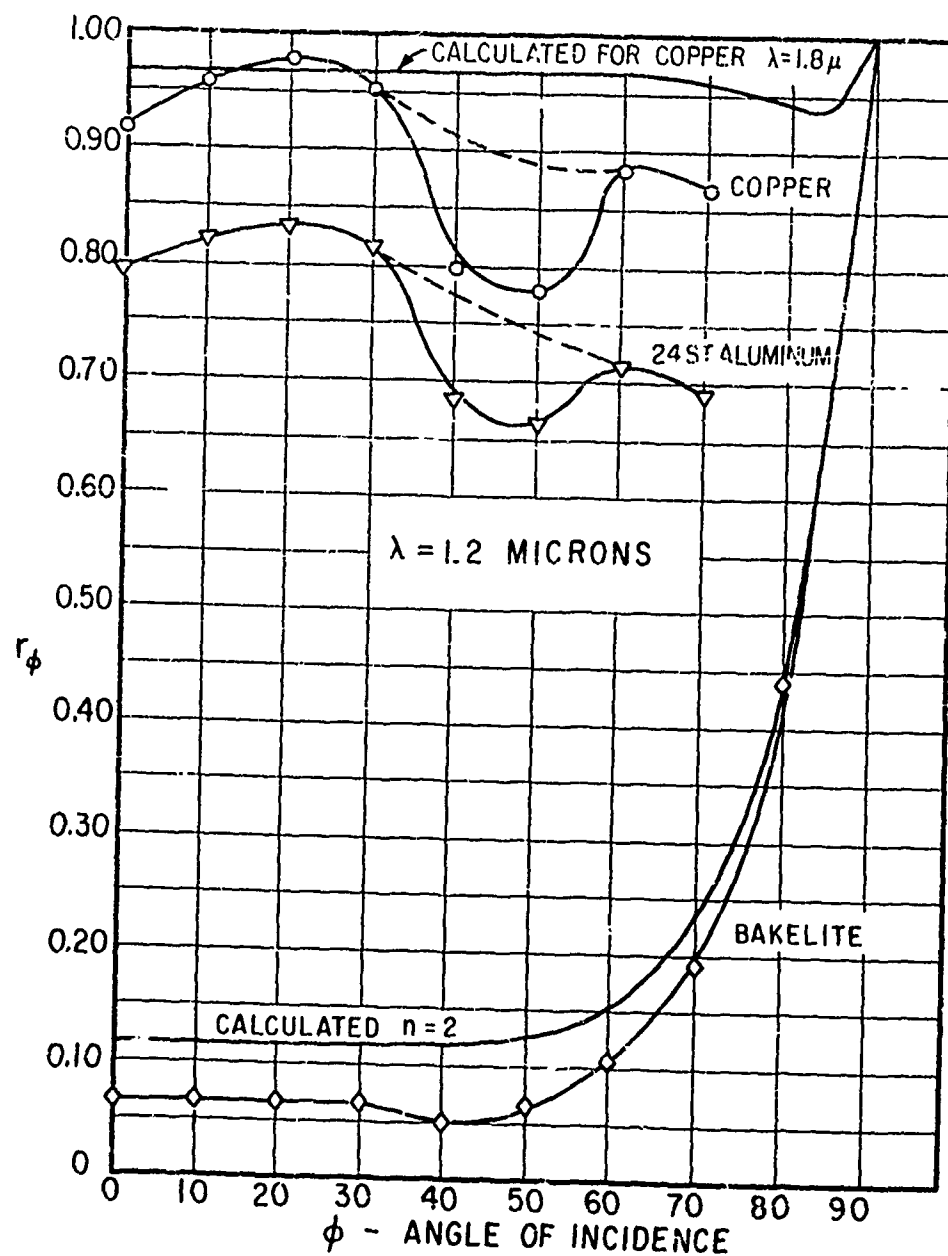


Figure 23. - Angular Reflectance of polished samples at 1.2 microns. Dashed portions show the magnitude after the correction associated with specular samples.

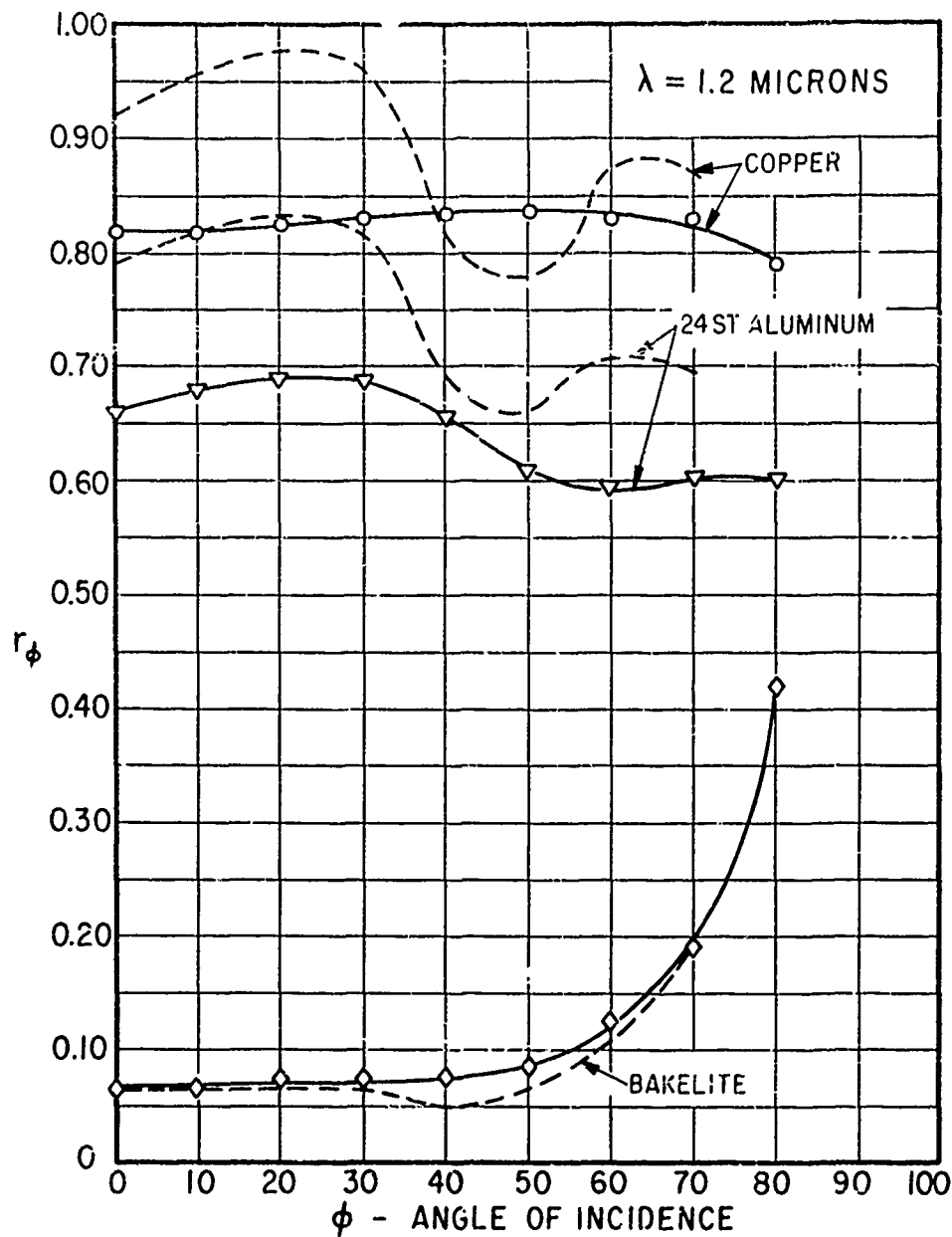


Figure 24. - Angular reflectance of roughened sample at 1.2 microns. Dotted curves are uncorrected results for polished samples of same material.

<u>Coarse Structure</u>	<u>24ST Aluminum</u>	<u>Bakelite</u>
Peak to Peak Depth	6.35	3
Spacing	34	24
<u>Fine Structure</u>		
Peak to Peak Depth	1	1

The reflectance of the copper has been reduced by the roughening and by the diffuse character of the reflection produced by the rough surface. The minimum at 45° found in the specular surface results has been eliminated. The form of the reflectance curve remains similar to that predicted for a smooth copper surface, but at reduced magnitude. The aluminum sample, grooved in only one direction, still has a significant specular component, as evidenced by the 55° minimum. Roughness has flattened out the curve, and lowered it approximately 10% in comparison with the polished sample. The bakelite data corresponds closely with polished sample results. Only the decrease due to the specular component of the polished sample distinguishes one sample from the other. It appears that the only effect of surface roughness, other than masking the specular spot error inherent in the sphere, is to lower the magnitude of the reflectance. The shapes of the curves remain the same, except at very high ($80^\circ+$) angles of incidence. The few modes of roughness studied indicate no strong aggregate effect on directional distribution. It appears most surfaces found in nature will conform to this observation.

Figure 25 presents some additional results for the dependence of reflectance on the angle of incidence for other samples, for which additional radiation properties have been determined, as specified in Section 7.

The information on the absorptance as a function of angle of incidence makes possible the evaluation of the ratio of the absorptance for hemispherical irradiation to that for normal irradiation, a ratio that is sometimes quoted as an appraisal of the departure from a constant absorptance with angle, which of course would make the ratio unity. It can be evaluated analytically for smooth surfaces from the reflectances specified from electromagnetic theory and of course for those surfaces it also is the ratio of the total emittance to that in the normal direction. This follows since $\epsilon_n = 1 - r_n$ and for specular surfaces $r_n = r_\theta$. This predicted ratio is often presented as a function of the normal value; Eckert⁽²⁾ has compared his measurements of emittance to such a prediction, to show that even relatively non-specular surfaces yield ratios of the order of magnitude that are predicted for specular surfaces.

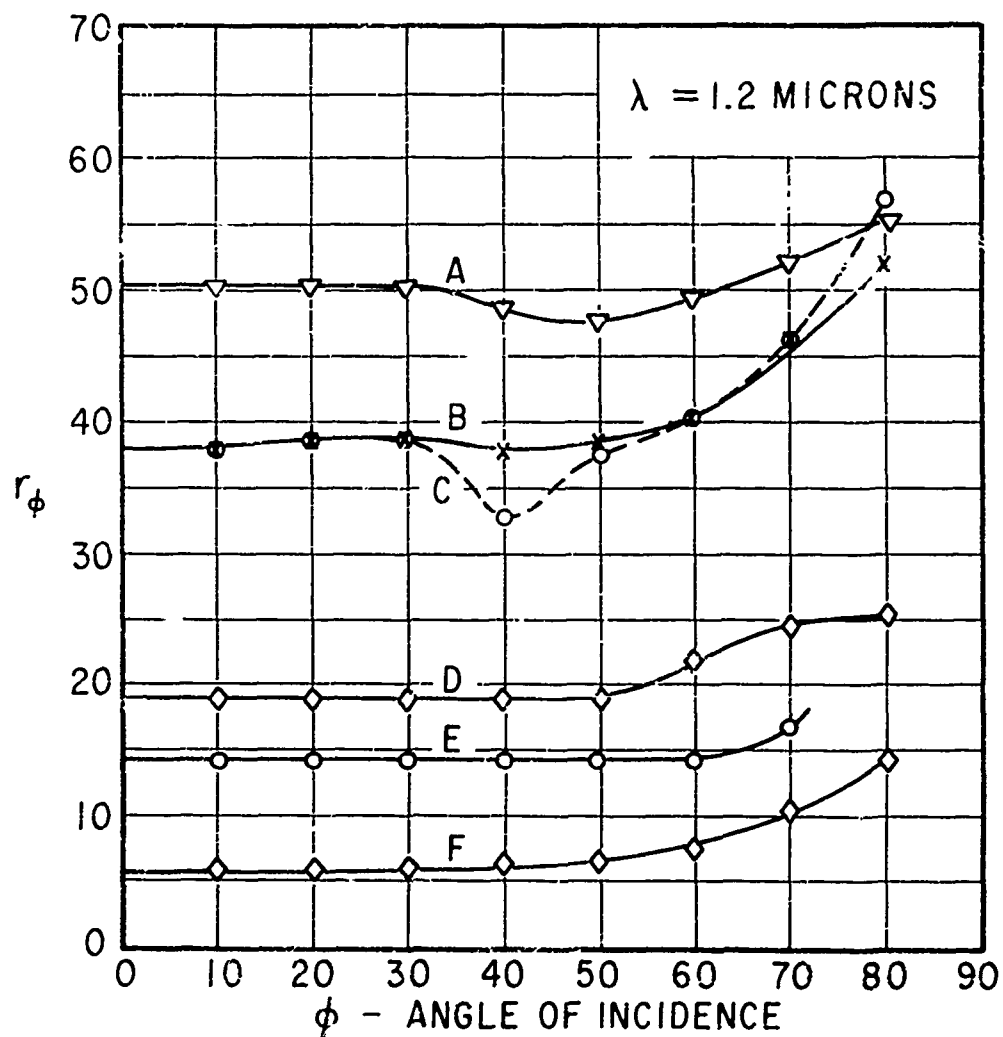


Figure 25. - Angular reflectance of several sample at 1.2 microns. Curve A, F120; Curve B, CTL 37-9X; Curve C, Alclad solar absorber; Curve D, oxidized Inconel; Curve E, M252, Curve F, Chromate on Inconel.

For all smooth surfaces the predicted absorptance is almost invariant for angles of up to 50° with the normal. Dielectrics, which generally are poor reflectors, experience an increase in reflectance beyond these angles, an increase which becomes large after 60° . Thus, the ratio of the normal to the hemispherical absorptance may turn out to be slightly less than unity. Metals indicate a less variable reflectance, which does, however, diminish significantly only at about 80° , with a return to higher reflectances at grazing angles. The decrease is enough to make the hemispherical absorptance exceed the normal value. The rough surfaces that were examined actually show a somewhat similar behavior, though of different magnitude; Table 3 contains the experimental values of the ratio α/α_0 obtained from these measurements. The predicted values for smooth surfaces having the same normal absorptance are contained in the Table as $(\alpha/\alpha_0)_T$ and similarity with the experimental values is indicated.

TABLE 3

	λ	α_0	α/α_0	$(\alpha/\alpha_0)_T$
Grooved Copper	1.2	0.18	0.94	1.15
	1.8	0.09	1.10	1.23
Alclad Absorber	1.2	0.620	0.94	1.00
	1.8	0.27	1.03	1.08
Oxidized Inconel	1.2	0.81	0.97	0.96
	1.8	0.76	0.93	0.97
Chromate on Inconel	1.2	0.95	0.97	0.95
	1.8	0.93	0.97	0.95
M252	1.2	0.86	0.96	0.95
	1.8	0.84	0.96	0.95
F120	1.2	0.50	1.0	1.04
	1.8	0.66	0.96	1.00
CTL37-3X	1.2	0.62	0.95	1.01
	1.8	0.78	0.89	0.97

11.0 PLASTIC SAMPLES

There has been a prior indication in Section 4 of the impediment on the methods of measurement described there that is imposed by high thermal resistance within the specimen. When either sample heating or cooling is involved and when the surface temperature must be known, the effect of high thermal resistance is to increase the uncertainty in the determined sample temperature. All the plastic samples fall into this category because of their low thermal conductivity. Because of this uncertainty the techniques that were used and the results that were obtained are discussed separately in this section.

11.1 Total Emittance

The back heated stand of the type discussed in Section 4.1 is fundamentally inappropriate for plastic samples because of the large temperature drop produced across the sample. For a typical plastic, Astrolite, this drop was of the order of 32°F when the surface temperature was 400°F. To determine surface temperatures under these conditions, with a gradient of the order of 256°F/inch, a primary attempt involved the placement of 40 gage thermocouples in fine slots cut into the back of the specimen, with the slots then filled with Sauereisen cement. The effective locations of the couples were then to be determined from a thermal conductivity test at room temperature, with the indication of the thermocouples at elevated temperatures to be extrapolated to give surface temperature, on the poor assumption of invariance of the conductances with temperature. Attempts at this method were not encouraging, the positioning of the couples was poor and the accuracy of temperature determination required in the thermal conductivity tests was not achieved.

As an alternate, a fine groove approximately 0.005" x 0.005" was cut into the front and back surfaces, and 40 gage thermocouples placed in the groove. A radiation balance predicts that such an installation will indicate a temperature considerably below the temperature of the surface, but apparently the indication is improved by actual contact between the wire and the surface. This conjecture was supported by the observation, made at low surface temperature, that the introduction of adhesive into the groove in the region of the thermocouple junction did not change the apparent emittance values. With this method, total emittances were determined for a few of the high temperature plastics, Astrolite, CTL37-9X, and F120, using the electrically heated stand, with the results evaluated from Equation 4.0.1.

11.2 Spectral Reflectance

Spectral reflectance data were obtained for all plastic samples in the Beckman reflectometer, with the results as given in Figures 26 to 31. These are the ratios of the sample reflectance to that of MgO. To obtain actual reflectances the values of the

ratio given on Figures 26 to 31 must be multiplied by the reflectance of the MgO as given in Figure 8. This routine determination involved no heat transfer through the sample and consequently the thermal resistance of the material produced no problem.

To obtain some results at the longer wavelengths a few of the plastic samples were tested in the heated cavity, using the water cooled sample holder. In this unit the irradiation is intense, the flux to the cooling water is large, and because of the high thermal resistance of the plastics there is consequently a large difference in temperature between that of the irradiated surface and that on the cooled side. Since the surface temperature was large enough to significantly affect the system response in the way described in Section 3.1 for the air cooled sample holder, the results were reduced according to Equation 3.1.5, with an assumed temperature for the sample surface. By adjustment of this temperature there could be obtained a reflectance distribution which on integration would yield an emittance comparable to what was measured. This does not belie the inaccuracy of the latter value but merely establishes a consistent reflectance curve. The final appraisal then involves the comparison of the estimated surface temperature, the thermal conductivity of the plastic measured at room temperature, its dimensions, and the estimated heat flux. For example, for the spectral reflectance results for Astrolite that are shown on page 100 the estimated surface temperature is 813°F and that of the cold side of the sample of the order of 80°F. The thermal conductivity was measured at room temperature as 0.15 Btu/ft.².hr.^{°F} and the thickness was 0.062 inch. This gives a flux of 7800 Btu/ft.²-hr. But in terms of this surface temperature and the estimated absorptance for irradiation at the cavity temperature the flux should have been 16000 Btu/ft.²-hr.

This twofold discrepancy points initially to the possible existence of a higher surface temperature, but the possibility is limited. Higher temperatures will produce lower indicated reflectances, and the values on page 100 are already as low as 0.05. With zero as a minimum, reference to Figure 5 indicates that little further increase is possible for the hypothesized surface temperature. The discrepancy between the heat fluxes therefore is attributed rather to a possible increase in the thermal conductivity with temperature and to a low extinction coefficient in the material, in which case the average conduction path would be less than the sample thickness.

The reflectance curves indicated for the plastics are therefore viewed with some confidence, and the total emittances obtained from them are probably satisfactory until major changes in the nature of the material occur.

11.3 Translucent Plastic

One sample, WWCNE-2, was translucent; therefore the transmittance had to be determined and used in the specification of the spectral reflectance.

When placed in the optical path of the heated cavity system at the shutter location, the normal transmittance of the sample for normal irradiation was found; reference to the incident radiation was made with the sample removed from the optical path. A transmittance was then determined which was different from the cavity reference reading by surface reflections, absorption, and side scattering. Small changes in sample orientation were possible, and small changes in the angle of incidence produced no observed change in transmittance. These results are shown in Section 13 page 108.

Situation of the sample at the inlet port of the integrating sphere of the DK2 reflectometer provided transmittance data for normal incidence on the range 0.30 to 2.7 microns but in this situation the total transmission was measured by the collection of all the transmitted energy in the integrating sphere. By locating a total absorption tube at the sample port the direct transmission could be removed. (This was approximately 10% of the total.)

Reflectance measurements were obtained from the heated cavity by placing the sample over a metal disc with a flat black surface held in the water cooled sample holder. Since the surface was not entirely black, some reflection occurred there to make somewhat uncertain the interpretation of the measured reflectance. With hemispherical irradiation, the irradiation of the black surface at the back of the sample is $t G_H$.

The transmittance t is taken as the measured normal transmittance, though this is known to be low. If, for instance, the transmission is assumed to be diffuse scattering, then the total transmittance is π times the normal values. But, where windows exist such a multiplication is obviously too large. Hence the normal value is used in the realization that it is too low.

Then the radiosity of the film and back plate combination is

$$J = r_s G_H + t^2 r_b G_H = [r_s + t^2 r_b] G_H \quad 11.3.1$$

Thus, the apparent reflectance is $r_s + t^2 r_b$; the results were calculated on this basis, with r_b the spectral reflectance of the black paint. As used, t is certainly too low and consequently the cited value of the reflectance of the plastic, r_s , is very slightly low.

When used in the DK2 reflectometer, the backing of the sample was a long paper tube with a closed end, painted inside with flat black. This was completely black, and for this measurement no transmission correction was needed.

11.4 Reflectance of Plastic Samples at Short Wavelengths

The difficulties associated with the plastic samples, discussed in Section 11.1 and 11.2, result in a limited number of results for the total wavelength range. The limitations of course did not exist in the integrating sphere devices, with the small irradiation of the sample that occurred in them. In particular, because of its automatic features, all the plastic samples were measured in the Beckman reflectometer in the spectral range from 0.3 to 2.5 microns. This range covers most of the solar spectrum so that these results are sufficient for the appraisal of solar absorptance.

Figures 26 through 31 present the direct Beckman results, as the ratio of the sample reflectance to that of MgO , as obtained for the plastic samples. In the Beckman unit, as described in Section 3.2, the detector is irradiated by the first reflection from the sample and the consequent dependence on the geometric nature of the reflection is important if the reflection is not isotropic. It was non-isotropic for a number of these sample and different results were obtained if the sample was rotated in the holder. In such cases the quotations on Figures 26 through 31 are the mean of the maximum and minimum reflectances obtained by changing the sample position.

Solar absorptances were calculated from the results of Figures 26 through 31 for zero air mass as indicated in Section 7, except that the reflectance of the MgO was accounted for by preparing an overlay for twenty equal increments of the quantity

$$\int_{\lambda}^{\lambda+\Delta\lambda} r_{MgO} G d\lambda$$

In this way the total absorptance for normal irradiation was obtained as

$$\alpha = 1 - r = 1 - \sum \left(\frac{r}{r_{MgO}} \right) \int_{\lambda}^{\lambda+\Delta\lambda} r_{MgO} G d\lambda \quad 11.4.1$$

These values are given on Figures 26 through 31.

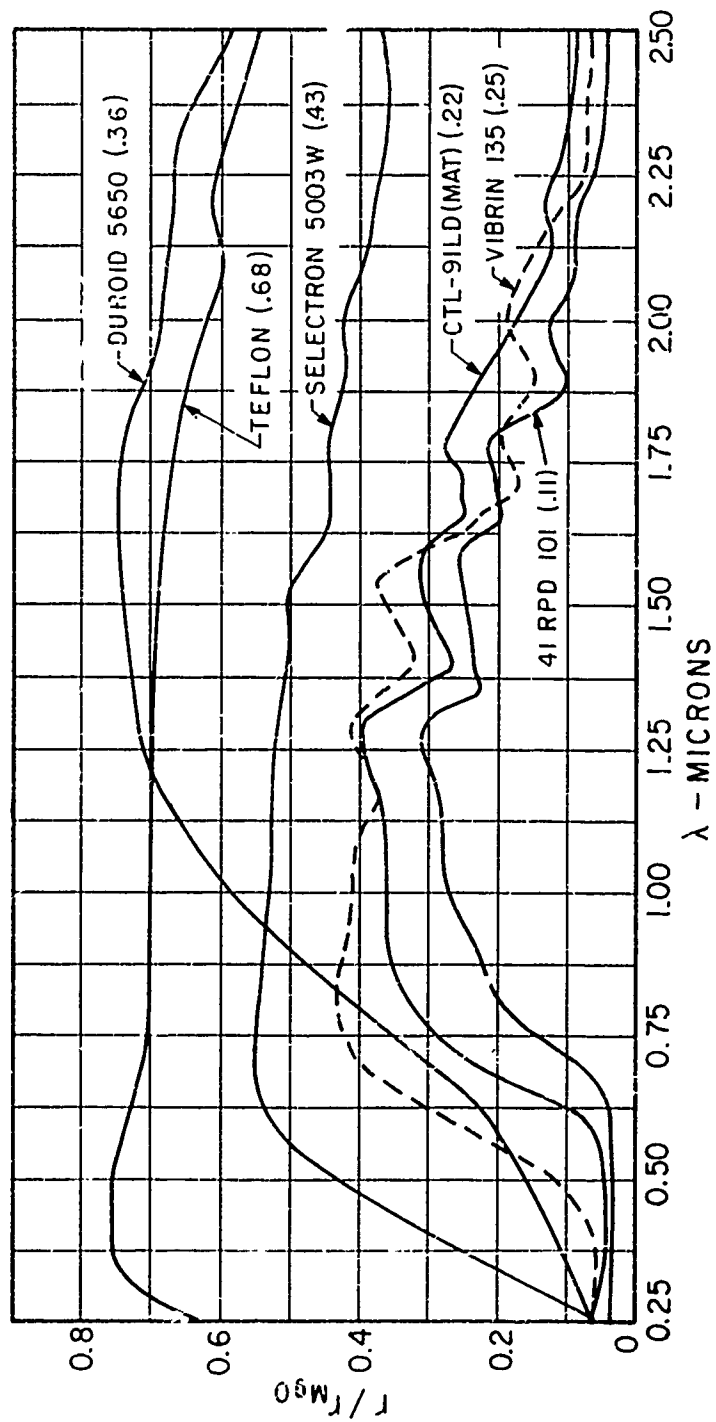


Figure 26. - Ratio of spectral reflectance to that of MgO. Zero air mass. Numbers in parenthesis are integrated solar reflectances.

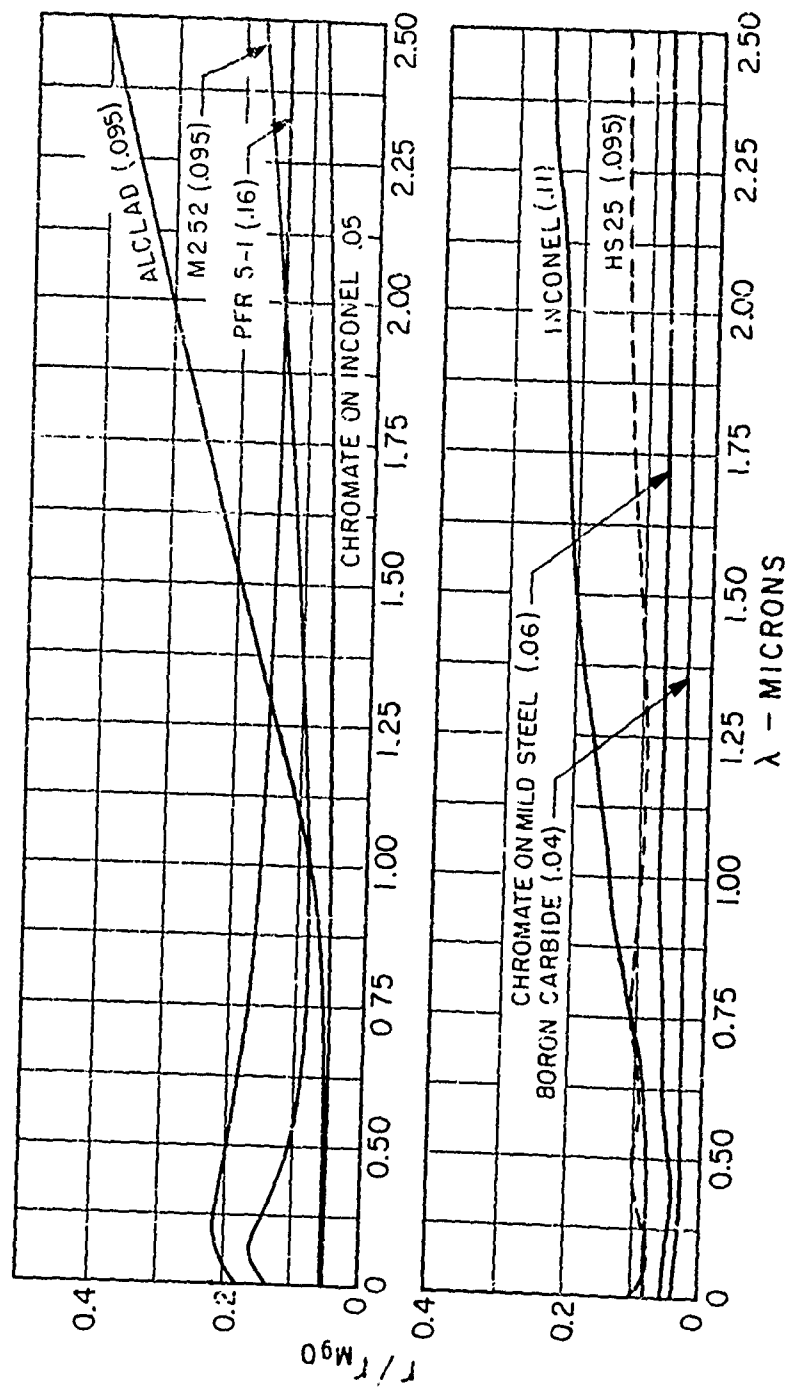


Figure 27. - Ratio of spectral reflectance to that of MgO. Zero air mass. Numbers in parenthesis are integrated solar reflectances.

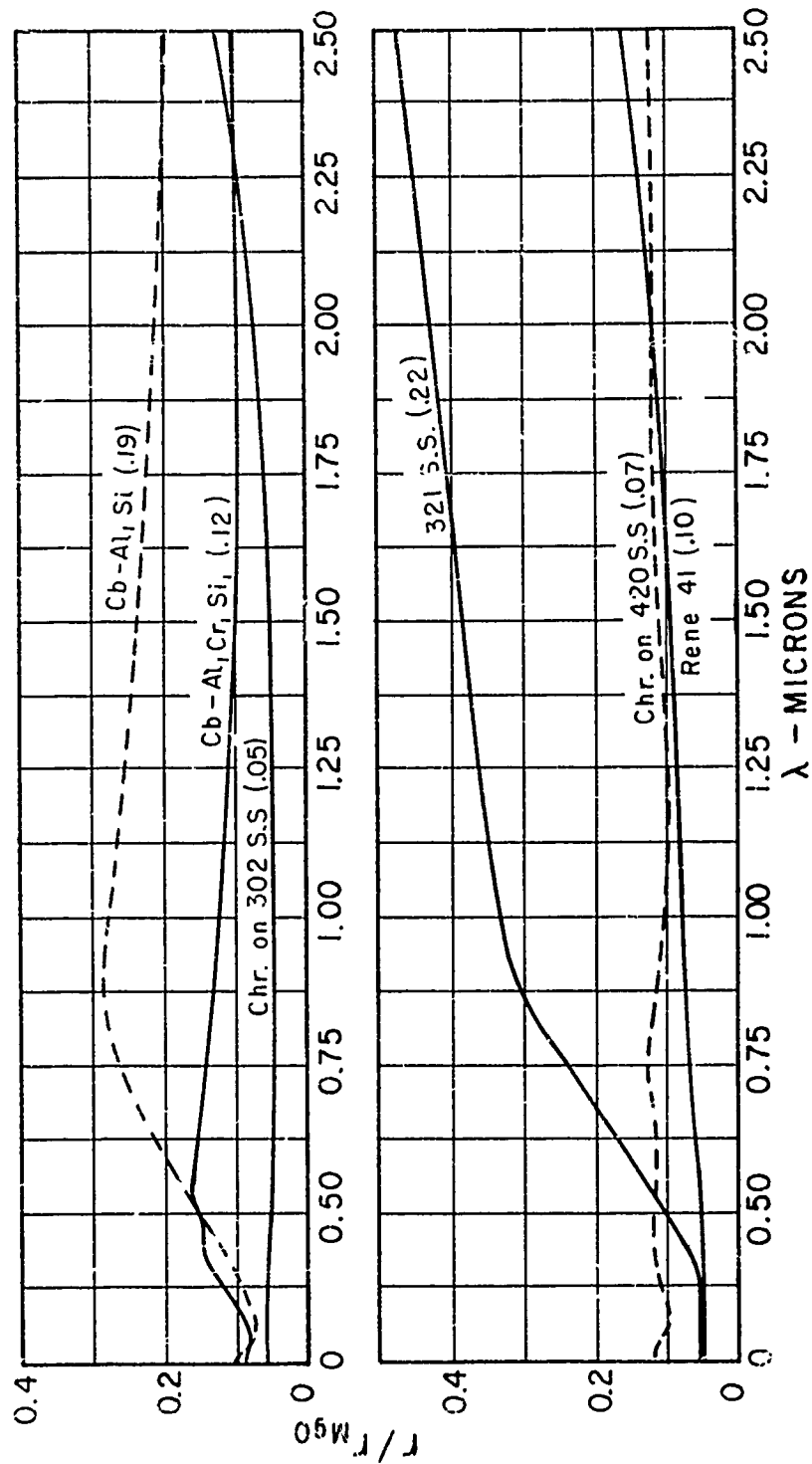


Figure 28. - Ratio of spectral reflectance to that of MgO. Zero air mass. Numbers in parenthesis are integrated solar reflectances.

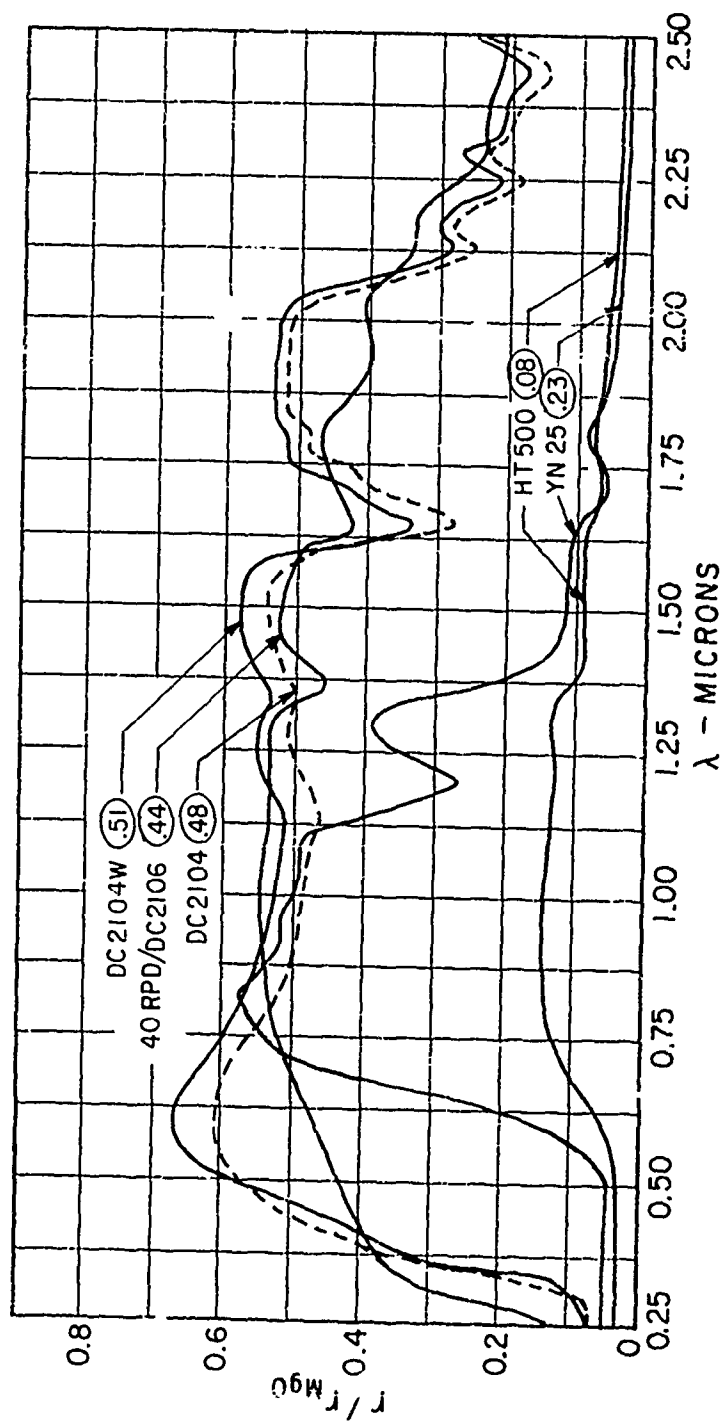


Figure 29. - Ratio of spectral reflectance to that of MgO. Zero air mass. Numbers in parenthesis are integrated solar reflectances.

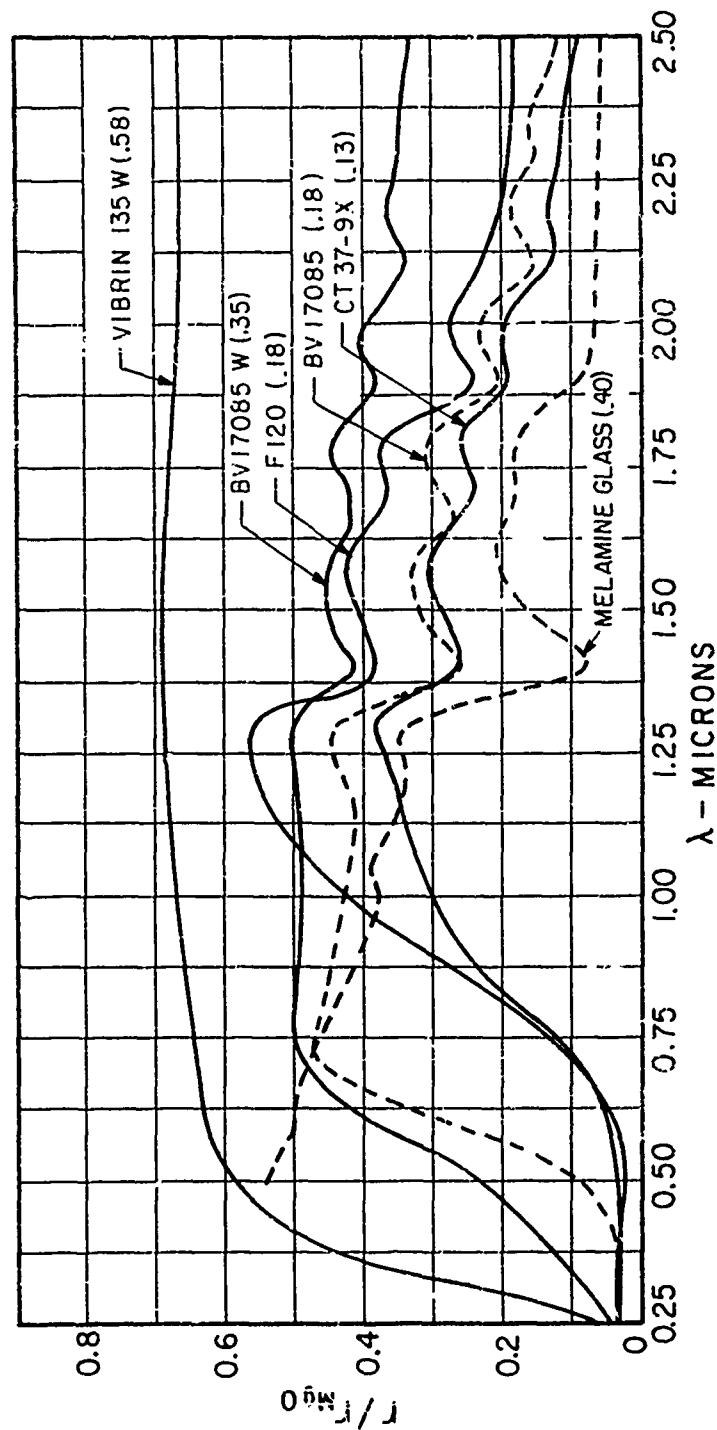


Figure 30. - Ratio of spectral reflectance to that of MgO. Zero air mass. Numbers in parenthesis are integrated solar reflectances.

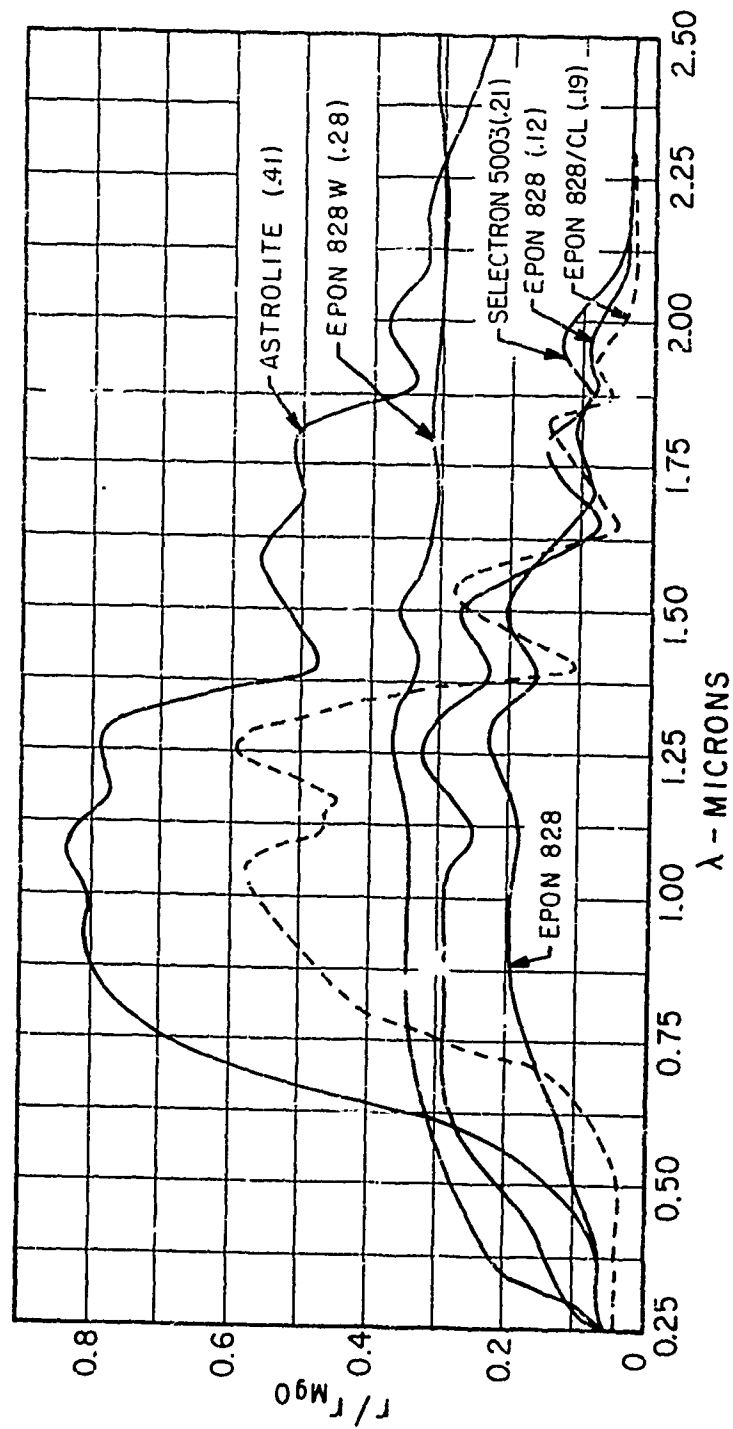


Figure 31. - Ratio of spectral reflectance to that of MgO. Zero air mass. Numbers in parenthesis are integrated solar reflectances.

12.0 SUMMARY AND CONCLUSIONS

The thermal radiation properties of 20 materials are given in Section 13, basically as the total normal emittance and the spectral reflectance. In some cases the former is more dubious or is omitted, because of difficulties in thermocouple attachment or of appraisal of the indicated value. This is particularly true of the plastic samples where the large temperature variation through the sample led to difficulty in the measurement of the total emittance and in the appraisal of the spectral reflectance results, as discussed in Section 11.

Other than to note that the majority of the materials were poor reflectors, no generalization is possible for the properties themselves, and the remainder of this summary is directed toward the methods of measurement.

The values of total normal emittance were determined from back heated samples by the methods discussed in Section 4. On the electrically heated system, used to temperatures of 1700°F, reproducibility of results was within 2% while on the gas heated unit, used up to 2500°F, the greater dependence on environmental conditions, increased this to 5%. The greatest source of absolute error is in the evaluation of the surface temperature from the thermocouple indication, for on some samples there is apparently appreciable contact resistance at the weld of the thermocouple to the oxidized or coated metal. The position of thermocouple attachment was such as to always make the measured emittance too high, and the general appraisal makes the excess no more than 5% of the actual value. However, in any particular measurement there is no absolute check on the uncertainty.

The spectral reflectance readings obtained with the cold samples in the heated cavity systems are subject to the minimal error of any of the major property determinations made and reported here. Since the prediction of the total normal emittance from reflectance values for temperatures at which such determinations were made involves essentially only the spectral range covered by that apparatus, those predictions are viewed with some confidence and indeed form a basis for the appraisal of the error in the measured total emittance.

An important question associated with the prediction of total emittance from the measured reflectance concerns the degree of temperature dependence of the reflectance itself. This dependence does of course exist for conductors, and it may for dielectrics if there is an alteration of the nature of the material or of its surface, as perhaps in thermal expansion. However, in any such change, progressive change as by oxidation, is not considered. Particularly when the dielectric is a surface on a metallic substrate, some temperature effect might occur, and to examine this question

reflectances were measured at elevated temperatures in the way described in Section 3.2. The procedure of necessity reduced the accuracy of the measured reflectance and made it acutely dependent on the measured sample temperature in part of the spectral range. These reflectances were always higher than those measured cold and the present view associates the excess with errors in the determination of the temperatures of the sample. But such corrections do not make the "hot" and "cold" reflectors coincide and there may still be some change of reflectance with temperature, which for the poor reflectors that were examined cannot be specified concretely because of the poor accuracy of the "hot" determination.

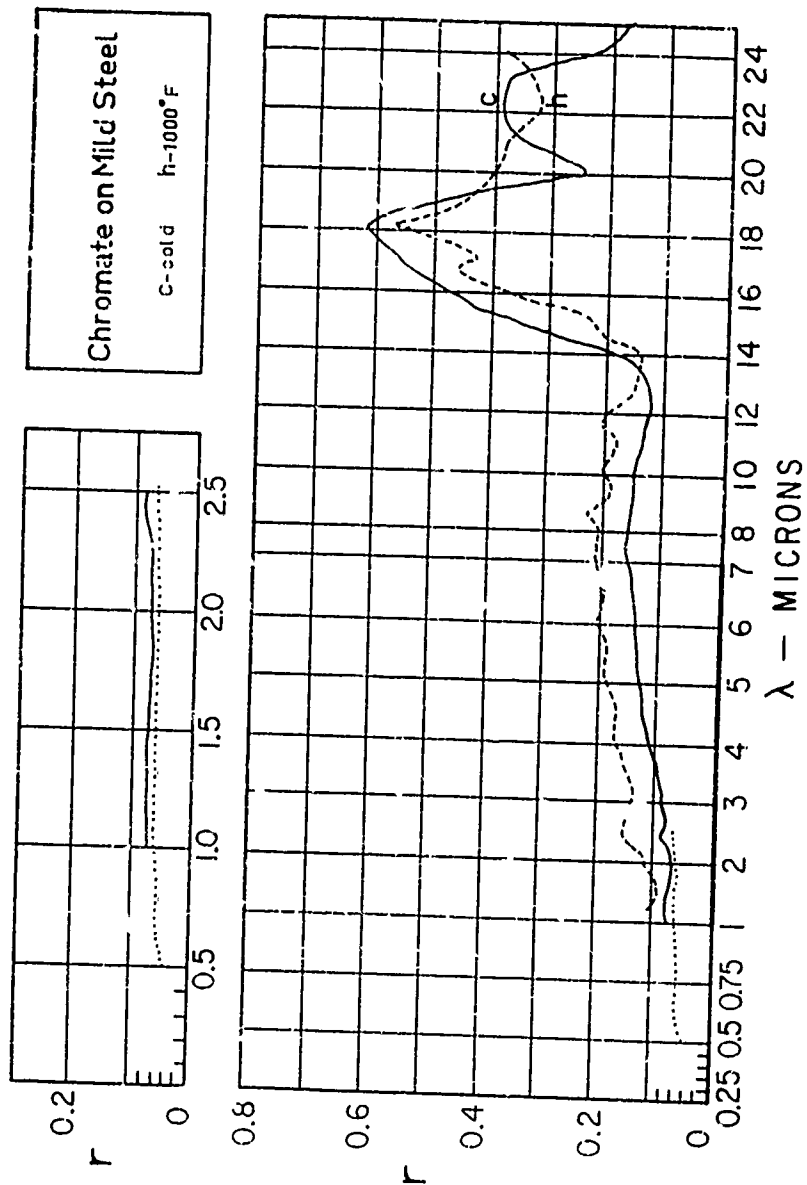
Spectral emittance values, determined of course with a hot sample should be more definitive in respect to the temperature dependence of the spectral values. These spectral emittances were only determined in a preliminary way, as described in Section 5.0 and a definite appraisal cannot yet be made. For one of the samples heated there were serious difficulties with contact resistance at the thermocouple weld, and the surface temperatures were uncertain; for the others, the best comparison was with the "cold" rather than with the "hot" reflectance values. This leads to the inference that for these samples at least, there was no significant temperature dependence of the spectral values and that in consequence the total emittance is best obtained from the "cold" reflectance results.

Reflectance values for "cold" samples were obtained in the spectral range $0.5 < \lambda < 2.5$ by the integrating sphere devices described in Section 3 and these reflectances are associated with the reflectances measured by the heated cavity system even though their true relation is still somewhat uncertain. Difficulty was experienced in relating the reflectances measured by the two spheres to each other and to the results from the cavity. Section 3.3 contains results which to some extent indicate that values from the Beckman unit may be slightly low. For the prediction of emittance at temperatures below 3000°F there is but a small amount of energy at wavelengths less than 1 micron and there differences are of minor importance. For the evaluation of the values of absorptance for solar energy the need for appropriate reflectance in the spectral range $0.25 < \lambda < 2.5$ microns is acute, and the question is then more important.

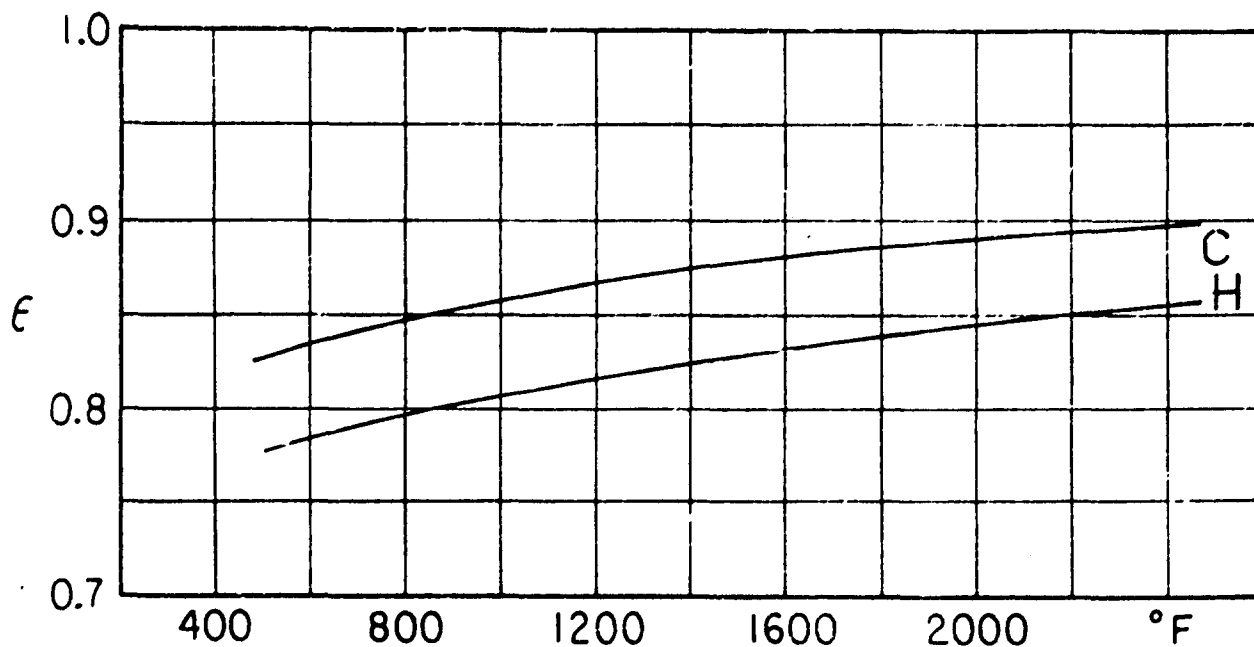
Absorptance as a function of angle of incidence was obtained with the variable angle sphere described in Section 3.3; these results are important in relation to problems involving the absorption of solar energy. These alone, of the present measurements, gave at least an indication of the relation of normal to hemispherical properties, and indicated that for most of the samples tested the normal values are easily within 5% of the hemispherical values.

13.0 RESULTS FOR THE VARIOUS SAMPLES

Results for each of the samples, indicated in Table I, are presented in the form outlined in Section 7.1.

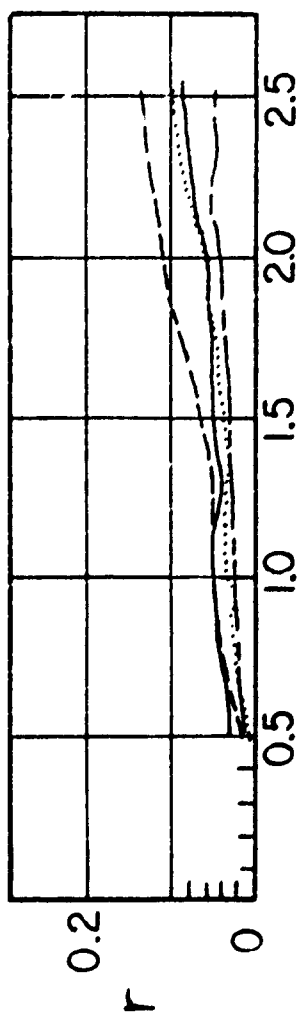


1. Material: Chromate on mild steel
2. Initial Treatment: None, all tests made after at least 3 hours at 1700°F.
3. Roughness: Fine structure 2.5 microns. Coarse structure 12 microns at intervals of about 300 microns.
4. Spectral Reflectance: Hot reflectance indicated to be .05 above cold reflectance except at long wavelengths.
5. Total Normal Emittance: (Predicted only)

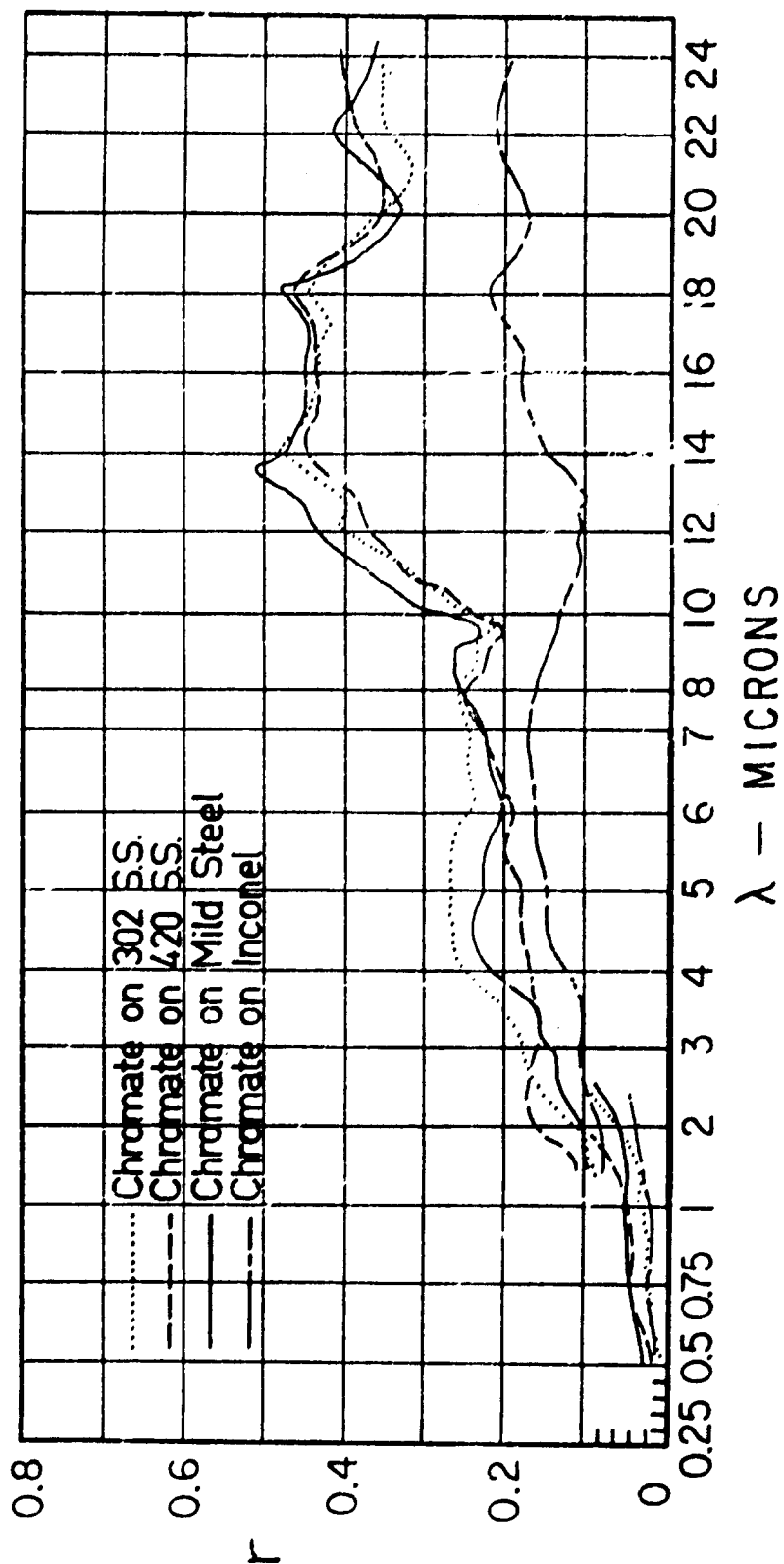


See page 73 for correspondence between this and other chromate coatings.

6. Solar Absorptance: Integrated from spectral results, 0.94.



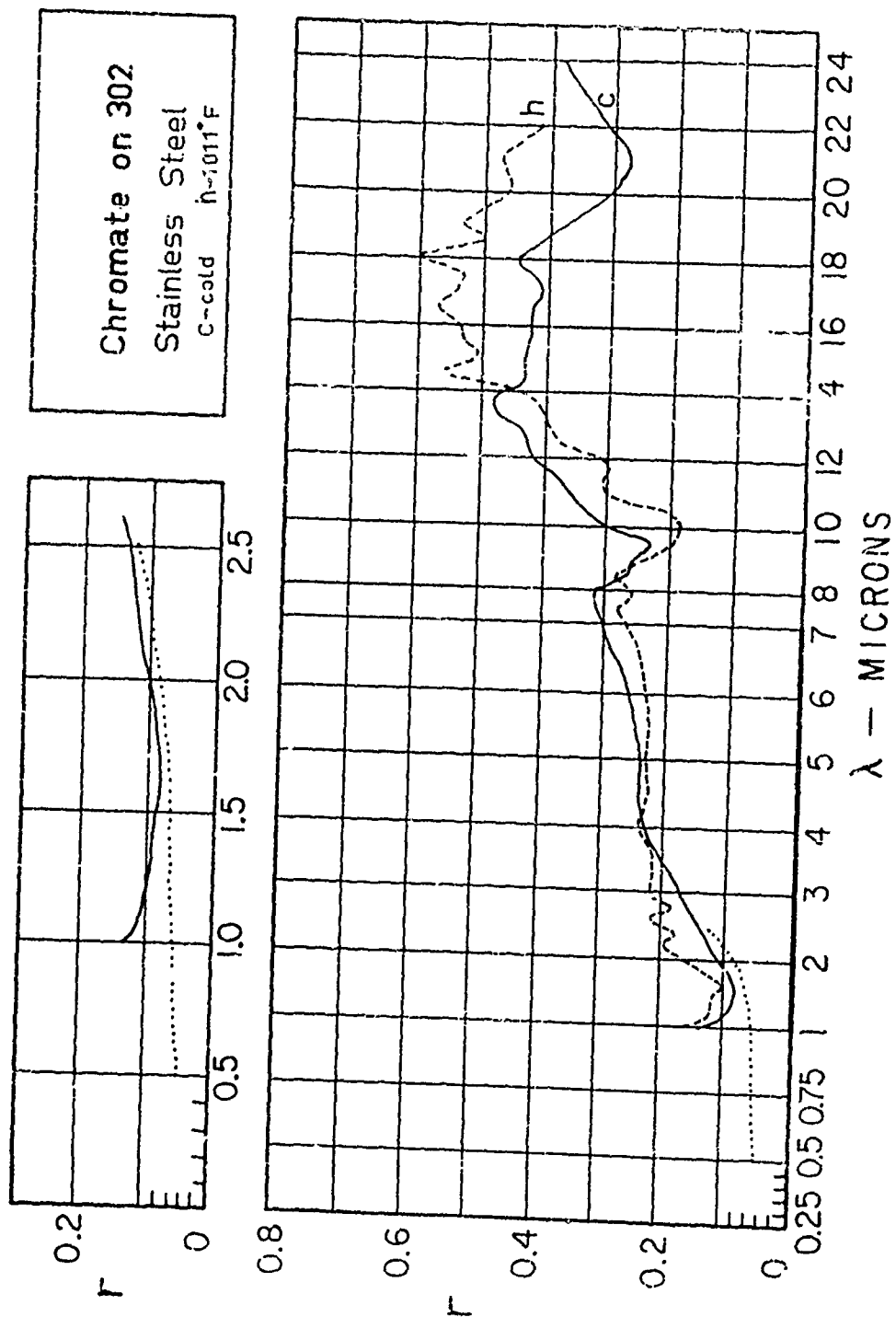
Comparison of
Chromate Coated
Samples



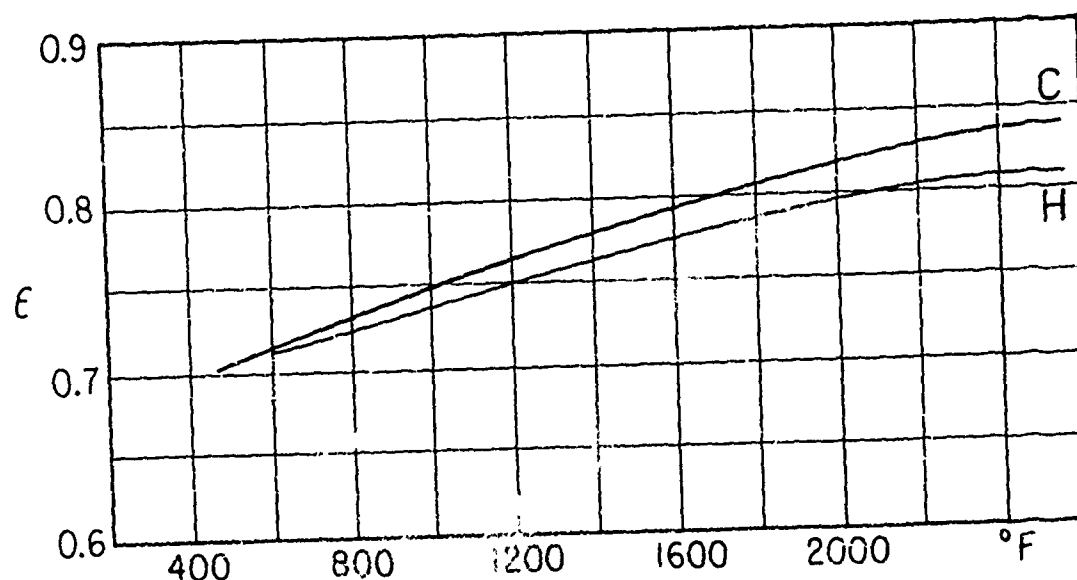
Spectral Reflectance of Chromate on: 302 stainless steel, 420 stainless steel, mild steel, and inconel.

The Figure on page 72 demonstrates the correspondence between the four chromate coatings. The spectral reflectance results for the four chromate coated samples, measured cold, were found to follow substantially the same general curve throughout the spectral range investigated with the exception of chromate on Inconel. The results for the chromate on Inconel show a slightly lower value of reflectance than the other three samples up to a wavelength of ten microns after which the inconel departs markedly below the values of the other samples.

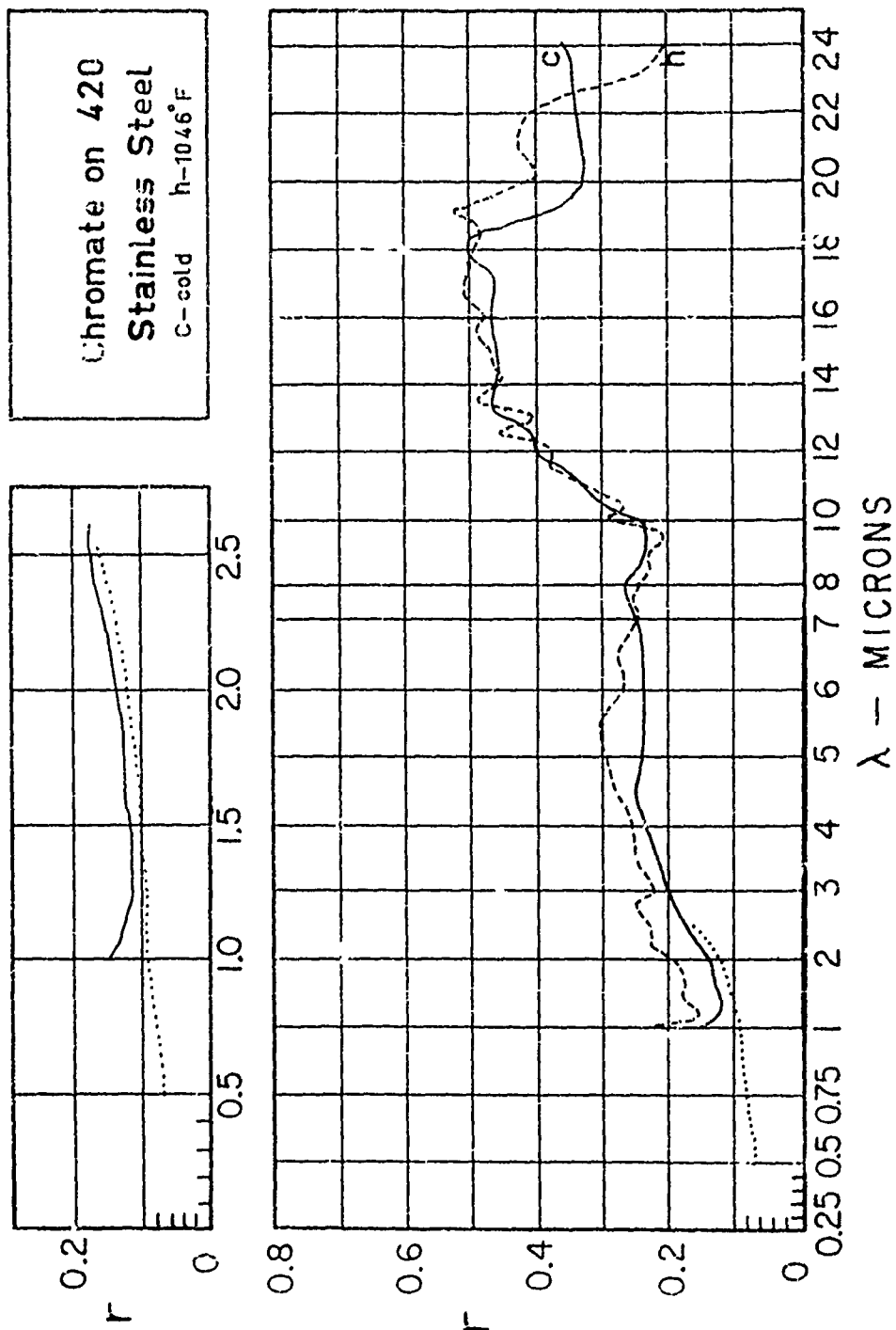
The reason for the difference in results between inconel and the other three samples could be due to differences in thickness or manner of application of the chromate coating.



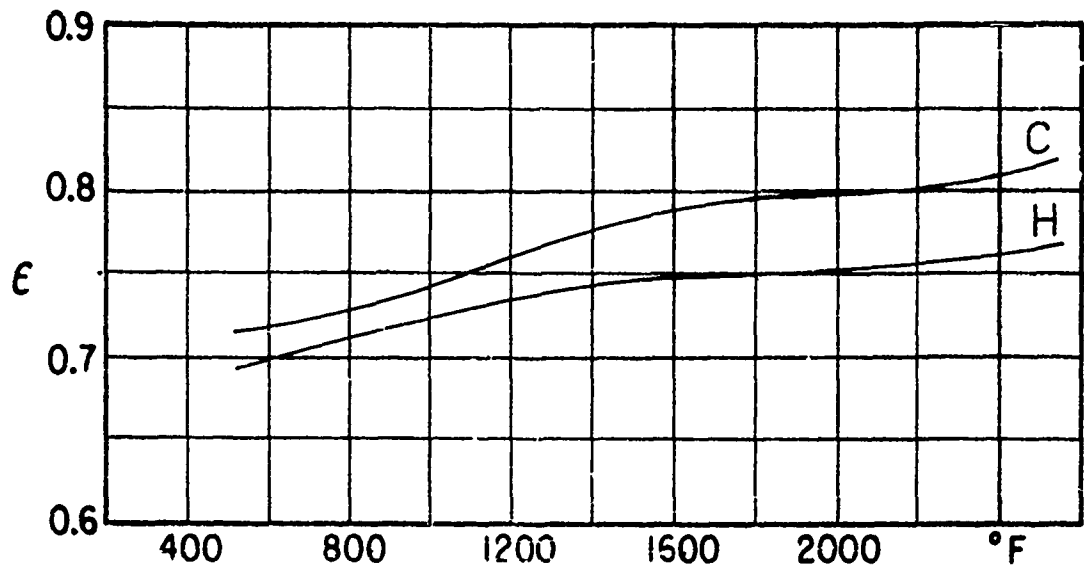
1. Material: Chromate on 302SS
2. Initial Treatment: None; aged as a result of use at high temperatures; 3 hours minimum at 1700°F in air.
3. Roughness: Fine structure 4 microns. Coarse structure 10 microns spaced at about 300 microns. As received sample similar to aged.
4. Spectral Reflectance: Hot reflectance shows only minor variations from cold value.
5. Total Normal Emittance: (Predicted only)



6. Solar Absorptance: Integrated from spectral results, 0.95.

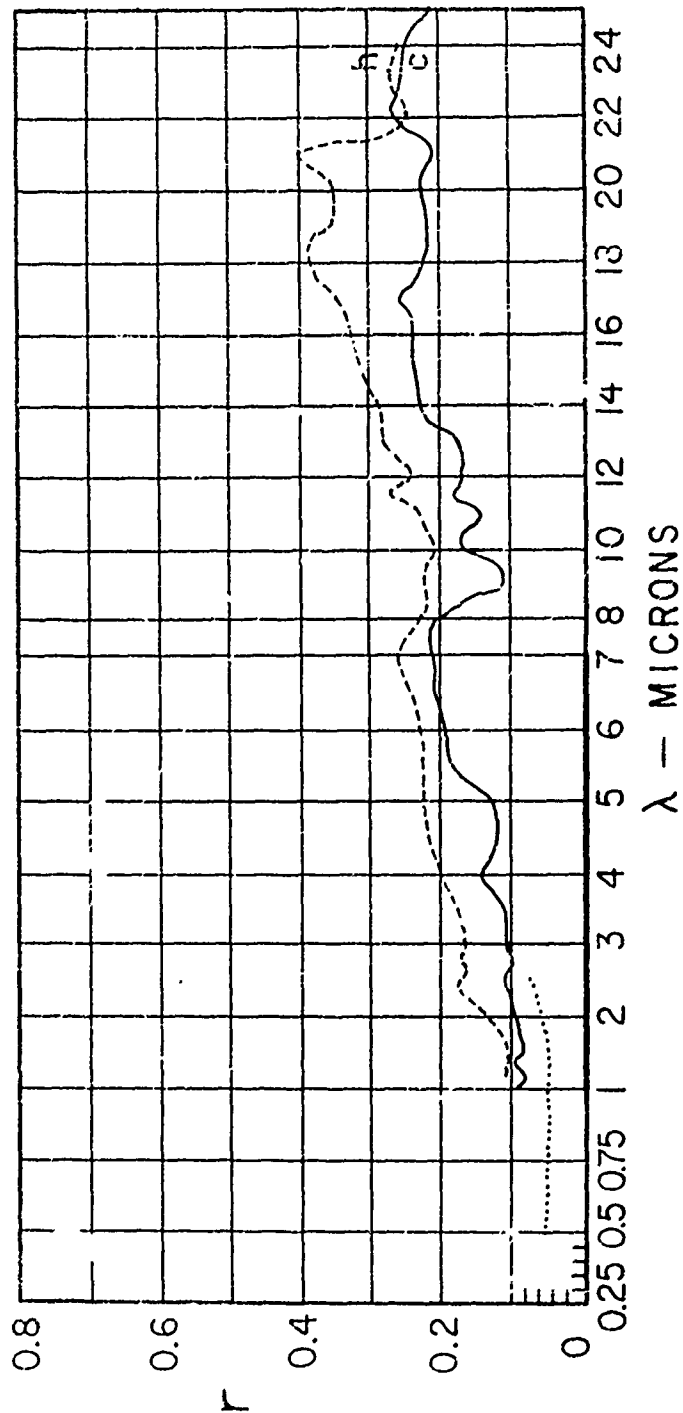
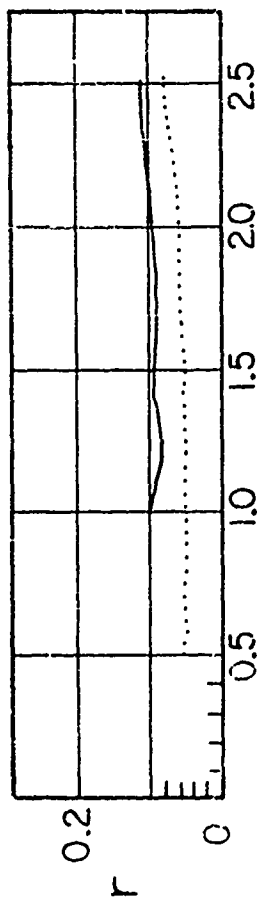


1. Material: Chromate on 420SS
2. Initial Treatment: None, all tests made after aging in air for 3 hours at 1700°F.
3. Roughness: Aged - fine structure sparse and of height 3 microns. Coarse structure about 15 microns at 200 microns intervals.
4. Spectral Reflectance: Hot reflectance results about 3 percentage points above cold reflectance for $\lambda < 7$. Close correlation above $\lambda = 7$.
5. Total Normal Emittance: (Predicted only)

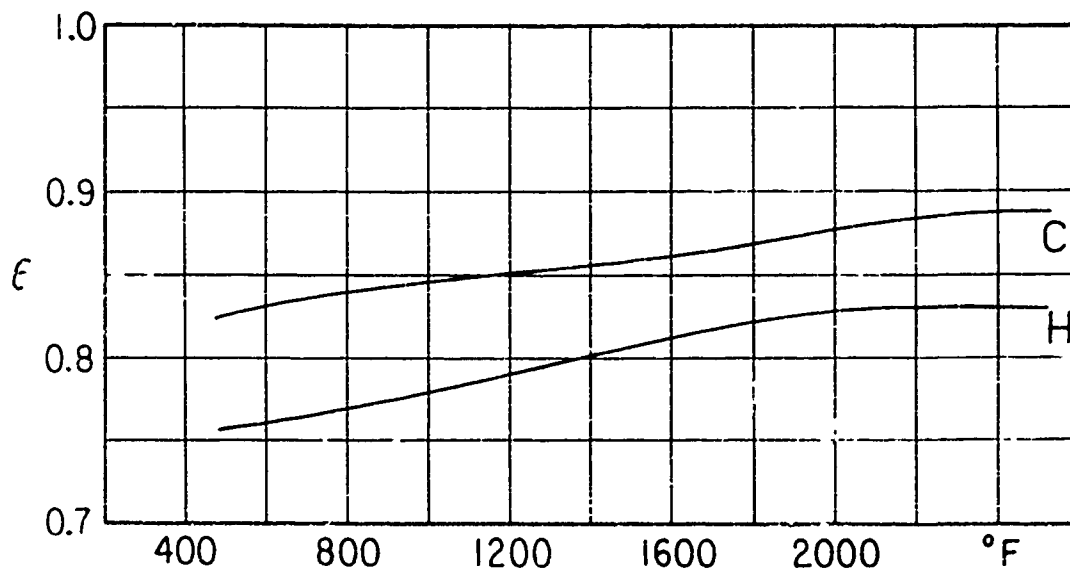


6. Solar Absorptance: Integrated from spectral results, 0.93.

Chromate on Inconel
C-cold h-1030°F

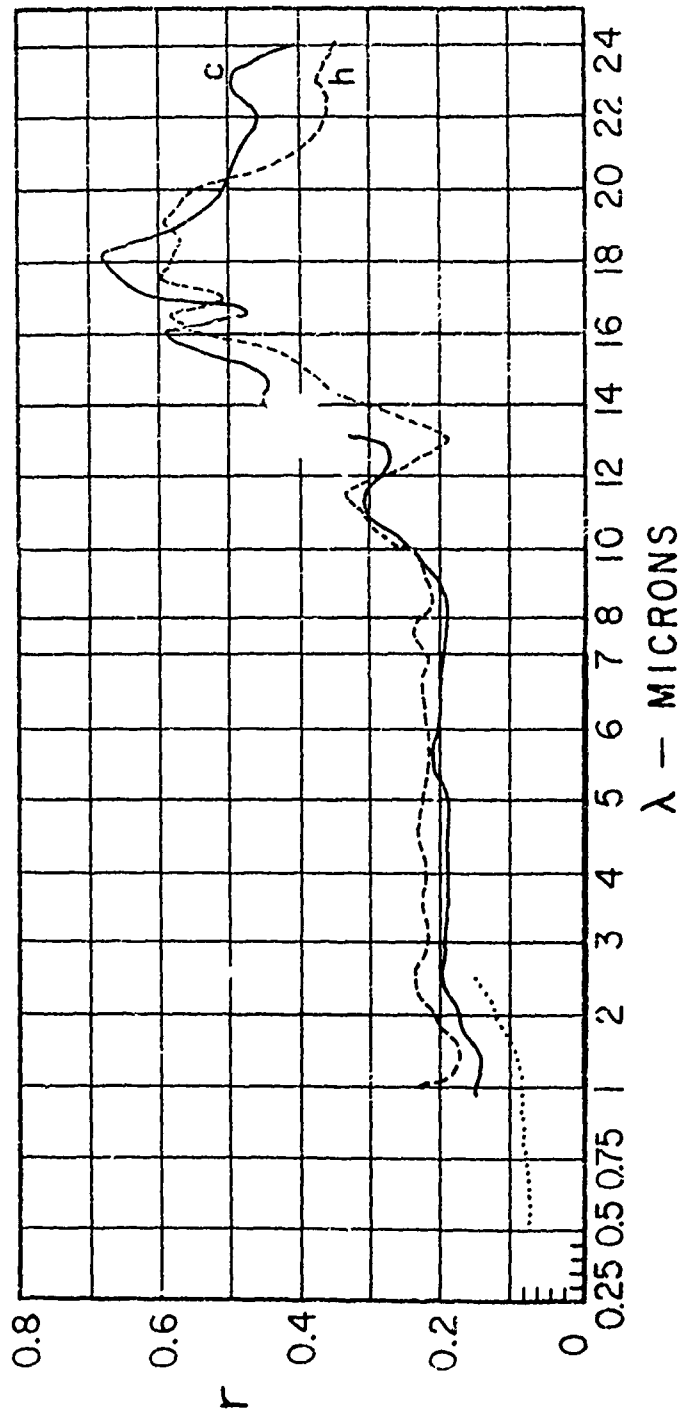
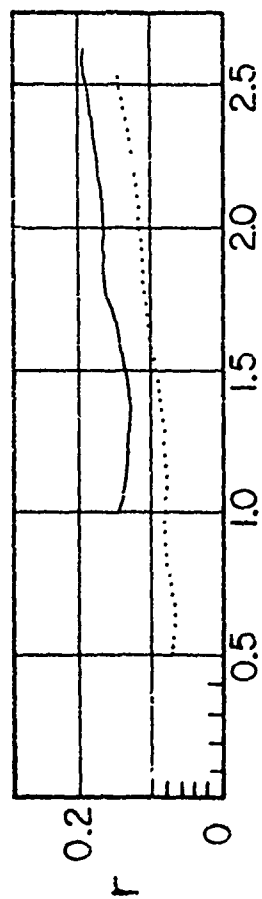


1. Material: Chromate on Inconel
2. Initial Treatment: None, all results taken after 3 hours in air at 1200°F.
3. Roughness: Fully aged: Fine structure sparse and of 4 microns. Coarse structure 18 microns at 250 micron intervals. "As received" sample very similar.
4. Spectral Reflectance: Hot reflectance results 0.95 to 0.10 above cold for $\lambda < 10$, substantial change for $\lambda > 10$. This sample shows good agreement between DK2 and heated cavity results. This is the chromate coating which produced reflectance data which differed from the other chromate samples.
5. Total Normal Emittance: (Predicted only)

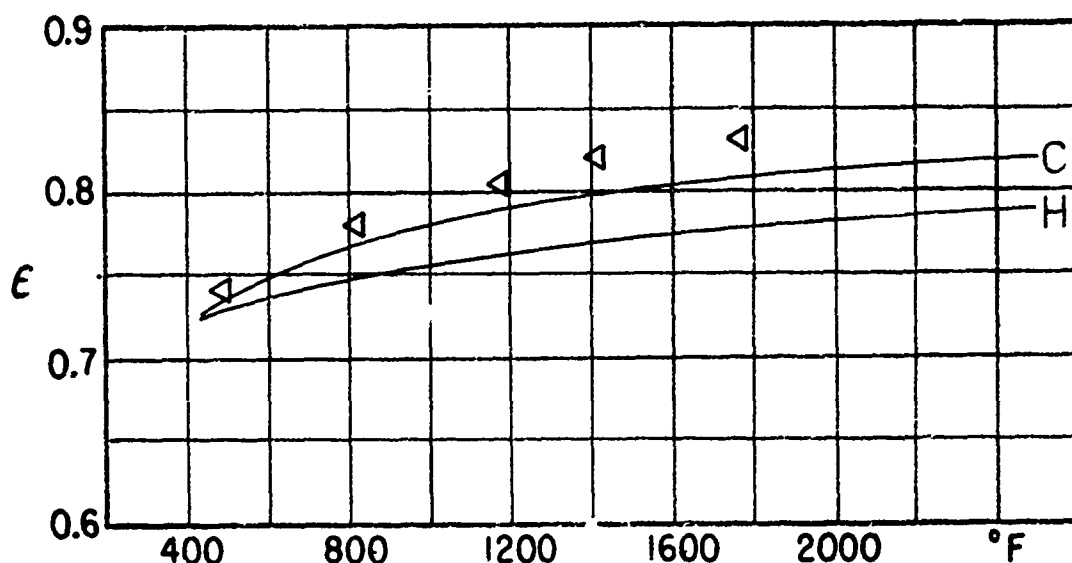


6. Solar Absorptance: Integrated from spectral results, 0.95.

M 252
C-cold h-1030°F

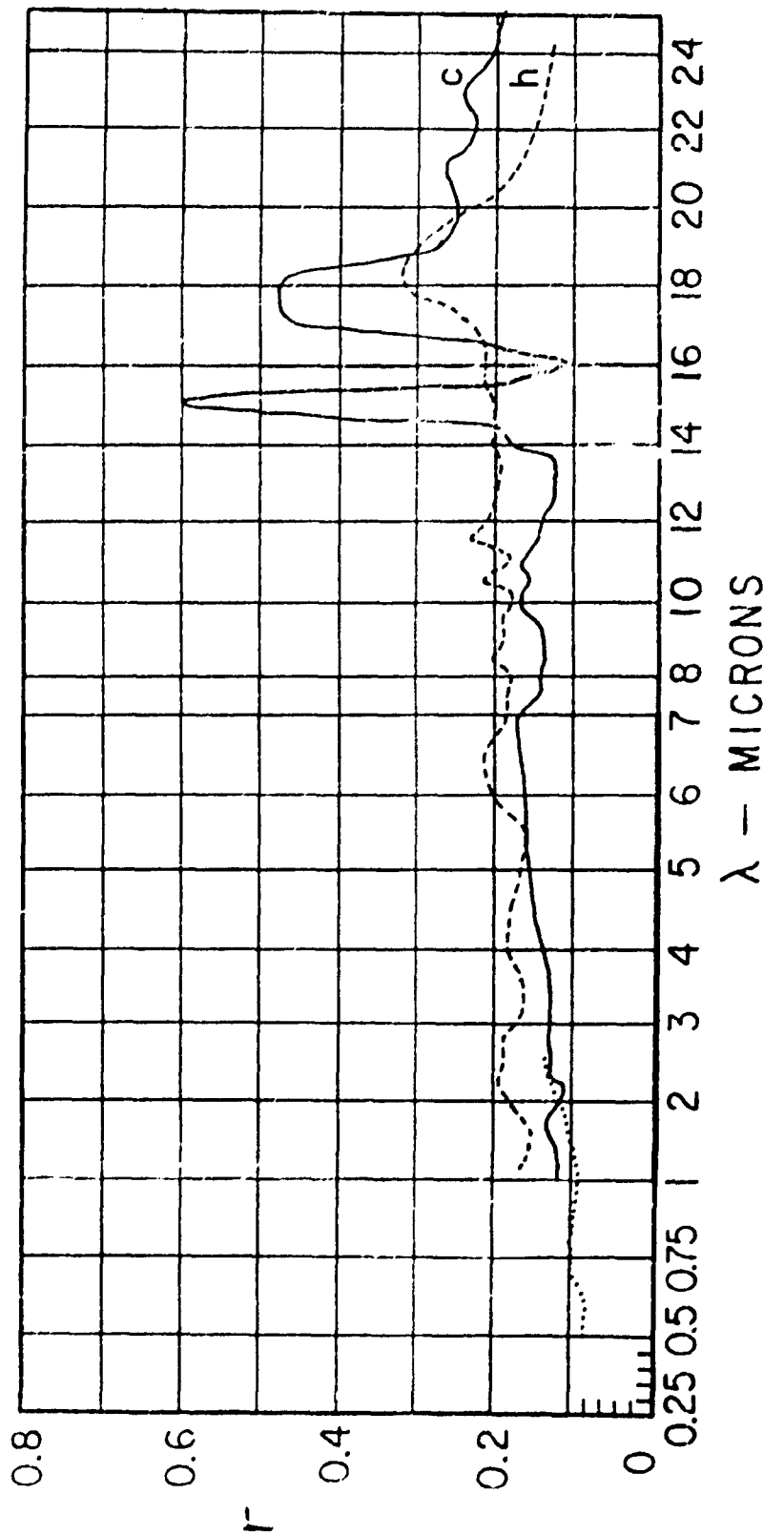
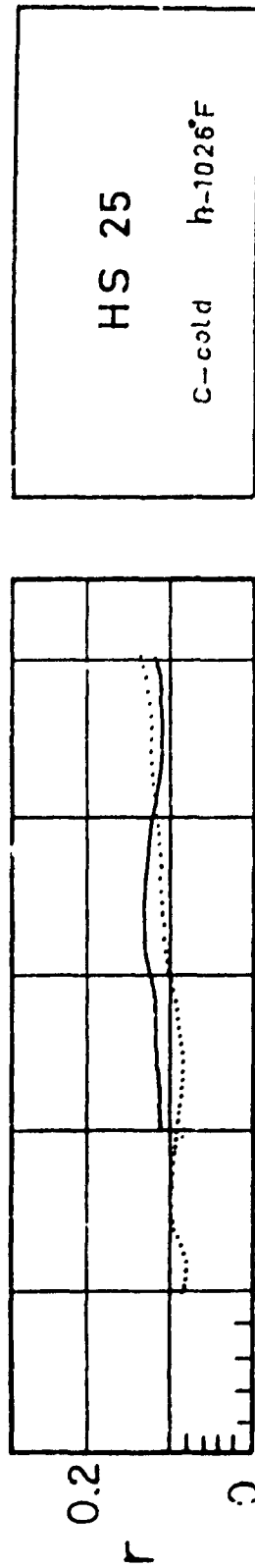


1. Material: M252 (SS 4781)
2. Initial Treatment: Cleaned in 1 to 1 water-diluted HF solution for 1 hour. Oxidized 3 hours at 1700°F in air.
3. Roughness: As received. Fine structure 2.5 microns amplitude
Fully aged: same.
4. Spectral Reflectance: Reflectance at 1000°F within about 0.05 of the reflectance at room temperature at low wavelengths. DK2 results low, estimate that they should be raised to coincide with cavity results.
5. Total Normal Emittance:

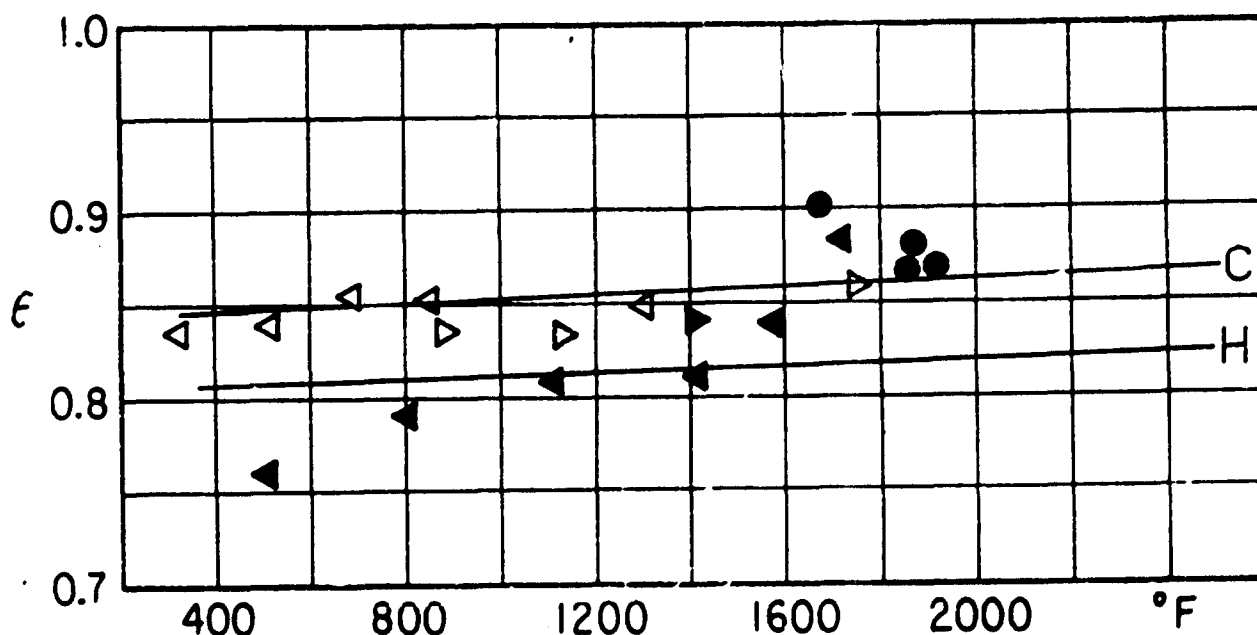


Measured values to 1600° follow trend of predicted values, predicted values low by 4%.

6. Solar Absorptance: Integrated from spectral results, 0.90.
7. Spectral Emittance: See page 32 . Angular dependence of absorptance, see page 55.



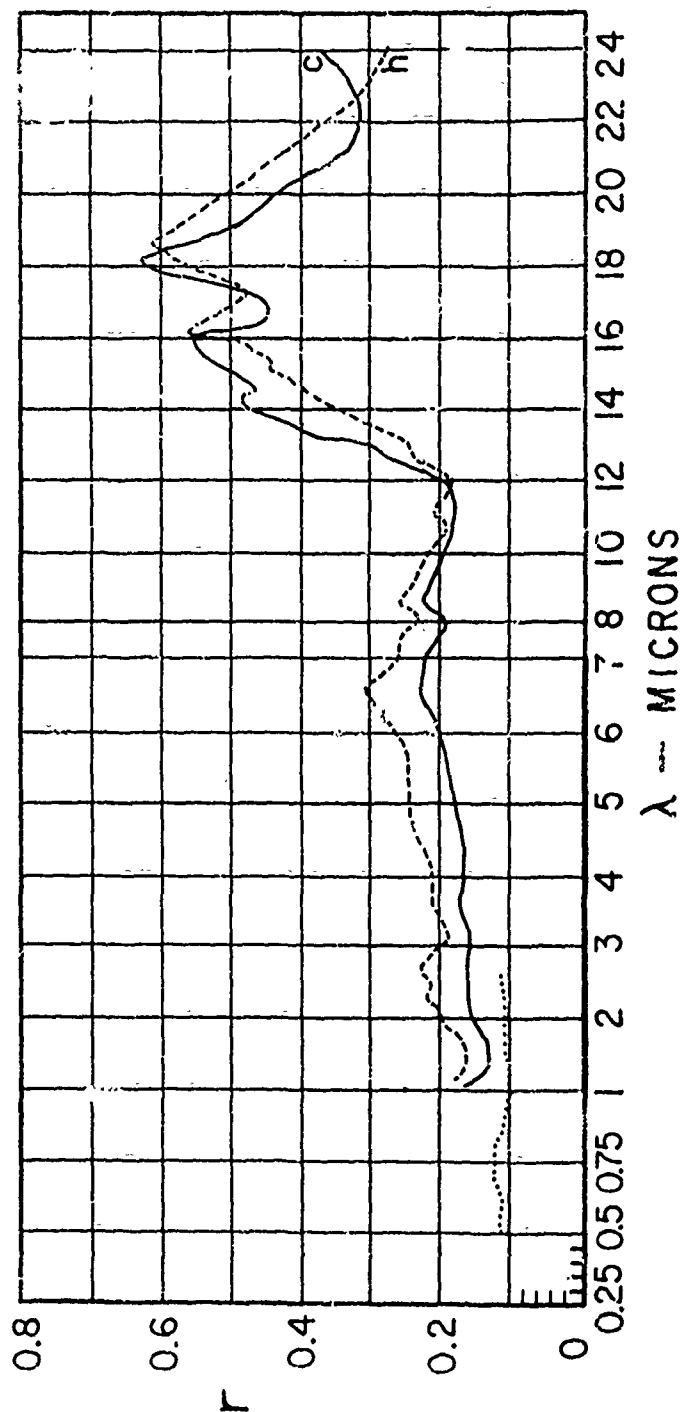
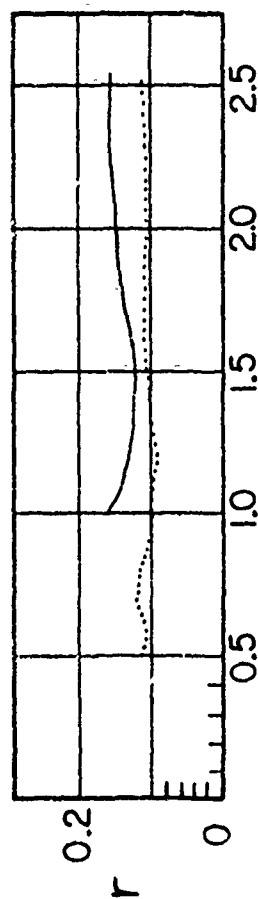
1. Material: HS25 (SS8178)
2. Initial Treatment: Cleaned in 1 to 1 water-diluted HF solution for 1 hour. Oxidized 3 hours at 1700°F in air.
3. Roughness: As received: Fine structure 2.5 microns. Coarse structure 6 microns at 250 micron intervals. Fully aged: Fine structure same. Coarse structure reduced to one in 2500 microns.
4. Spectral Reflectance: Reflectance at 1000°F within 0.05 of reflectance at room temperature, except near 15 microns: there an absorption peak did not appear with high temperature. Cold reflectance run with fully aged sample after it was used for total emittance measurement.
5. Total Normal Emittance:



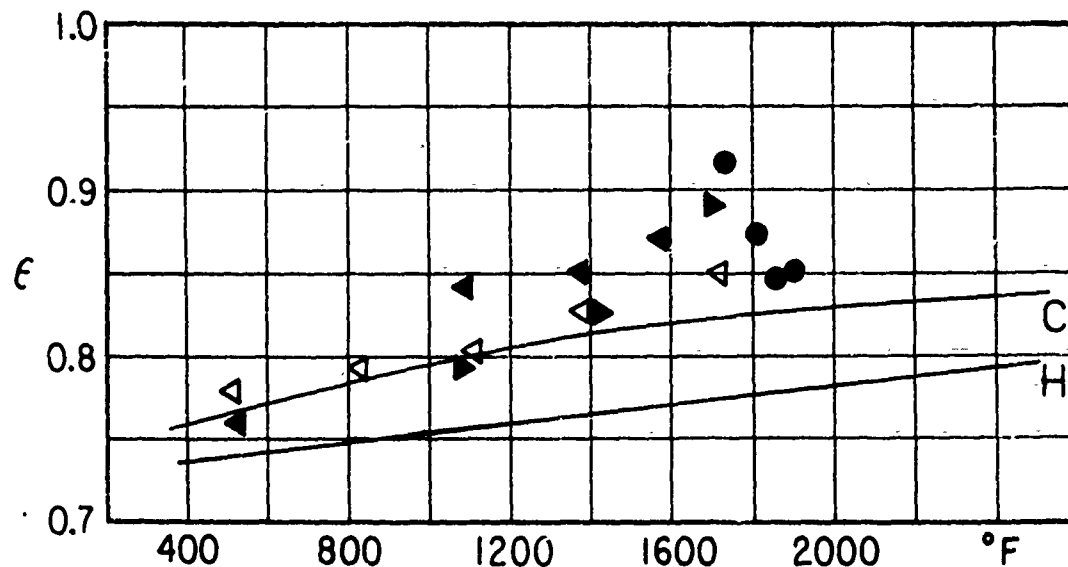
Original sample (WADD delivered) within 3% of prediction from cold reflectance, hot prediction 5% low. Second sample (received from Boeing 6/60) shown by solid points, indicated lower emittance up to 1500°F, then increases. Increase verified by repetition. Results from gas fired stand erratic within 3%, but check higher magnitude above 1700°F. No reflectance results obtained with second sample.

6. Solar Absorptance: Integrated from spectral results, 0.90.
7. Spectral Emittance: See page 32

Rene 41
 C-cold h-1031°F

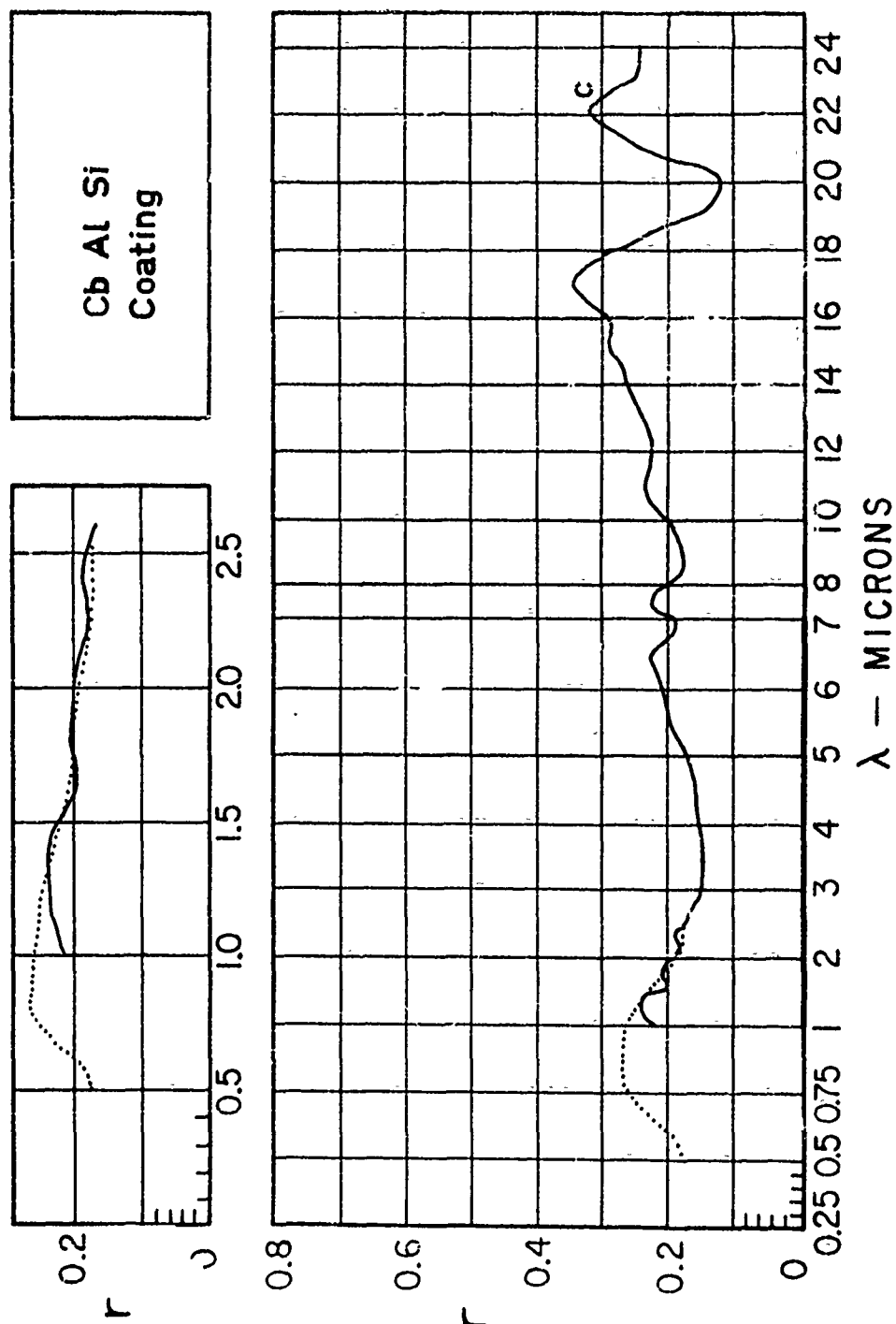


1. Material: René 41 (SS 8080)
2. Initial Treatment: Cleaned in 1 to 1 water-diluted HF solution for 1 hour oxidized 3 hours at 1700°F in air.
3. Roughness: Fully aged: Fine structure 2 microns high.
Coarse structure 5 microns at 200 micron intervals.
4. Spectral Reflectance: Sample at 1000°F .05 higher than at room temperature. DK2 results should probably be increased by 0.04.
5. Total Normal Emittance:

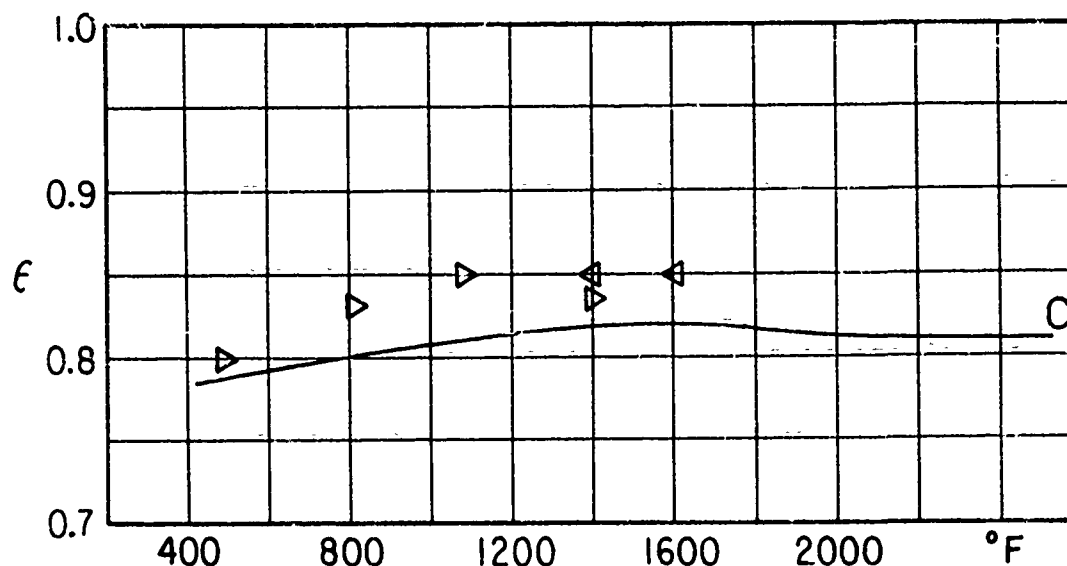


Original sample corresponds well with prediction from cold reflectance values. Second sample (solid point, Boeing 6/60) gives similar values but they become 4% higher at 1700°F. Emittances from gas fired unit vary but agree with other values within 5%. The second sample was used on the gas fired stand.

6. Solar Absorptance: Integrated from spectral results, 0.89.

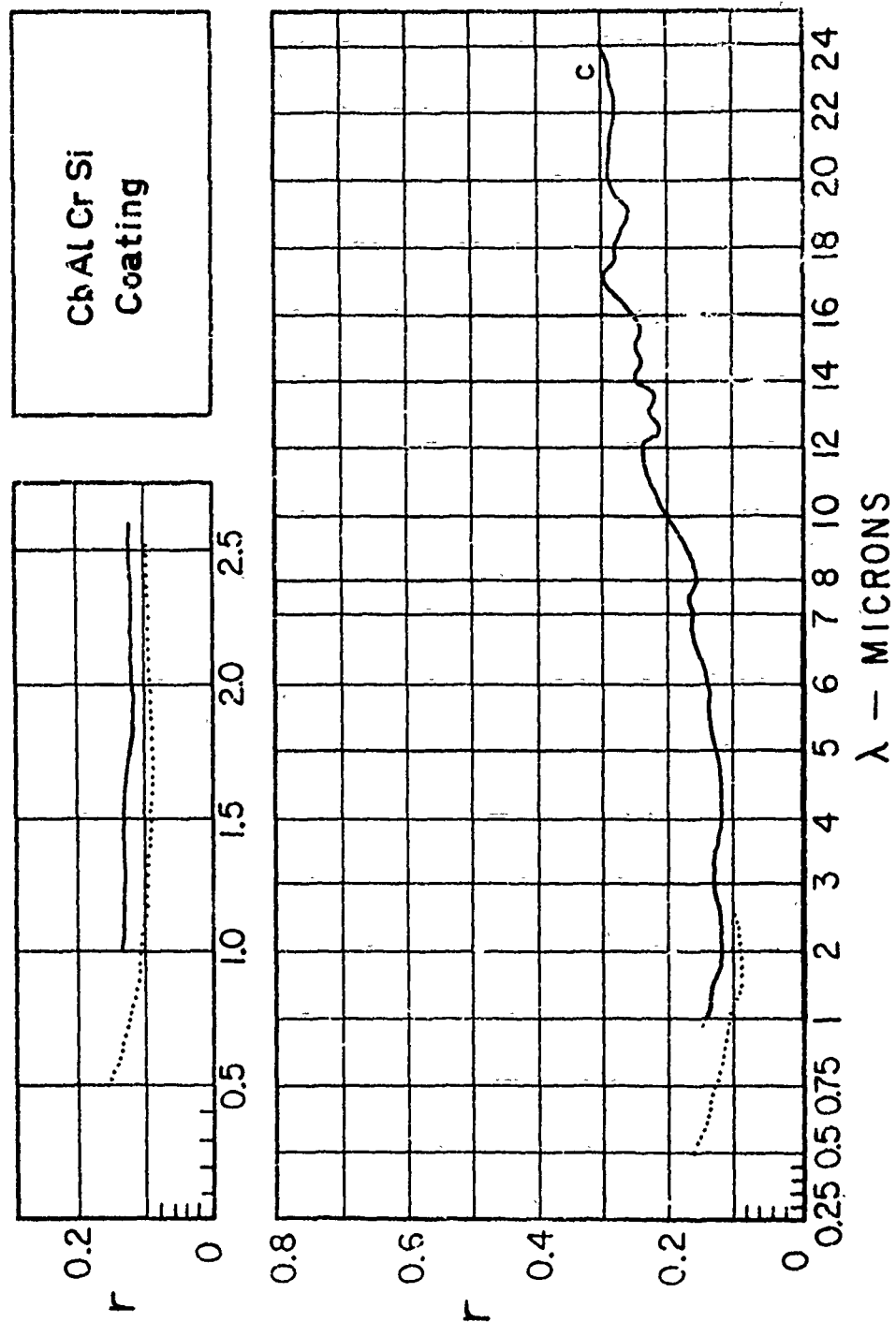


1. Material: Nb dipped in slurry of Al-Si.
2. Initial Treatment: (Before delivery) Unalloyed Cb aluminized by Al-Si hot slurry dip at 1700°F for 3 minutes. Diffusion heat treated at 1900°F for 1 hour in a vacuum. No further treatment before test.
3. Roughness: Fine structure - 1 micron. Coarse structure about 4 microns at 150 micron intervals.
4. Spectral Reflectance: One cold run taken with this sample. Good agreement between DK2 and cavity system.
5. Total Normal Emittance:

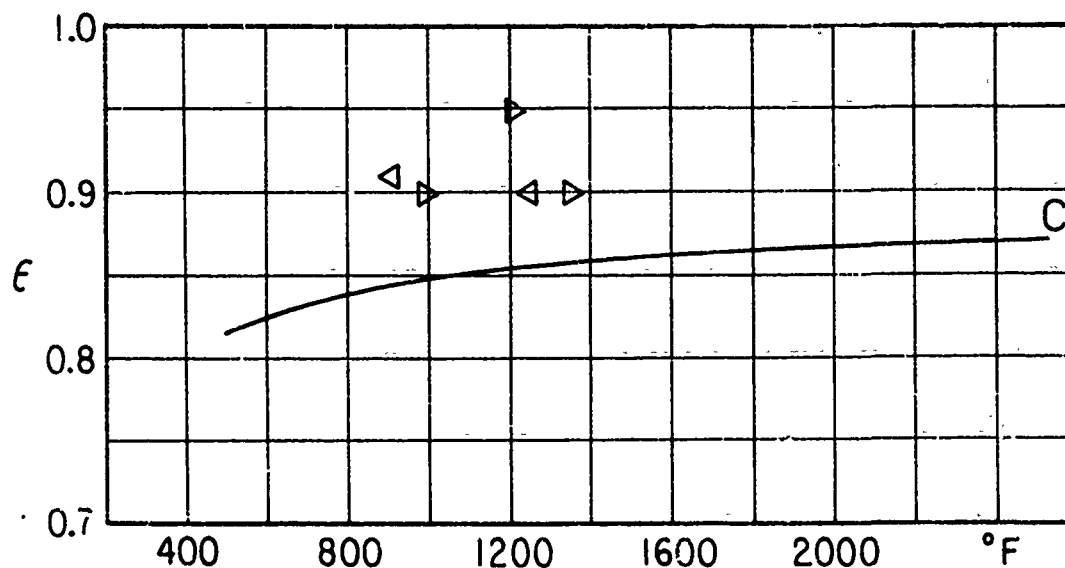


Measured total emittance 3% above prediction from cold reflectance results. Substrate would oxidize and thermocouple weld would separate after about 45 minutes of high temperature operation.

6. Solar Absorptance: Integrated from sphere results, 0.80.

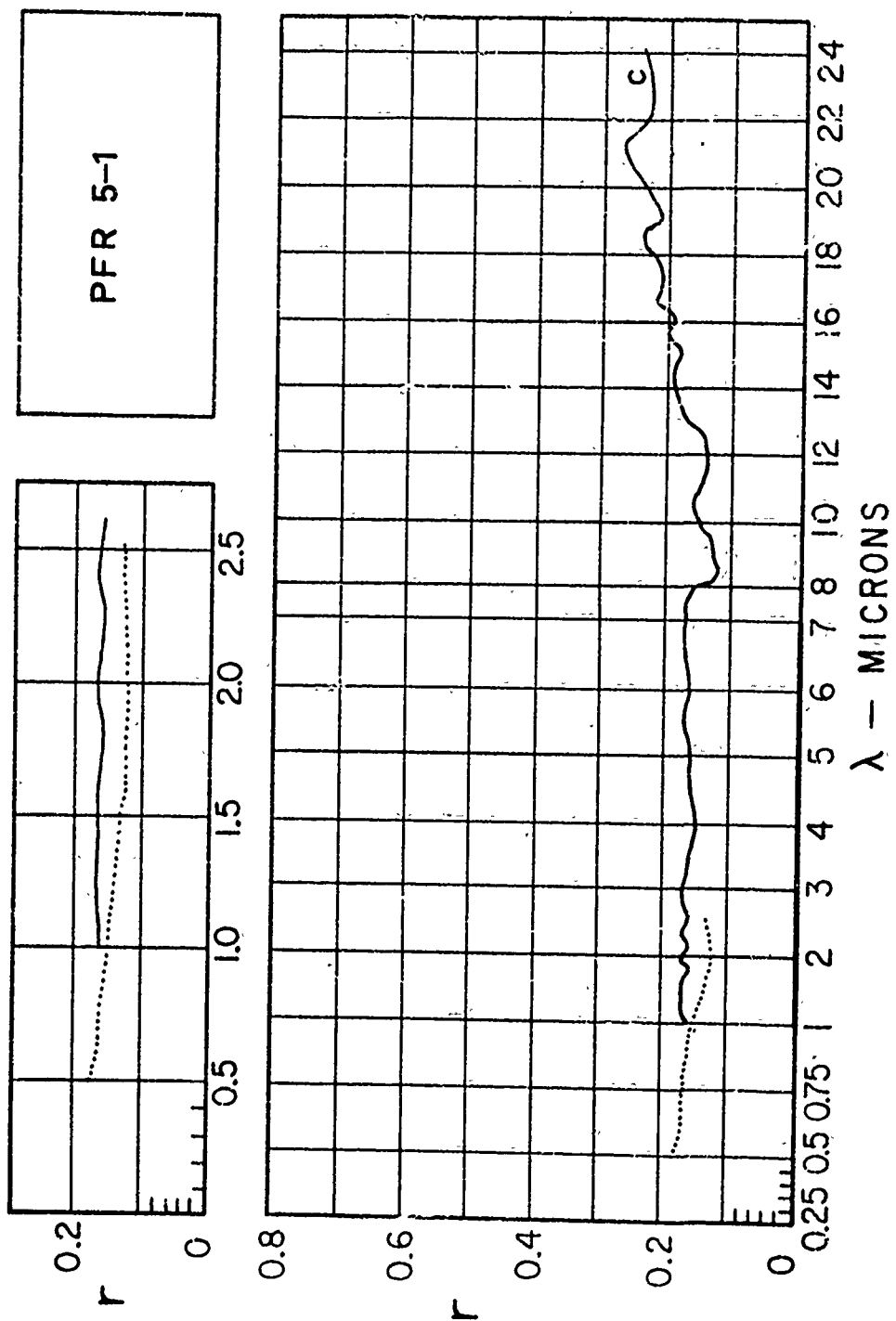


1. Material: Nb dipped in slurry of Al-Cr-Si. Unalloyed niobium aluminized by Al-Cr-Si hot slurry dip at 1700°F for 3 minutes. Diffusion heat treated at 1900°F for 1 hour in vacuum.
2. Initial Treatment: None.
3. Roughness: Fine structure about 1 micron in height. Coarse structure about 5 microns at 100 micron intervals.
4. Spectral Reflectance: Cold results obtained for sample after emittance determinations had been made.
5. Total Normal Emittance:

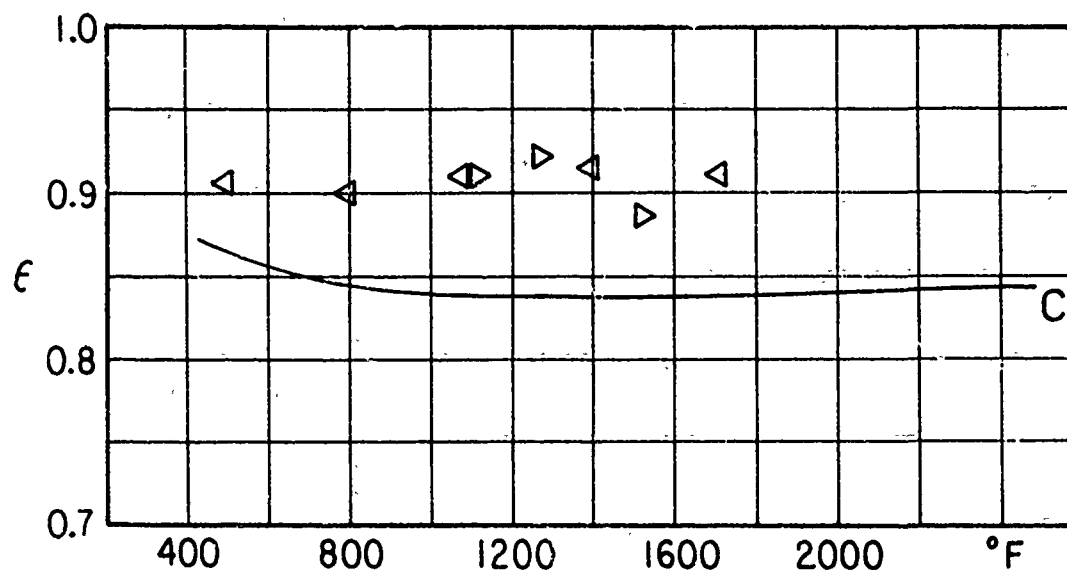


Majority of results 5% above prediction. Experimental results limited because of difficulty in maintaining thermocouple attachment. Probe thermocouple unsuccessful when tried. See section 8.

6. Solar Absorptance: Integrated from spectral results, 0.87.



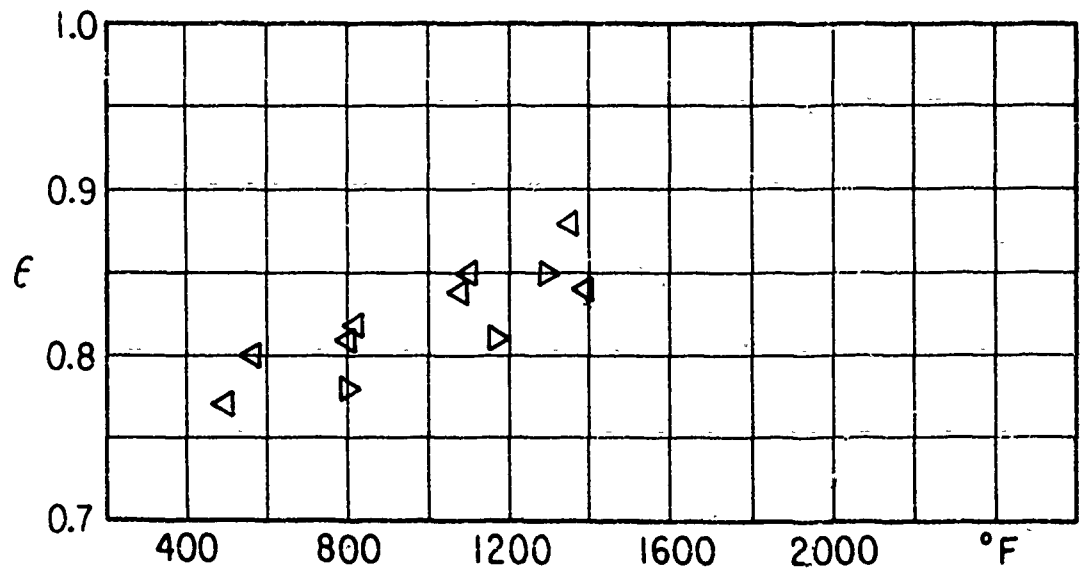
1. Material: PFR5
2. Initial Treatment:
3. Roughness: Fine structure 1.5 microns. Coarse structure about 18 microns at 200 micron intervals.
4. Spectral Reflectance: Reflectance data for sample cut from total emittance sample, after material used for emittance runs. Cold sample only.
5. Total Normal Emittance:



Measured total values exceed the prediction by 6%. Difficulty was experienced with deterioration of sample. Oxidation of substrate occurred, with visible changes of surface at any place where coating was punctured as at point of thermocouple location.

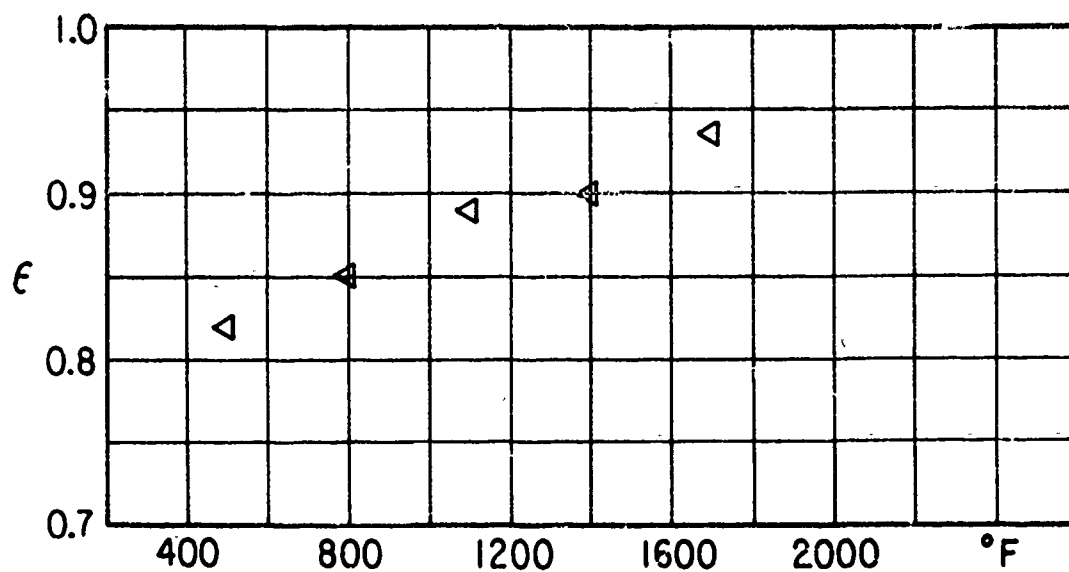
6. Solar Absorptance: Integrated from spectral results, 0.83.

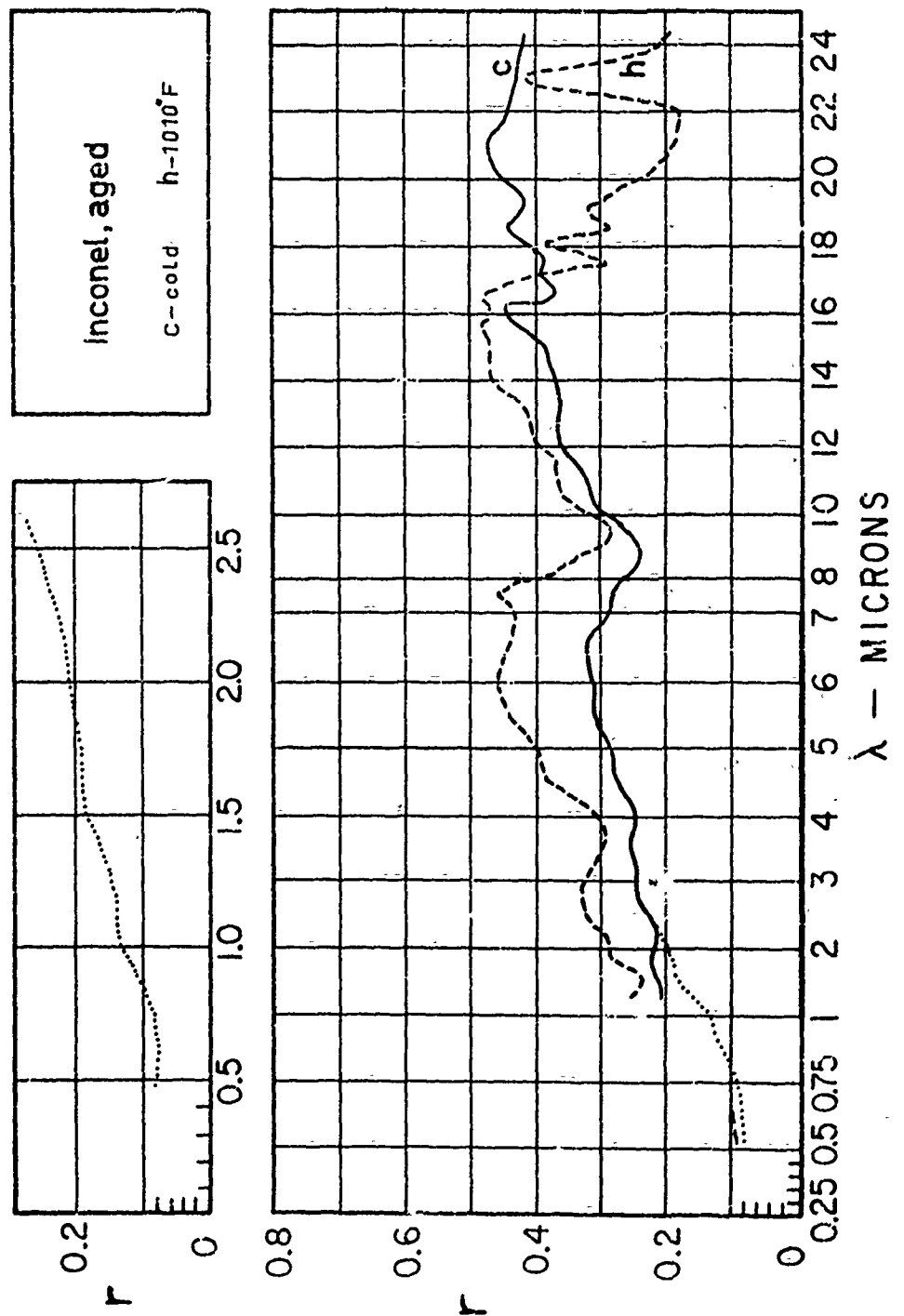
1. Material: PFR4
2. Initial Treatment:
3. Roughness:
4. Spectral Reflectance: Not obtained. Surface coating destroyed in total emittance tests before sample could be obtained for a determination.
5. Total Normal Emittance:



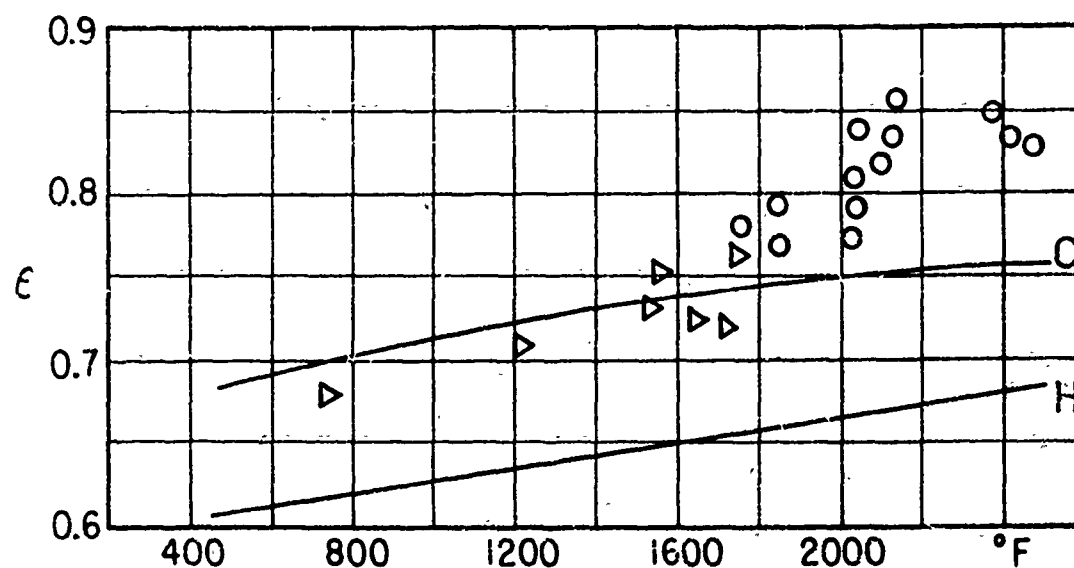
Only experimental values obtained. Progressive failure at higher temperatures due to progressive penetration of oxide through the surface coating.

1. Material: SS286
2. Initial Treatment: None
3. Roughness:
4. Spectral Reflectance: Not yet obtained.
5. Total Normal Emittance:





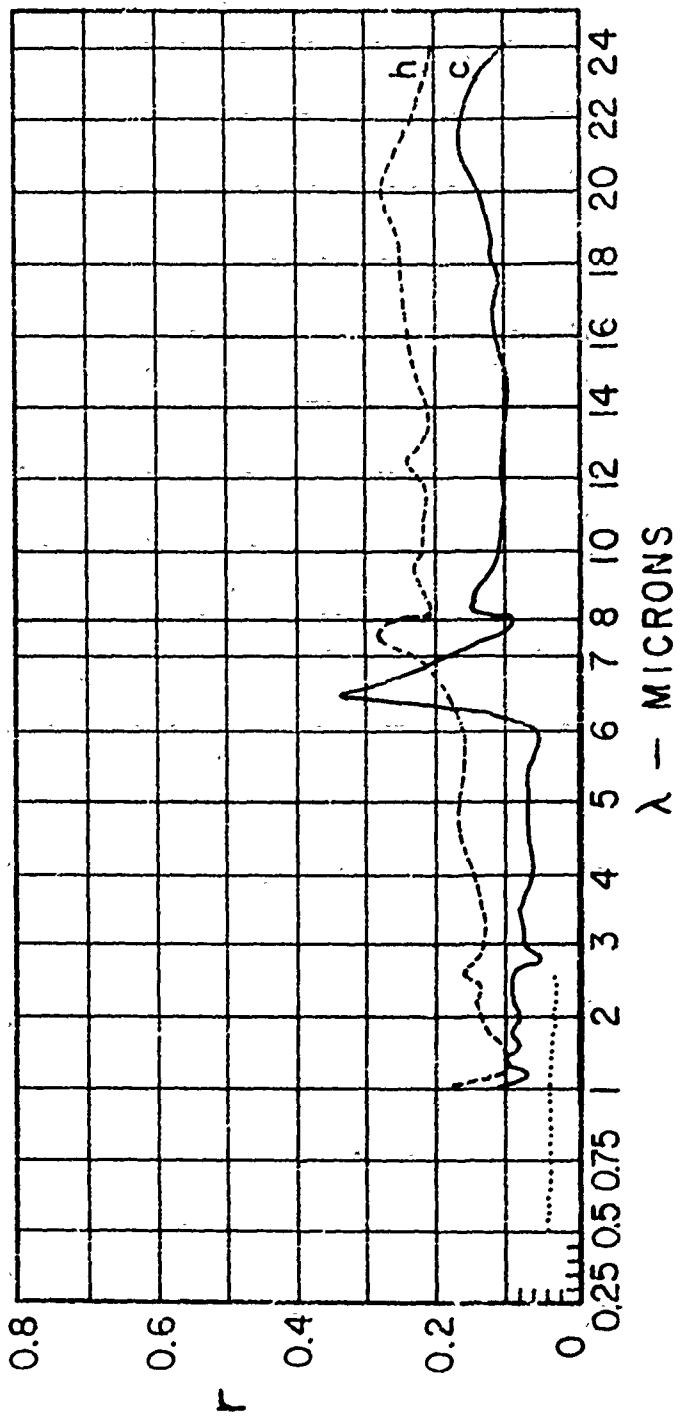
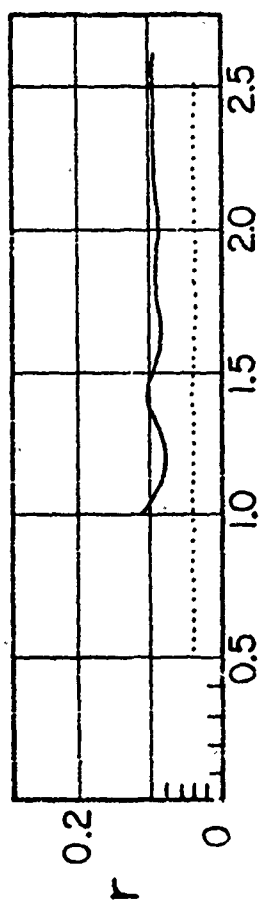
1. Material: Inconel
2. Initial Treatment: A number of different samples were involved and were heated 3 hours at 1700°F in air but their subsequent history differed and the oxide did not appear to have been exceptionally stable. Two different samples, giving different spectral reflectance values, are presented as examples for that measurement. The data presented are representative of all samples.
3. Roughness: Fine structure - 1 micron. Coarse structure about 2.5 microns at 60 micron intervals.
4. Spectral Reflectance: Results are shown for hot and cold samples.
5. Total Normal Emittance:



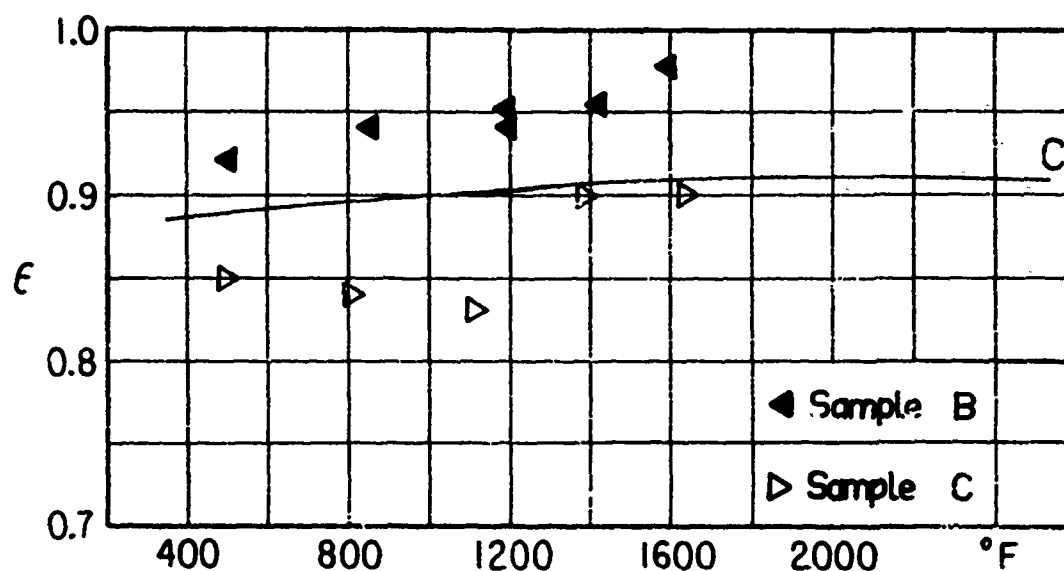
Total emittance values were obtained on the electric furnace and provided values corresponding to predictions made for that sample with a sample temperature of 1500°F. Results from the gas fired unit were made with different samples and indicated much higher values, as much as 10% above the prediction made from the reflectance data.

6. Solar Absorptance: Integrated from spectral results, 0.88.

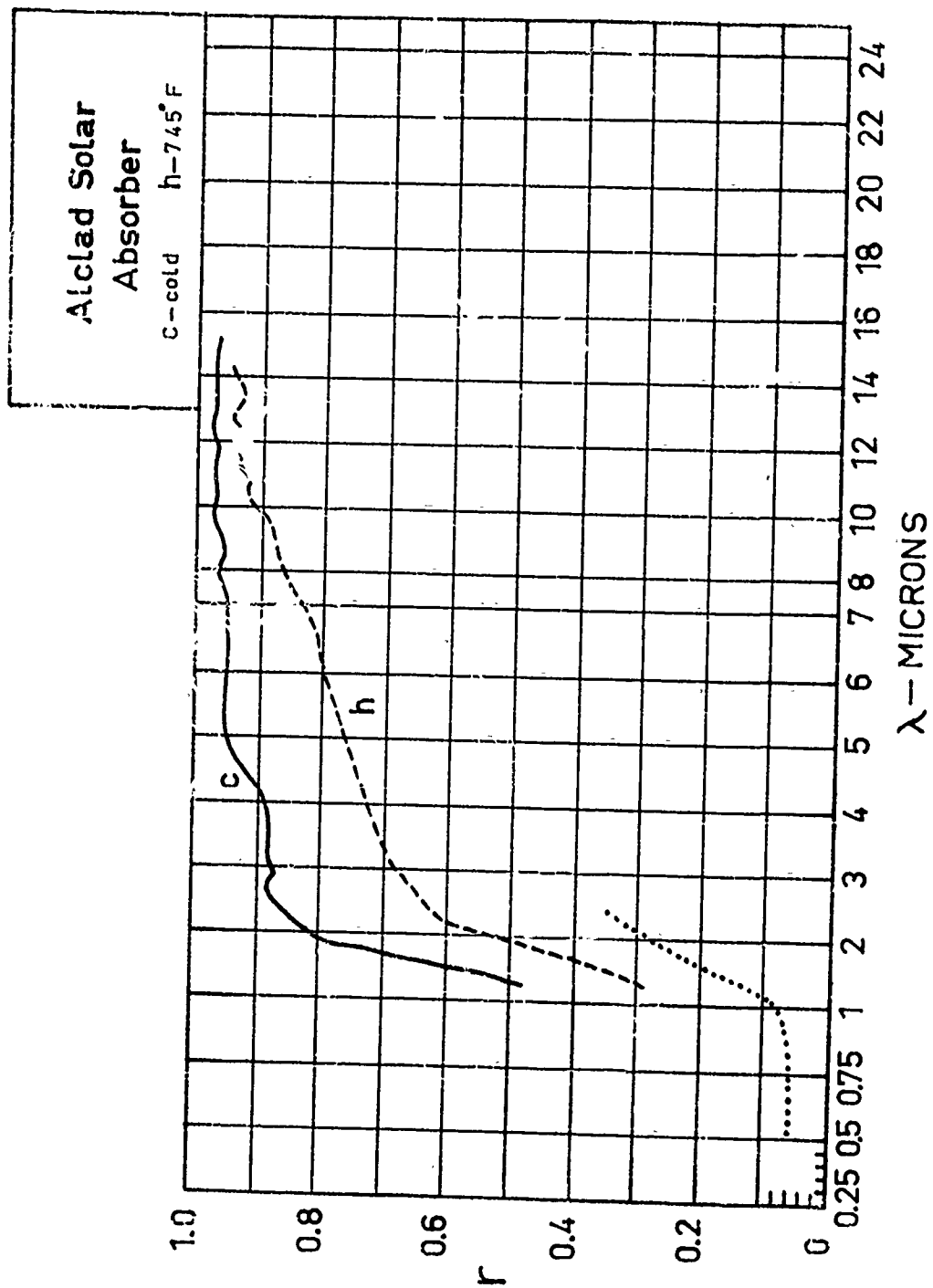
Boron Carbide
 Coating
 C-cold h-998°F



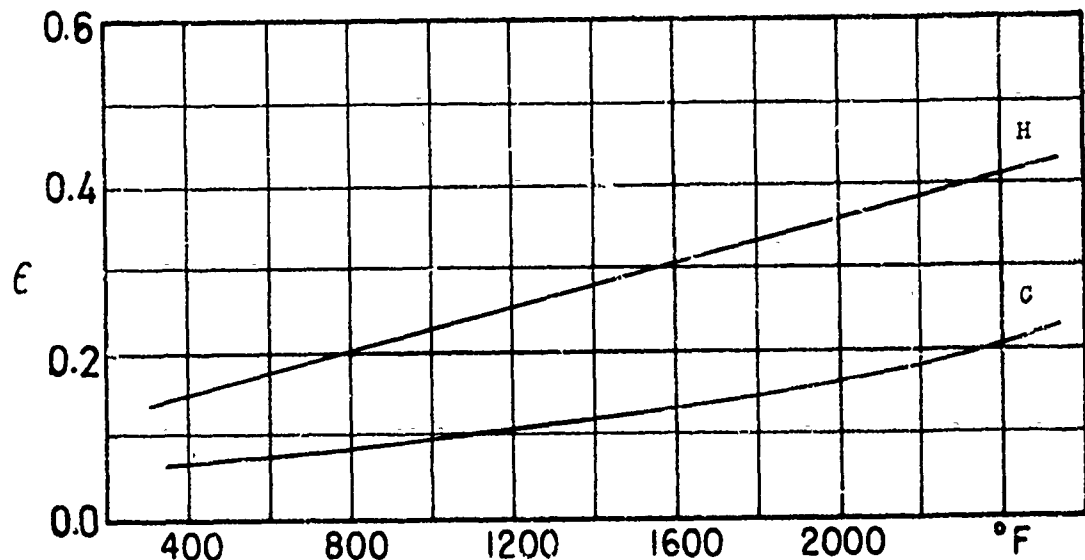
1. Material: Boron Carbide Coating
 Sample A: reflectance sample, same as Sample B.
 Sample B: total emittance sample (obtained at Boeing 6/60) Substrate: unknown.
 Sample C: Total emittance sample. Prepared at UCB according to Boeing recipe, using their materials. Substrate: stainless steel.
2. Initial Treatment: None.
3. Roughness: Samples A and B: Fine structure sparse and of about 4 microns height. Coarse structure about 20 microns.
4. Spectral Reflectance: Obtained only with Sample A. Cold reflectance $\lambda > 1$ somewhat higher than anticipated. DK2 readings, cold, appear to be low and results for integrating sphere, Section 4, are also shown as Curve E. Hot results substantially higher, may be due to excess sample temperature. See Section 8.
5. Total Normal Emittance: Sample B shows a 5 to 6% higher emittance than the value predicted from the cold reflectance data. Sample C gave lower results, and evidenced a change in nature at 1300°F to higher values. No further results were obtainable due to failure of sample coating on cooling from 1640°F, with total separation of the boron carbide from the substrate.



6. Solar Absorptance: Integrated from spectral results, 0.63.



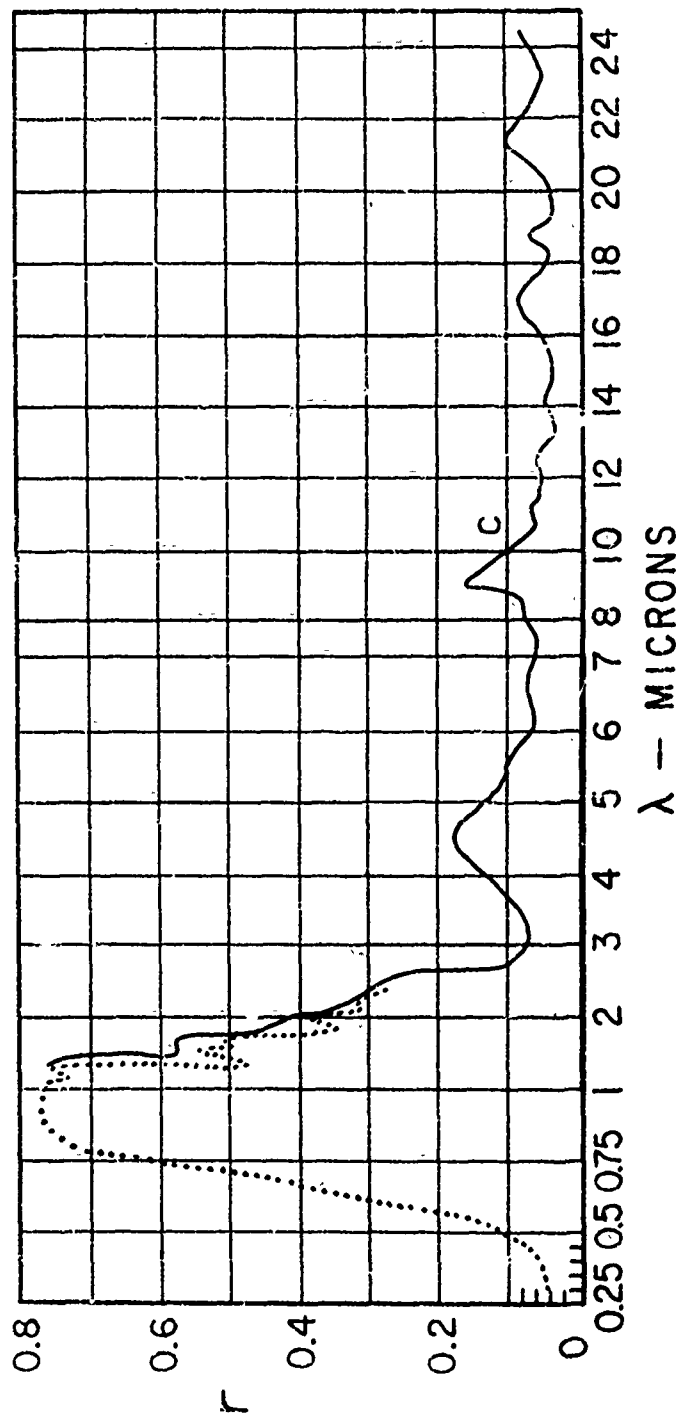
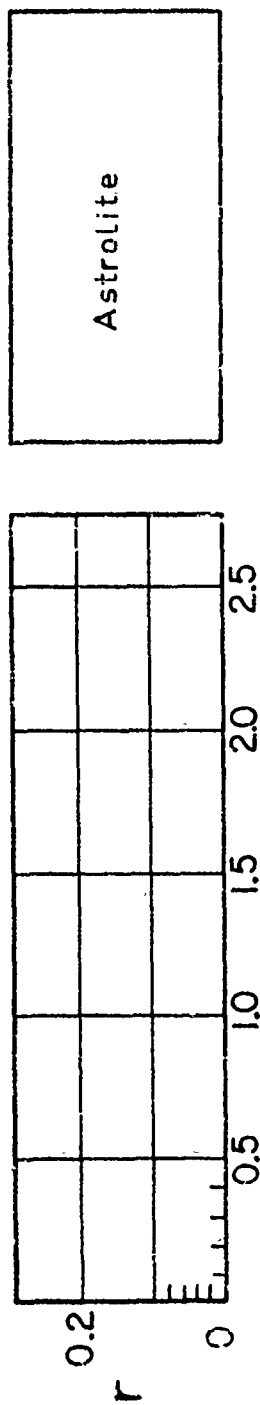
1. Material: Alclad solar absorber
2. Initial Treatment: None.
3. Roughness: As received: Fine structure - 0.3 microns. Coarse structure 1 micron at 250 micron intervals.
4. Spectral Reflectance: Only cold run, taken with sample as received, is of significance. Sample surface changed with exposure at higher temperature. Hot result shown is for sample at 754°F, with about 1 hour at this temperature. Substantial discrepancy between cavity and Beckman results.
5. Total Normal Emittance:



Total emittance corresponds well with "cold" prediction.

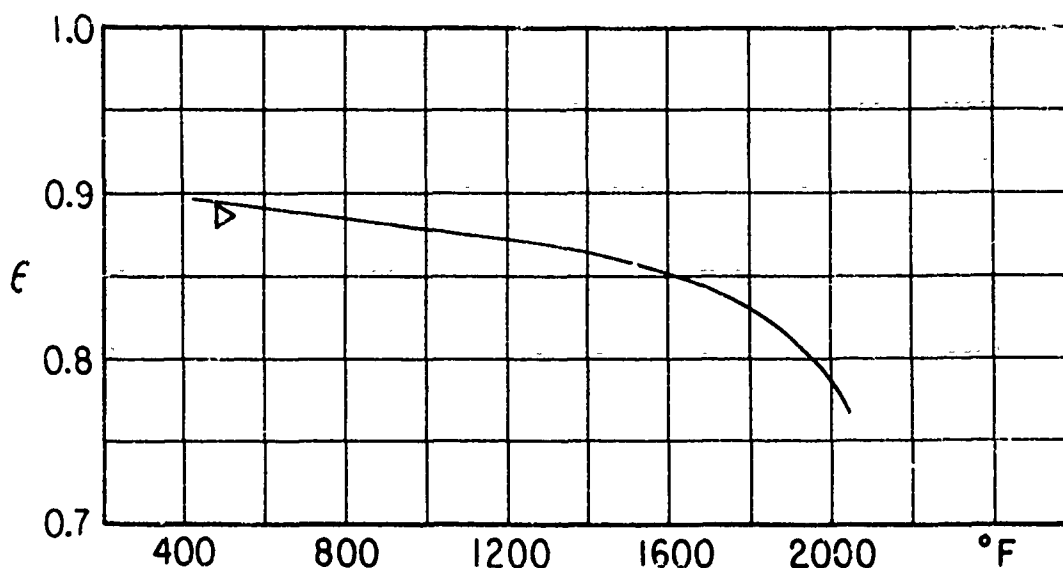
6. Solar Absorptance: Integrated from spectral results, 0.90.
Angular dependence of reflectance - see page 55

WADD TR 60-370

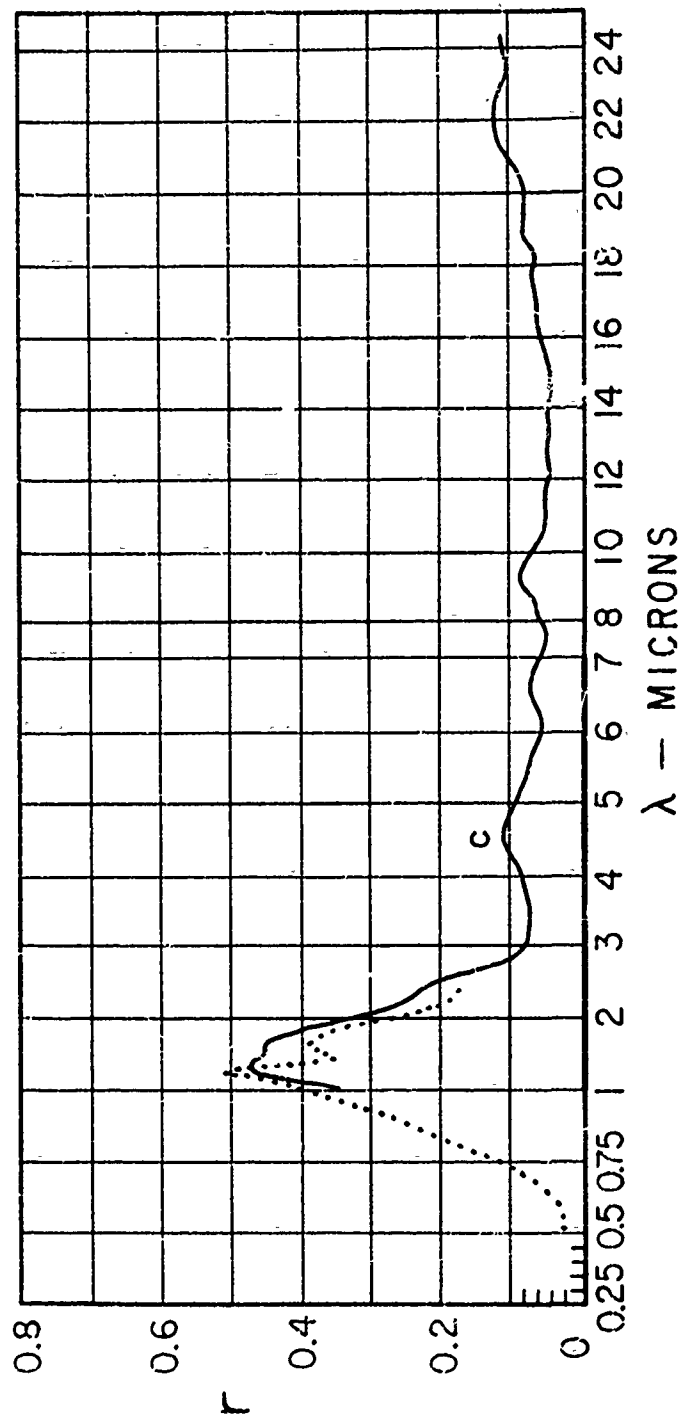
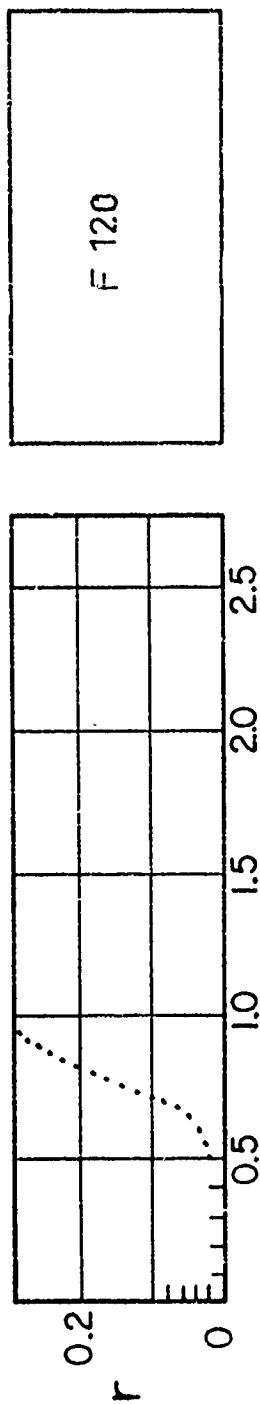


100

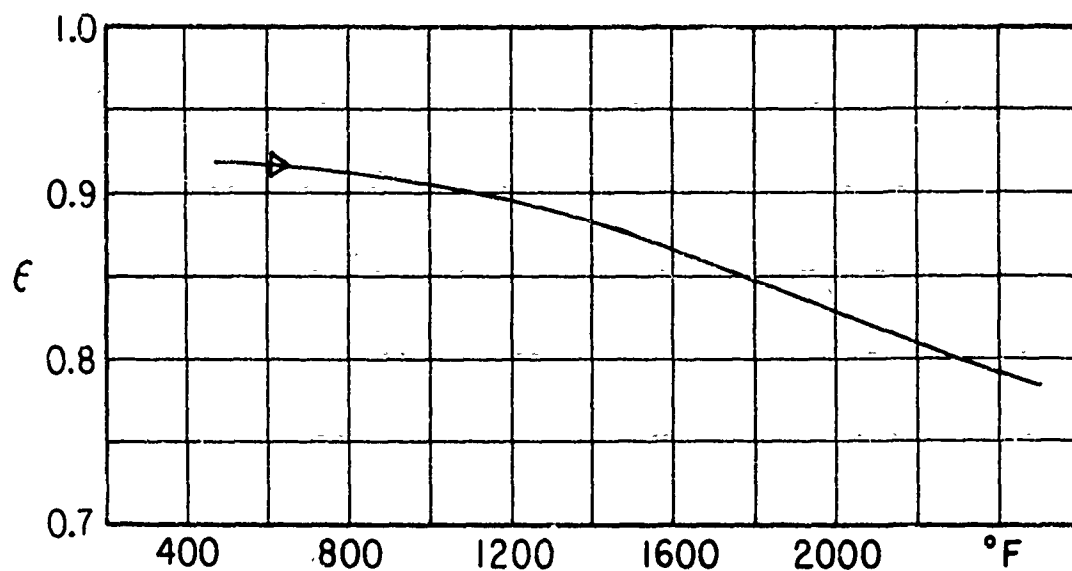
1. Material: Astrolite
2. Initial Treatment: None.
3. Roughness:
4. Spectral Reflectance: Obtained with 1/16 inch thick sample in water cooled sample holder. Estimated surface temperature was 353°F. There is a particularly good check with values of $\phi = 5^\circ$, from the Beckman reflectometer. The sample temperature does not affect the heated cavity values in this spectral region.
5. Total Normal Emittance:



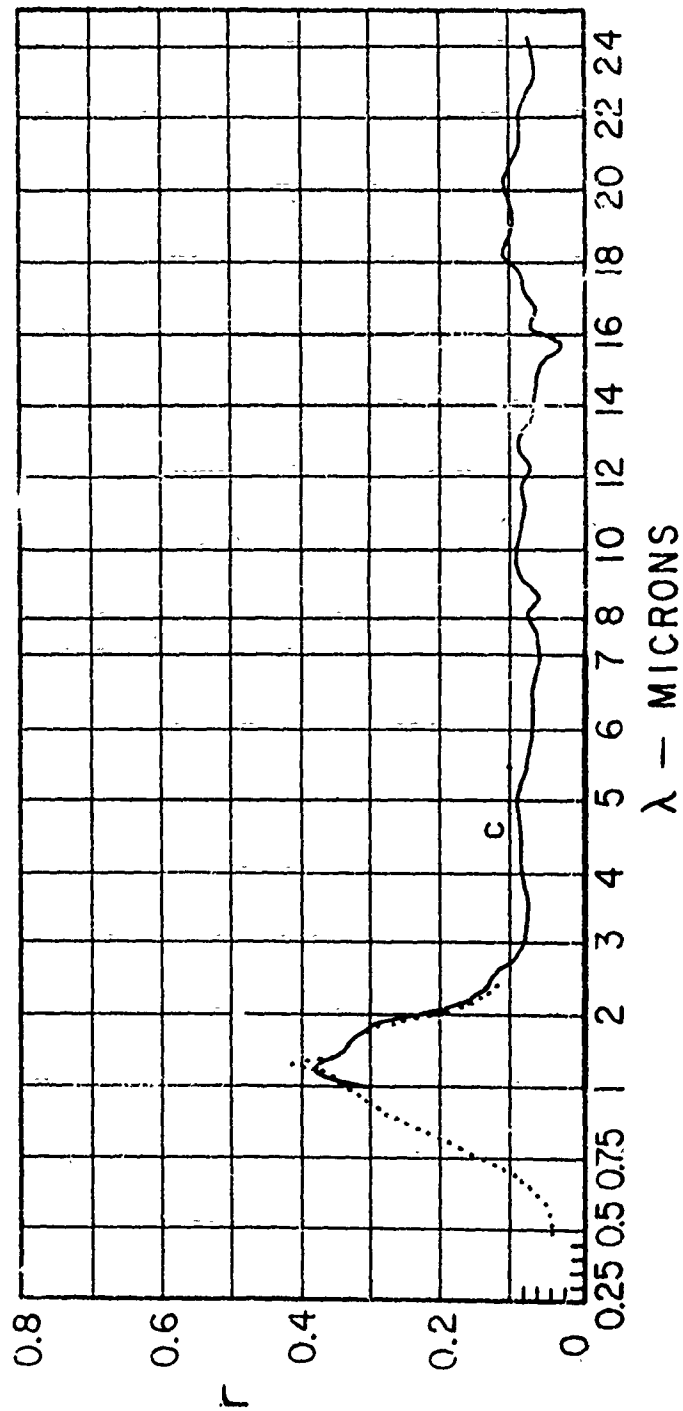
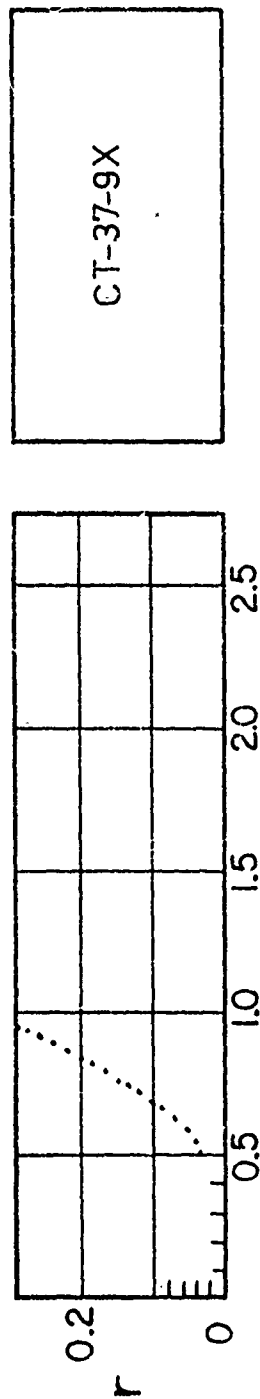
The measured values were obtained as indicated in Section 12.1. At a surface temperature of 903°F the temperature at the back of the sample was 1281°F and disintegration occurred. The binder vaporized completely, leaving only the glass cloth.



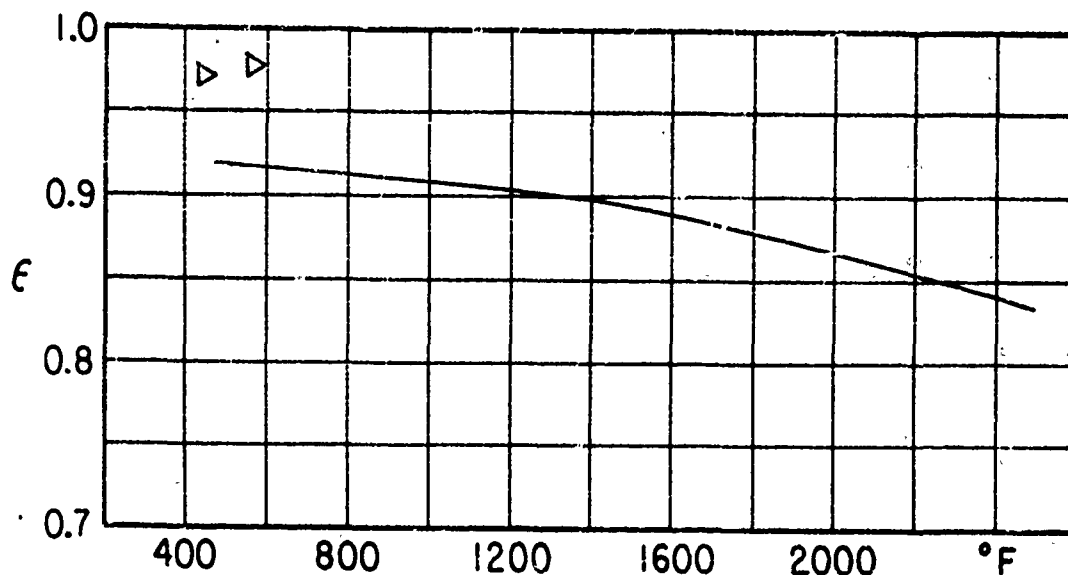
1. Material: F120
2. Initial treatment: None.
3. Roughness:
4. Spectral Reflectance: The position of the curve was chosen to give a reflectance of 0.07 at $\lambda = 10\mu$, to indicate a surface temperature of 787°F. This was done to produce an integrated reflectance corresponding to the measured total emittance.
5. Total Normal Emittance:



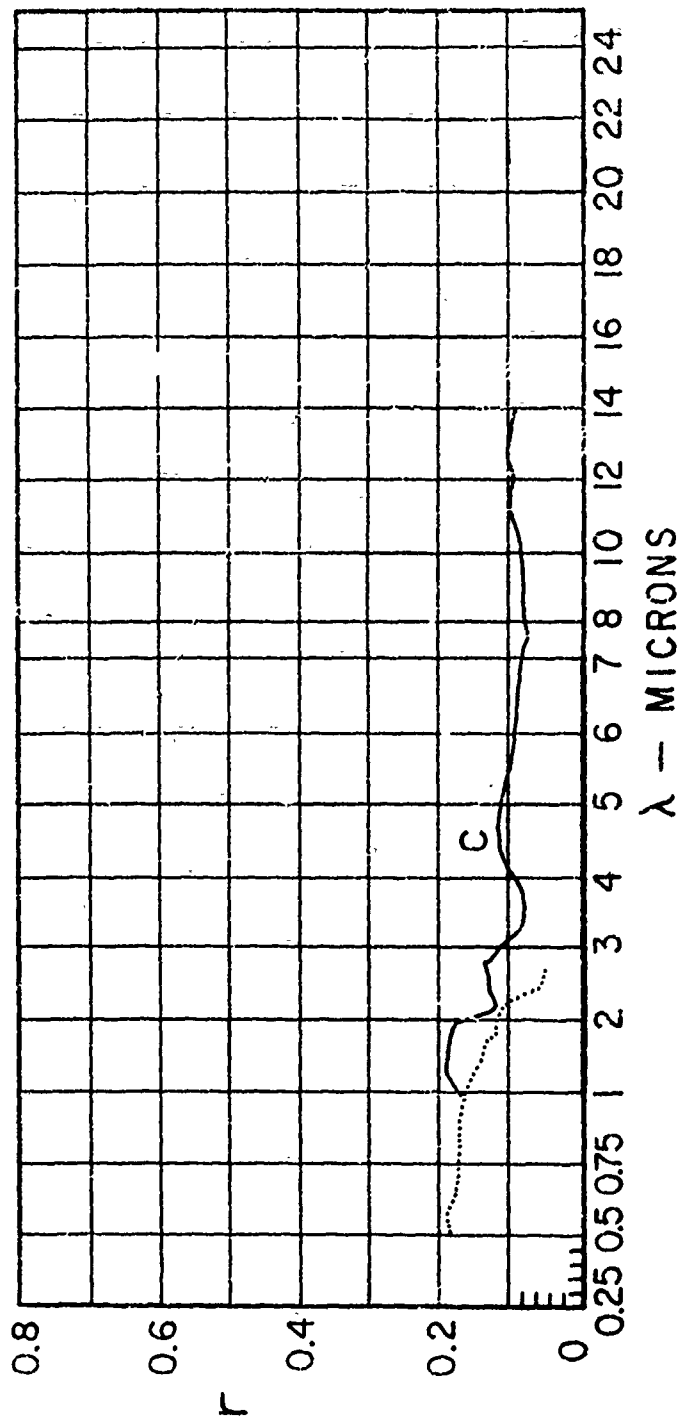
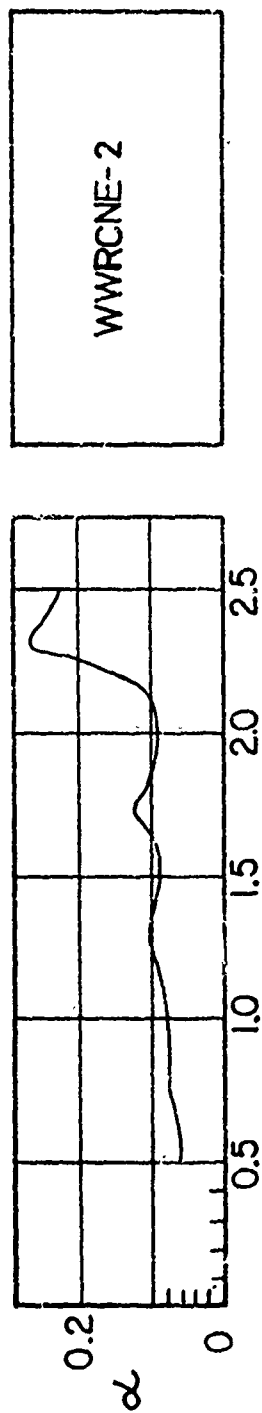
The measured value of total normal emittance at 610°F was important in determining the nature of the reflectance curve.



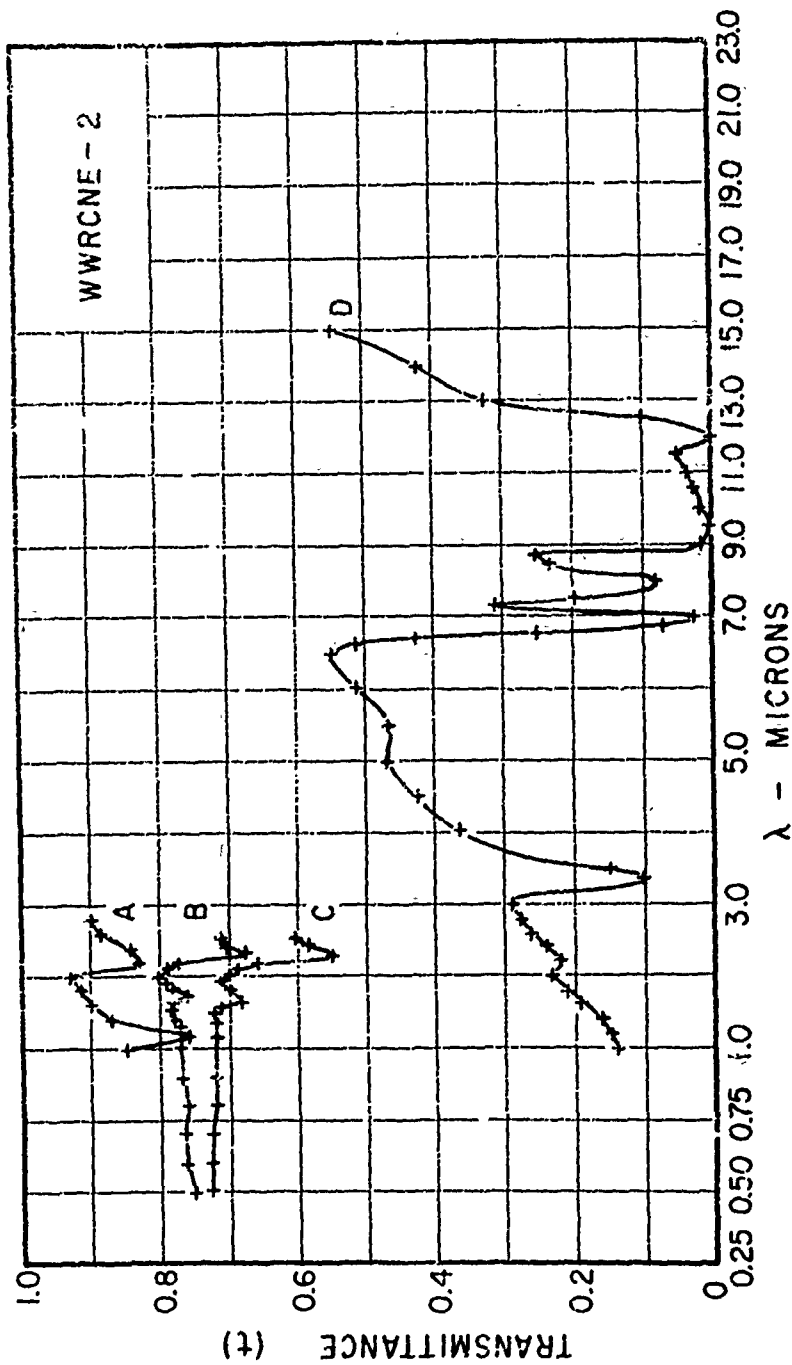
1. Material: CTL37-9
2. Initial Treatment: None
3. Roughness:
4. Spectral Reflectance: The position of the curve was chosen to give a reflectance of 0.10 at $\lambda=10\mu$, to indicate a surface temperature of 793°F. This choice of temperature was based upon our assumed value of 0.90 for the total normal emittance at 793°F.
5. Total Normal Emittance:



Experimental determinations of total normal emittance with this sample, with values of about 0.99 being attained. This high value is attributed to the difficulties in evaluating the surface temperature of the emittance sample as previously described.



1. Material: WWCNE-2 (Translucent plastic)
2. Initial Treatment: None.
3. Roughness: Not measured.
4. (a) Spectral Transmittance
Page 108 shows transmittance results, both normal and total. The total transmittance obtained from the integrating sphere (Section 3.3) is high and the discrepancy with regard to the Beckman values has not been resolved.
- (b) Spectral Reflectance
Spectral reflectances have been evaluated as indicated in Section 11.3, using the results for normal transmittance and the cavity results for $\lambda > 1.0$. For lower wavelengths the Beckman results are given directly. There is only fair correspondence in the region of overlap, $1.0 < \lambda < 2.5$ microns.
5. Solar Absorptance: Spectral absorptance can be calculated from the transmittance and reflectance data for normal incidence and this can be done with confidence for $\lambda < 2.5$ microns, where the total transmittances are known. Using the solar irradiation values for zero air mass, there is found in this way an absorptance of 0.07 for solar irradiation. The spectral absorptances from which this value was calculated are shown on page 106.



Transmittance of WVRCNE-2, translucent plastic, Curve A, total diffuse transmittance from integrating sphere, Curve B, total diffuse transmittance from Beckman DK2; Curve C, total diffuse transmittance from Beckman DK2; Curve D, approximate diffuse component from heated cavity reflectometer.

14.0 NOMENCLATURE

A = Area
 C, C_1 = Planckian Constants
 $C(\lambda) = E/\sigma T^4$
 E = Black body spectral emissive power
 F = Fahrenheit degrees
 F = Shape factor for diffuse energy exchange
 G = Irradiation Btu/hr.ft.²
 I = Intensity Btu/hr. ft.² - steradian
 K = Directional radiometer constant
 R = Reflected energy
 S = Detector output
 T = Absolute temperature °R
 V = Radiometer output mv.
 W = Energy rate

 r = Spectral reflectance

 α = Normal spectral absorptivity
 α_s = Hemispherical spectral absorptivity
 β = Ratio of emissive powers $(E_H - E_c) / (E_R - E_c)$
 r = Ratio of emissive powers $(E_s - E_c) / (E_H - E_c)$
 Δ = Incremental difference
 ϵ = Spectral emittance
 ϕ = Angle between incident beam and normal to sample surface
 ψ = Polar angle in plane of sample surface
 μ = Angle between reflected or emitted beam and normal to sample surface
 λ = Wavelengths - microns
 σ = Stefan - Boltzmann constant
 π = Ratio of diameter to circumference of a circle
 Ω = Solid angle in steradians

Subscripts

B = Backing plate
 C = Chopper blade
 H = Hohlraum area
 O = Sphere wall
 R = Reference area
 S = Sample area
 T = Denotes properties on a total basis, not spectrally

 ∞ = Ambient conditions
 \bar{r} = Average value of reflectance over small $\Delta\lambda$
 $\bar{\epsilon}$ = Average value of emittance over small $\Delta\lambda$

15.0 REFERENCES

1. Muench, B., Die Richtungsverteilung bei der Reflexion von Wärmestrahlung. Dissertation, Eidgenossischen Technische Hochschule, Zurich, 1955.
2. Eckert, E. R. G., Forschung des Gebiete der Ingenieurwesens, #6, p. 175, 1936, Heat and Mass Transfer, p. 377, 2nd Ed., McGraw Hill Book Co., 1959.
3. Gier, J. T., R. Dunkle, J. Bevans, "Measurement of Absolute Spectral Reflectivity from 1.0 to 15 microns", Jour. Opt. Soc. America, vol. 44, 1954, p. 558.
4. Tellex, P. and J. Waldron, "Reflectance of Magnesium Oxide", Jour. Opt. Soc. America, vol. 45, 1953, p. 19.
5. Jacquez, J. and H. Kuppenheim, "Theory of the Integrating Sphere", Jour. Opt. Soc. America, vol. 45, 1955, p. 460.
6. Betz, Olson, Schurin and Morris, "Determination of Emissivity and Reflectivity Data on Aircraft Structural Materials", Wright Air Development Center Technical Report 56-222, Part II.
7. Gier, J. and L. Boelter, "The Silver Constantan Plated Thermocouple Radiometer", Temperature and Its Control in Science and Industry, Reinhold Publishing Company, New York, 1941, p. 1284. Also: Snyder, N., J. Gier and R. Dunkle, "Total Normal Emissivity Measurements on Aircraft Materials between 100 and 800°F. Trans. Amer. Soc. of Mech. Engrs., vol. 77, 1955, p. 1011.
8. Johnson, F. S., "The Solar Constant", Jour. of Meteorology, vol. 2, #6, 1954.
9. Harrison, W., et.al., "Standardization of Thermal Emittance Measurements", WADC TR 59-516. WADD, USAF, 1960.
10. Etemad, A., Discussion on "Comparison of Total Emittances with values Computed from Spectral Measurements", by Bevans, et.al., Trans. Amer. Soc. Mech. Engrs., vol. 80, 1958, p. 1405.
11. Clayton, W and R. Evans, "Total Normal Emittance Measurements at Boeing Airplane Company", Boeing Airplane Co., Seattle, Washington, Jan. 1960.

<p>UNIVERSITY OF CALIFORNIA, Berkeley. CONFIDENTIAL THERMAL RADIATION PROPERTIES OF MATERIALS, by R. A. Seban and R. E. Rolling, June 1961, 110 p. incl. figs. and tables. (Project No. 9(8-7360; Task 73603) (WADD TR 60-370) (Contract AF33(616)-6630)</p> <p>Unclassified report</p> <p>Methods are described for the measurement of total normal emittance, in air, for temperatures up to 2500°F; for normal spectral reflectance, in air, at 1000°F, from 1 to 25 microns. Results of this type are given for twenty samples of different materials and the measured total emittances are generally</p> <p>(over)</p>	<p>U.C. Classified</p>	<p>UNIVERSITY OF CALIFORNIA, Berkeley. CONFIDENTIAL THERMAL RADIATION PROPERTIES OF MATERIALS, by R. A. Seban and R. E. Rolling, June 1961, 110 p. incl. figs. and tables. (Project No. 9(8-7360; Task 73603) (WADD TR 60-370) (Contract AF33(616)-6630)</p> <p>Unclassified report</p> <p>Methods are described for the measurement of total normal emittance, in air, for temperatures up to 2500°F; for normal spectral reflectance, in air, at 1000°F, from 1 to 25 microns. Results of this type are given for twenty samples of different materials and the measured total emittances are generally</p> <p>(over)</p>	<p>U.C. Classified</p>
<p>within 5% of values predicted from reflectance measurements.</p> <p>Reflectances were also measured as a function of angle for wavelengths of the order of 1 micron, to give absorptances as a function of angle of incidence that are useful in the appraisal of solar irradiation.</p> <p>A spectral emittance unit is described and the preliminary results from it for samples at 1400°F show general agreement with the measured values of spectral reflectance</p>	<p>U.C. Classified</p>	<p>within 5% of values predicted from reflectance measurements.</p> <p>Reflectances were also measured as a function of angle for wavelengths of the order of 1 micron, to give absorptances as a function of angle of incidence that are useful in the appraisal of solar irradiation.</p> <p>A spectral emittance unit is described and the preliminary results from it for samples at 1400°F show general agreement with the measured values of spectral reflectance.</p>	<p>U.C. Classified</p>
	<p>U.C. Classified</p>		<p>U.C. Classified</p>